# A-21 Valkyrie II

## A-10 Replacement

AIAA Undergraduate Individual Aircraft Design Competition 2017 - 2018


Frank Bonet AIAA # 922248

Advisor: Dr. R. Barrett-Gonzalez

## Abstract


This document explains in detail the preliminary sizing through class I and class II designs of the A-21 Valkyrie II, a ground attack aircraft capable of a long airborne armed overwatch (AAO) missions. Having the ability to loiter for long periods of time

with its advanced 35mm cannon and large amount stores, it will be shown that the A-21 Valkyrie II has the ability to provide airborne armed overwatch in a large range around its stationed base on rough terrane runways. The document begins with an overview of the mission specifications provided by the American Institute of Aeronautics and Astronautics (AIAA) 2017 - 2018 Undergraduate Individual Aircraft Design Competition. By interviewing experienced operators and other industry professionals, an optimized objective function and design vector were determined. To take advantage of the market sales of attack aircraft, a Statistical Time and Market Predictive Engineering Design (STAMPED) dataset was drawn up. With the data accumulated and expertise input used, a method for an effective design was made. From historical trends collected, a STAMPED vector analysis was used to establish a class I and class II attack aircraft with optimal weight and powerplant sizing. An estimate of drag throughout every possible scenario was drawn up to provide an accurate model of how the payload would affect the performance in all situations.


## Acknowledgements


The author would like to thank his Mother and Father for their support to their son with his aerospace engineering degree path. The author is also very grateful for the Aerospace Design Lab at the University of Kansas in G400 for providing a good work environment. Additionally, the author would like to thank Colonel Roger Disrud for his advice and expertise in the A-10. As well, the author would like to thank Dr. Ron Barrett and Dr. Willem Anemaat for the time they have taken to help with the design. Finally, the author would also like to thank the man, the myth, the legend, Dr. Jan Roskam for being such an inspiration to us all.

# Table of Contents

## List of Figures

## List of Tables

## List of Symbols

| Symbol | Description | Units |
|---|---|---|
| A | Aspect Ratio | ~ |
| b | Span | ft |
| c | Cord | ft |
| $C_D$ | Coefficient of Drag | ~ |
| $C_{D,0}$ | Zero Lift Drag Coefficient | ~ |
| $\Delta C_{D,0}$ | Change in Zero Lift Drag Coefficient | ~ |
| $c_j$ | Specific Fuel Consumption | lbm/lbf/hr |
| $c_{h\delta}$ | hinge moment coefficient | 1/rad |
| $C_L$ | Coefficient of Lift | ~ |
| d | Diameter | ft |
| D | Drag | lbf |
| E | Endurance | hr |
| h | Height | ft |
| i | incidence Angle | deg. |
| K | Flap Coefficient | ~ |
| K | Gain | deg/deg |
| K | Correction Factor | ~ |
| l | Length | ft |
| L | Lift | ~lbf |
| l | Distance | ft |
| L/D | Lift to Drag Ratio | ~ |
| n | Load Factor | ~ |
| N | Number of Engines | ~ |
| N | Moment | ftlbf |
| P | Pressure | psi |
| P | Force | lbf |
| R | Range | nmi |
| Rn | Reynolds Number | ~ |
| S | Area | $ft^2$ |
| $S_{wf}/S$ | Wing Flap Area Ratio | ~ |
| SM | Static Margin | % |
| T | Thrust | lbf |

| Symbol | Description | Units |
|---|---|---|
| T | Temperature | °F, °R |
| T/W | Thrust to Weight Ratio | ~ |
| V | True AirSpeed | kts, ft/s |
| $\bar{V}$ | Volume Coefficient | ~ |
| $w$ | Width | ft |
| W | Weight | lbf |
| W | Watts | W |
| W/S | Wing Loading | $lbf/ft^2$ |
| X | Distance | ft |
| $\bar{X}$ | Distance with Respect to MGC | ~ |
| $y$ | Distance | ft |

**Greek Symbols**

| Symbol | Description | Units |
|---|---|---|
| α | Angle of Attack | deg. |
| Γ | Dihedral Angle | deg. |
| δ | Pressure Ratio | ~ |
| δ | Deflection Angle | deg. |
| Δ | Change in | ~ |
| Η | Percent Span | % |
| θ | Temperature Ratio | ~ |
| λ | Bypass | ~ |
| Λ | Taper Ratio | ~ |
| $\mu_G$ | Friction Coefficient | ~ |
| ρ | Density | $Slugs/ft^3$ |
| τ | Torque | ft-lbf |

**Subscripts**

| | |
|---|---|
| a | Aileron |
| α | Lift Curve Slope |
| β | Side Slip Angle |
| ac | Aerodynamic Center |
| c/4 | Quarter Cord |
| crt | Critical |
| D | Drag |
| e | Empty |
| e | Elevator |
| f | Fuselage |
| f | Flaps |
| F | Fuel |
| FF | Fuel Fraction |
| h | Horizontal Tail |
| l | Airfoil Lift |
| l | Roll Rate |
| L | Landing |
| L | Lift |
| m | Main Landing Gear |
| m | Pitch Rate |
| MAX | Maximum |
| MIN | Minimum |
| n | Nose Landing Gear |
| n | Yaw Rate |
| oe | Operating Empty |
| PL | Payload |

r ........ Root
r ........ Rudder
t ........ Tip
TO ........ Take-Off
v ........ Vertical Tail
w ........ Wing
wett ........ Wetted Area
wf ........ Wing Fuselage

**Acronyms**

AAA ........ Advanced Aircraft Analysis
AC ........ Aerodynamic Center
AIAA ........ American Institute of Aeronautics and Astronautics
BL ........ Butt Line
CAD ........ Computer Aided Design
CG ........ Center of Gravity
FAA ........ Federal Aviation Administration
FAR ........ Federal Aviation Regulation
FS ........ Fuselage Station
MGC ........ Mean Geometric Cord
MTOW ........ Maximum Take-Off Weight
NACA ........ National Advisory Committee for Aeronautics
NASA ........ National Aeronautics and Space Administration
RFP ........ Request for Proposal
STAMPED ........ Statistical Time and Market Predictive Engineering Design
TOG ........ Take-Off Groundrun
CGR ........ Climb Gradient Request
OEI ........ One Engine Inoperable
AEO ........ All Engines Operable
CAS ........ Close Air Support
WL ........ Water Line

# 1 Introduction, Mission Specification & Profile

The Mission Specification obtained and used for this study was posted by the American Institute of Aeronautics and Astronautics (AIAA) at http://www.aiaa.org. The Request for Proposal (RFP) version referenced in this report was posted on 23 August 2017 (Ref. 1).

Due to the success of the A-10 thunderbolts II seen in the Gulf War and other encounters, the usefulness and need for a new ground attack aircraft could be seen. Because of the age of the A-10, a replacement for the aircraft could be used in a future scenario. The A-10 was built around the use of the GAU-8 30mm Gatling gun which was crucial to the effectiveness of the plane on the battlefield. Thus, the replacement would be built around a 35mm cannon to potentially have an increase in ground attack effectiveness.

The RFP released is in search of a viable replacement for the A-10 Close Air Support (CAS) aircraft for an entry into service date of 2025 that would have a higher effective and endurance. More specifically, the replacement should be able to carry more payload in weapon stores and be airborne for a longer period of time. Additionally, the plane would be able to provide similar or better protection as well as higher power than the A-10. Design considerations will also include addressing observability of the aircraft as well as lifetime and operation cost.

The following sections in this document discuss the design process utilized to approach the replacement for the A-10. These sections include calculations and reasoning that were used to develop an effective design first through statistics, and then through Class I and II design.

## 1.1 Mission Specification

Using the RFP provided by the AIAA for the 2017 – 2018 Individual Aircraft Design Competition seen in Reference 1, the mission specifications can be used to design a ground attack aircraft. All requirements used are for FAR 25 climb and military aircraft. Finally an objective function was to be optimized for the design seen in Equation 1 from Reference 1.

OF = [(Actual Range with 4 hrs AAO)/(500 nm)]$^2$ + [Actual Dash Speed/(300 KTAS)]$^2$ + [Actual Cruise Speed/(200 KTAS)]$^2$ + [\$40M /(Actual Fly-Away Cost)]$^2$ + [\$3000/hour /(Actual Direct Operating Cost)]$^2$ + [6,000 ft /(Fully Loaded Minimum Runway Length)]$^2$ + [(Max Positive Load Factor with 50% Internal Fuel, Gun, and Gun Ammo)/8]$^2$ + Observable (= 0 if missiles/sensor pod/ gun/fuel tanks are externally carried, 1 otherwise)

**Equation 1:** Objective Function

**Table I:** A-10 Replacement Mission Specifications and Requirements (Ref. 1)

| | |
|---|---|
| **GENERAL DESIGN REQUIREMENTS** | |
| Crew Members | 1 to 2 |
| Additional Considerations | 20 MIN of Fuel Reserves |
| **PERFORMANCE REQUIREMENTS** | |
| Range | 1,000 NAUTICAL MILES |
| Take-off Runway Length at MTOW | 6,000 FEET |
| Take-off Conditions (Altitude and Temp.) | 5,000 FEET at 20°F Increase |
| Min Cruise Speed | 200 Knots True Airspeed (KTAS) |
| Minimum Max Speed | 300 KTAS |
| Maximum Design Load Factor | 8 g |
| Service Celling Altitude | 45,000 FEET |
| **PAYLOAD REQUIREMENTS** | |
| Weapon | 1x 35mm Cannon |
| Payload | 750 Rounds and 14,000 $lb_f$ of Stores |
| **AIRBORN ARMED OVERWATCH REQUIREMENTS** | |
| Radius | 500 NAUTICAL MILES |
| Loiter Time | 4 hr. |
| **ADDITIONAL CONSIDERATIONS** | |
| Crew Member Weight | 200 $lb_f$ |
| **ENTRY INTO SERVICE** | 2025 |

## 1.2 Mission Profile, Performance, Payload-Range Requirements

The mission profile is a long and changing one, and will be difficult for a ground attack aircraft such as this one. This mission profile is derived from the RFP (Ref. 1) and Aircraft Design book 1 (Ref. 2). The aircraft will take off from a field at 5,000 ft and climb to cruise at 25,000 ft. The aircraft will then cruise at 300 kts to a position 500 mi away where it will loiter for approximately 4 hrs while commencing attack runs. Finally, the aircraft will return home with similar conditions. As well, using the mission specifications, a payload-range diagram can be drawn up for the worst case scenario from the criteria of the mission.

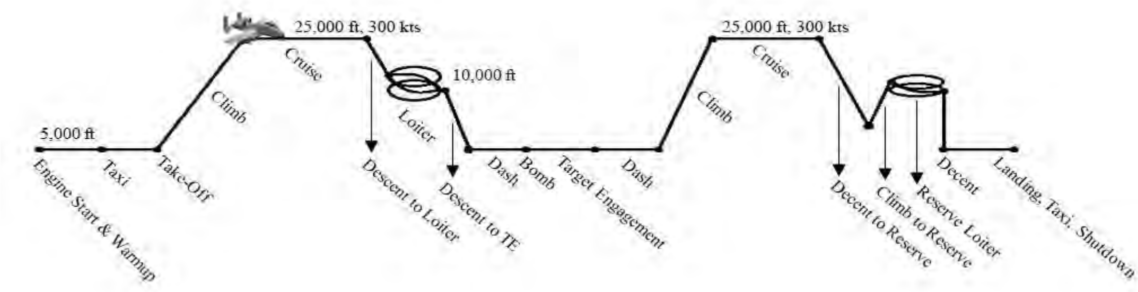


**Figure 1.1:** A-21 Mission Profile (Derived from Mission Specifications, Ref. 1)

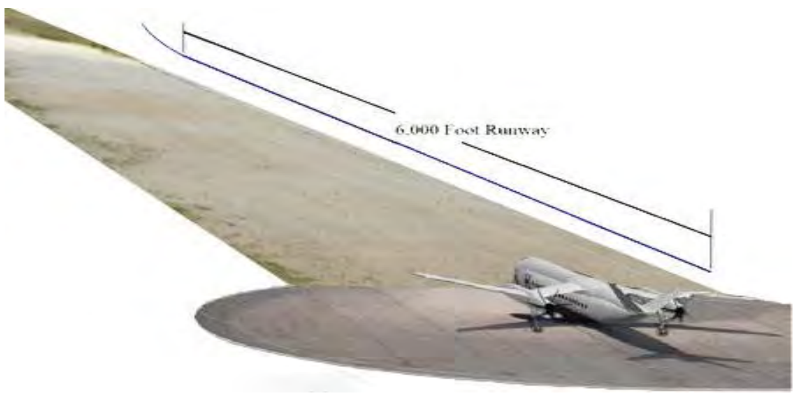


**Figure 1.2:** Field Length Requirements under Hot/High Conditions (Ref. 1)

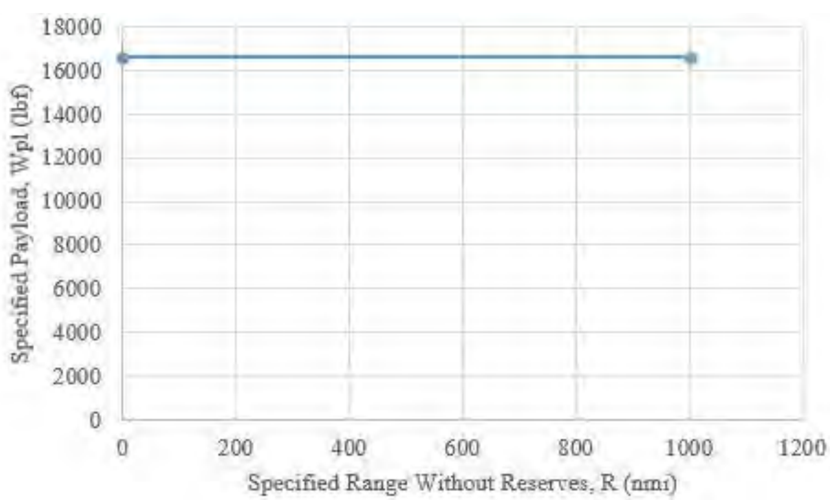


**Figure 1.3:** Required/Specified Payload-Range Performance for a Crew of 1 (Ref. 1)

## 1.3 Overall Design Methods and Process

For the design process, the general method used for the analysis was from Aircraft design series seen in Reference 2-9 by Dr. Jan Roskam. A well as Advanced Aircraft Analysis (AAA) software. For the assembly of this document, Adobe Photoshop was utilized to achieve quality images. Finally, Microsoft Excel was used in the preliminary design phase for calculations. The steps in approaching the design can be seen below.

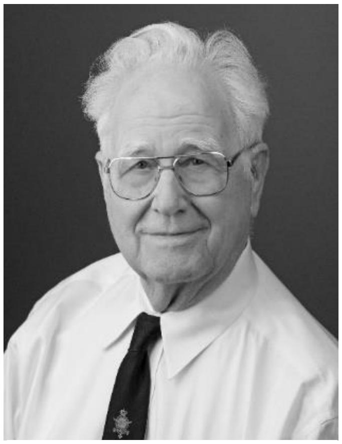

**Figure 1.4:** Dean E. Ackers Distinguished Professor Emeritus, Dr. Jan Roskam (Ref. 10)

1. Identification of the Mission Specification

Time will be used to find the exact mission for this ground attack aircraft to fulfill the criteria in the RFP.

2. Historical Overview & Completion

Many aircraft of similar purposes were found and studied. With the purpose of understanding the market to outperform the current standards.

3. Statistical Time and Market Predictive Engineering Design (STAMPED) Analysis

STAMPED analysis is used to evaluate the market to identify a preliminary design point from the large range of values. STAMPED will be discussed in more detail in a later sections.

4. Class I Designs

Class I design will be done on variety of configurations. For the preliminary calculations, a narrowing of the configurations based on the criteria provided is used to decide the final design.

5. Class II Design and Evaluation of the Final Design

By narrowing of the configurations to achieve the final design configuration, Class II calculations were done followed by the evaluation of the final configuration such as strategies on cost and manufacturing.

## 2 Historical Review & Competition in the Market

The use of a ground attack style of aircraft began in the First World War, for the use in supporting the ground troops on the battlefields. The creation of the attack aircraft class came out of the need for a style of aircraft similar to both bombers and fighter aircraft. This need was seen when the bomber class of aircraft would take fire from ground forces due to their slow speed. The idea for the new attack aircraft was to be able to survive ground-fire through speed and armored "bathtub" to protect the engine and crew. Germany became the first country to use an attack aircraft with their most recognizable being the Junkers J.I in 1917 (Ref. 11 & 12).

**Figure 2.1:** Junkers J.I (Ref. 13)

**Figure 2.2:** Bowing GA-1 (Ref. 16)

After World War One the popularity of the attack style of aircraft fell till the United States started research in the 1920s. During this time, Boeing built a twin-engine triplane called the GA-1, and the PG-1 was developed by Aeromarine that used a 37mm cannon. Through the United States Army Air Corps the "A" series designation was given to attack aircraft which first consisted of the Curtiss A-2 Falcon and the A-12 Shrike. Similar to the US, Germany was developing attack aircraft with their Heinkel He series in the 1930s. As well, many other countries such as Japan and Britain during this time began developing attack aircraft (Ref. 14 & 15).

During World War 2 the Germans used the Junkers Ju 87 attack aircraft which experienced success during the early years of the war (Ref. 17). The Allied forces first use of attack class craft came from the British with their Curtiss P-40 and Hurricane Mk IID which was very effective agents tanks (Ref. 19). Using a more old and simple design, the Soviets experienced success in their Polikarpov Po-2 which were converted from trainers into fighters (Ref. 20). During this time attack aircraft would carry an assortment of weapons such as cannons, bombs, and rockets. As the

**Figure 2.3:** Junkers Ju 87 (Ref. 18)

war continued more attack aircraft where experimented with and used such as the Focke-Wulf Fw 190 and the P-47 Thunderbolt which would be where the A-10 Thunderbolt II would get its name from (Ref. 22).

**Figure 2.5:** Hawker Typhoon (Ref. 21)

After World War 2 and during the production of jet propulsion aircraft, attack aircraft continued to use piston engines due to the fuel consumption problem jets had at this time. During the Korean and Vietnam Wars piston driven aircraft where used, such as the Hawker Sea Fury and Douglas A-1 Skyraider (Ref. 24). The A-1 Skyraider was one of the most influential and successful propeller driven ground attack aircraft at the time. The reluctance for jet propelled attack aircraft was sparse, but they saw use in the form of the "A" series US attack aircraft like the A-5 Vigilante, A-6 Intruder, and even the introduction of the A-10 Thunderbolt II.

**Figure 2.4:** P-47 Thunderbolt (Ref. 23)


**Figure 2.6:** A-1 Skyraider (Ref. 25)

In more recent history, ground attack aircraft have experimented with attack helicopters like the AH-64 Apaches (Ref. 26), but due to helicopters having slow deployment time and being vulnerability to small-arms fire the US is favoring ground attack aircraft over attack helicopters. In the 1960s, the US Air Force gave the role of a dedicated attack aircraft to the A-10 Thunderbolt II. The A-10 had experienced immense success in the Gulf War, Afghanistan, and Iraq War. This success caused the service life of the A-10 to be extended and the US interest in attack aircraft expanded.

The development of the A-10 Came from the need for the Air Force to find an effective attack aircraft to supplement for the F-4 and the F-111. During the development of the A-10 the market for the craft experienced competition in the form of AH-1 Cobra and AH-56 Cheyenne attack helicopters. In 1966 the US requested an attack

**Figure 2.7:** AH-64 Apache (Ref. 27)

**Figure 2.8:** A-10 Thunderbolt II (Ref. 29)

aircraft which was issued to 21 different defense contractors in the name of the A-X program. At the same time General Electric and Philco-Ford were asked to build the GAU-8 Gatling gun for the aircraft. A YA-10 prototype was chosen over its competition, the YA-9, for the contract and the production of the A-10 aircraft began. The A-10 Thunderbolt II first flew on 10 May 1972 (Ref. 28). Through the years the A-10 has been improved on with mostly computing upgrades seen in the advancement of the A-10B and A-10C.

**Table II:** Important Weights & Performance Characteristics of Attach Aircraft

| Aircraft | Weight | | | | Loading | | Ratios |
|---|---|---|---|---|---|---|---|
| Aircraft Model | Max TO Wt. (lbf) | Empty Wt. (lbf) | Max. Fuel Wt. (lbf) | Max. Useful Load (lbf) | Wing Loading | Power Loading | We/Wto |
| Chengdu J-10 | 41005 | 21495 | 9920 | 14550 | 115.086 | 0.751 | 0.524 |
| Dassault Rafale | 54000 | 21715 | 26456 | 32085 | 109.800 | 1.600 | 0.402 |
| Eurofighter Typhoon | 51808 | 24581 | 9920 | 16534 | 84.020 | 1.100 | 0.474 |
| F-16 Fighting Falcon | 48000 | 20868 | 10072 | 21241 | 160.000 | 0.611 | 0.435 |
| F/A-18 Super Hornet | 66600 | 32082 | 16272 | 8029 | 132.000 | 1.500 | 0.482 |
| F-35 Lightning II | 70,000 | 29,300 | 18,250 | 40,700 | 152.170 | 0.614 | 0.419 |
| HAL Tejas | 29762 | 14462 | 6199 | 7165 | 37.985 | 1.180 | 0.486 |
| JF-17 | 29762 | 14134 | 5130 | 10141 | 106.600 | 1.500 | 0.475 |
| JH-7 | 62776 | 31900 | 14418 | 14330 | 111.520 | 1.530 | 0.508 |
| KAI T-50 Golden Eagle | 27300 | 14600 | 4895 | 10500 | 116.470 | 1.500 | 0.535 |
| MiG-29 | 54013 | 24030 | | | 119.471 | 0.735 | 0.445 |
| Sukhoi Su-25 | 38800 | 21605 | | | 106.970 | 1.950 | 0.557 |
| Sukhoi Su-27 | 50706 | 36111 | 20723 | | 108.940 | 1.300 | 0.712 |
| Sukhoi Su-30 | 85539 | 39021 | 21252 | 17636 | 128.710 | 0.644 | 0.456 |
| Sukhoi Su-32/34 | 97797 | 49608 | 30553 | 17636 | 146.534 | 0.609 | 0.507 |
| Saab JAS 39 Gripen | 36376 | 17,636 | 15440 | 3300 | 112.619 | 0.498 | 0.485 |
| MiG-29 | 49383 | 24030 | 11552 | 9920 | 109.230 | 0.804 | 0.487 |
| Mitsubishi F-2 | 29672 | 21003 | | | 129.910 | 1.600 | 0.708 |
| F-22 | 60000 | 31670 | | | 71.430 | 0.860 | 0.528 |
| IAR 99 | 12258 | 7055 | 2425 | 2778 | 60.860 | 3.060 | 0.576 |
| Saab JAS 39 Gripen | 30,864 | 15,652 | 11,030 | 4182 | 95.554 | 0.586 | 0.507 |
| Mirage 2000 | 37480 | 16755 | 9039 | 13890 | 84.920 | 1.750 | 0.447 |
| Mitsubishi F-2 | 29672 | 21003 | | | 129.910 | 1.600 | 0.708 |
| BAE Hawk 200 | 20061 | 9810 | 3000 | 7251 | 111.700 | 3.430 | 0.489 |
| Aermacchi MB-339 | 14000 | 7363 | 3153 | 3484 | 67.390 | 3.500 | 0.526 |
| Aero L-159 | 17636 | 9590 | 3571 | 5952 | 87.150 | 2.800 | 0.544 |
| AMX | 28660 | 15432 | 5997 | 8377 | 126.790 | 2.600 | 0.538 |
| F-15 Eagle | 81000 | 32000 | 34420 | 24500 | 133.220 | 1.730 | 0.395 |

# 3 Design Vector & Weights Establishment

For the preliminary design of the aircraft, before a design can be started and expanded upon, it is imperative to determine what RFP is looking for. This will often be given in the form of criteria from a company or agency sponsoring the individual design. In the case of this attack aircraft, the AIAA has left little guidance as to the design vector conditions which are to be prioritized over others and how each should be weighted. It is important to determine which design variables are the most important. By conducting this, it becomes possible to determine what variables most influence the design of the aircraft and therefore the selection of the optimum arrangement.

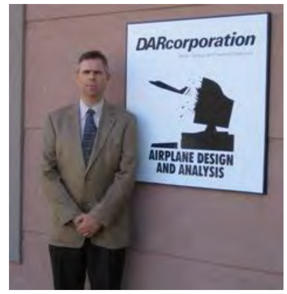


**Figure 3.2:** Dr. Willem Anemaat President of DAR Corporation (Ref. 30)

**Figure 3.1:** Colonel Roger Disrud and the Author

## 3.1 Selection of Design Vector Components

To establish the design vector, two of the top aerospace designers was consulted. As well, a top A-10 operator and ground army officer. Dr. Willem Anemaat, Colonel Roger Disrud, and 1SG Karl Utter were asked about the relative importance of each variable on the design of the aircraft. Similarly, Major Adrian Lewis contributed to the weightings. Table III shows the complete list of variables for the design vector chosen before industry professionals were consulted. It is known that many of the variables are tied together and may hinder one another.

**Figure 3.3:** Major Adrian Lewis, University of Kansas Professor (Ref. 31)

**Figure 3.4:** Karl Utter, Retired Aviation 1SG

**Table III:** Principal Design Vector Prior to Consulting

| | Variable Type | Optimization Direction | Suitable For Weighting By Experts and User |
|---|---|---|---|
| Crew Members | Binary | Minimize | NO |
| Payload | Binary | Must Meet Spec. | NO |
| Range at Given Payload | Gradient | Must Meet | YES |
| Dash Speed | Gradient | Maximize | YES |
| Cruise Speed | Gradient | Maximize | YES |
| Acquisition Coast | Gradient | Minimize | YES |
| Life Cycle Coast | Gradient | Minimize | YES |
| Balance Field Length | Gradient | Must Meet Spec. | YES |
| Max Load Factor | Gradient | Must Meet Spec. | YES |
| Observables (0 = External, 1 = Internal) | Binary | Maximize | YES |

## 3.2 Experts and Operators for Weights Determination

A pilot of ground attack aircraft and two industry expert were consulted to determine the weightings for each item on the list below, shown in Table IV. The individuals who participated include (Ref. 32 &33):

Dr. Willem Anemaat, DAR Corporation, Kansas

1SG Karl Utter, Retired Aviation 1SG

Colonel Roger Disrud, A-10 Top-Gun Pilot

Professor and Major Adrian Lewis, University of Kansas, Kansas

## 3.3 Weighting Survey and Results

The three people that were surveyed had were averaged and arranged. All participants were personally interviewed. The experts recommend to comply with most of the RFP requirements, but some of the variables were not as important or did not seem realistic. Colonel Disrud found that as a pilot the four hours of airborne armed overwatch was "ridiculous" and the operators would not have enough ordinance for a mission of that length (Ref. 32). Similarly, the price factor for the aircraft seemed to be less important due to the military aspect of the aircraft. Major Adrian Lewis said for the future of the aircraft may want to be A.I. controlled and put a higher emphasis on stealth (Ref. 33). For the most part most of the people found that all of the variables should be met to the best ability.

**Table IV:** Averaged Weights of Design Variables from Survey of Experts & Operators (Ref. 32 & 33)

| | Variable Type | Optimization Direction | Weighted Percentage |
|---|---|---|---|
| Range at Given Payload | Gradient | Must Meet | 13% |
| Dash Speed | Gradient | Maximize | 15% |
| Cruise Speed | Gradient | Maximize | 15% |
| Acquisition Coast | Gradient | Minimize | 7% |
| Life Cycle Coast | Gradient | Minimize | 7% |
| Balance Field Length | Gradient | Must Meet Spec. | 20% |
| Max Load Factor | Gradient | Must Meet Spec. | 17% |
| Observables (0 = External, 1 = Internal) | Binary | Maximize | 6.67% |
| | | **Total:** | 100% |

# 4 Statistical Time and Market Predictive Engineering Design (STAMPED) Analysis Techniques

For the initial sizing process to be completed, a technique used by many engineering firms in many different industries is used. This technique is used by highly advanced design teams and product development groups. This method is utilized in airlines to military sectors, but not much is found in the open, as most of it is proprietary or classified. The Statistical Time and Market Predictive Engineering Design (STAMPED) Analysis Techniques can be used to find engineering variables throughout time as the variables vary as a function of the market share or military mission of a given product (Ref. 34). This chapter explains the basis for the vector analysis by laying out the method used for the design of this aircraft. This details how STAMPED analysis is used for the preliminary design of aircraft. Figure 4.1 shows an example a design parameter for power loading as a function of the shares it achieved in the market. All information was received from Reference 34.

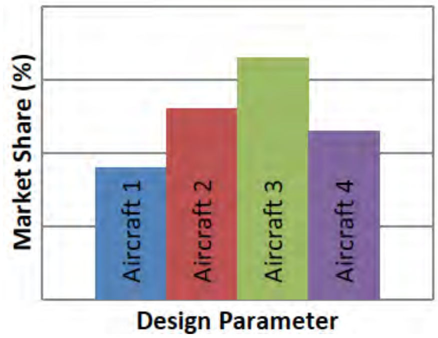


**Figure 4.1:** Example of Design Parameter Distribution on Market Share (Ref. 34)

Using the STAMPED analysis technique allows engineers to predict and track a design vector of engineering variable at any point in time. This technique can be utilized for anywhere from strength-to-weight ratio of a material to empty-to-takeoff weight ratio of the entire aircraft, the method can be used for any part of the aircraft that needs to be tracked. When considering an aircraft design problem, which can be seen in Figure 4.2, the first flight data can be considered a point of reference. With the data the aircraft can be taken threw its life cycle starting with its design data prediction. Using the aircraft type, the schedule of the entire market can be drawn up using different types and manufactures of aircraft. The design variables can be extrapolated as the market is matured as more aircraft of the same type are used.

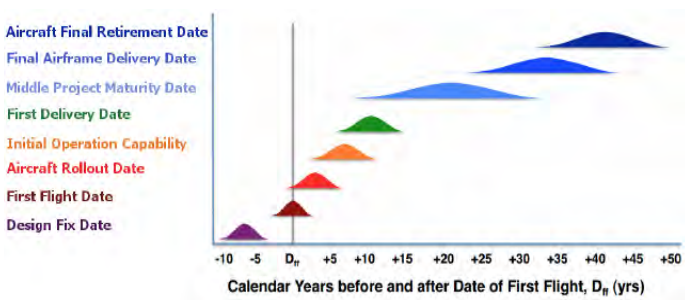


**Figure 4.2:** Example of Typical Major Aircraft Program Events WRT Date of First Flight, Dff (Ref. 34)

# 5 Wing Sizing

Threw the mission specification and profile provided, the weight sizing of the aircraft was performed using STAMPED analysis to make predictions of variables to achieve market dominance.

## 5.1 Empty-to-Takeoff Weight Ratio Determination

Examining relevant data of an assortment of ground attack aircraft that have been bot and sold throughout the years provides useful data to predict the design weight. The most recent empty-to-takeoff weight ratios for the planes examined can be seen in Figure 5.1. Data of the empty-to-takeoff weight ratios can be weighted with the sails numbers to determine the average weight ratio each year. This data can be taken and extrapolated to the entry into service date of 2025, seen in Fig. 5.2. The A-10 thunderbolt II has an empty to take-off weight of 0.57 as reference. For the preliminary design of the aircraft, the line of market domination can be followed to determine the empty-to-takeoff weight ratio of 50% with the STAMPED data this was about 50% aggressive. The value chosen corresponds to predicted value of the maximum market domination by the entry into service date of 2025.

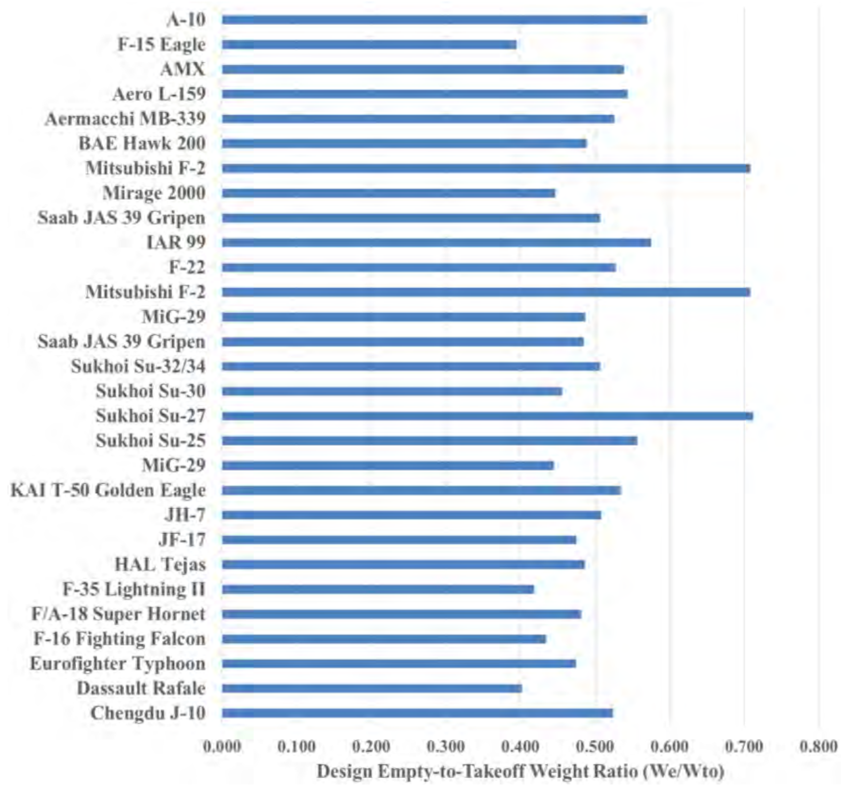


**Figure 5.1:** Empty-to-Takeoff Weight Ratio of Ground Attack Aircraft Considered for STAMPED Analysis

## 5.2 Determination of Preliminary Design Weights

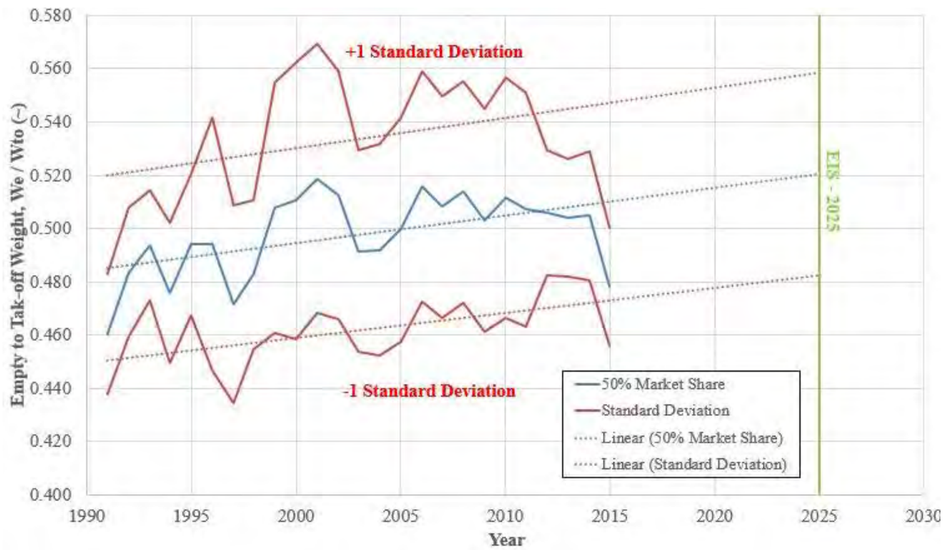


**Figure 5.2:** STAMPED Empty-to-Takeoff Weight Ratio over Each Year

Through using STAMPED analysis of jet fighter ground attack aircraft, the takeoff weight of the aircraft designed can be determined. From Airplane Design Part I: Preliminary Sizing of Airplanes (Ref. 2) the aspect ratio used is 5.34. The aspect ratio was chosen due to the role of a ground attack aircraft being between a fighter and a bomber. This was also taken into consideration when estimating the lift to drag ratios. The assumptions made resulted in the following weights for the preliminary design for the aircraft, shown in Table V.

**Table V:** Ground Attack Aircraft Weights

| Aircraft Weights | |
|---|---|
| Take-off Weight (lbf) | 77,800 |
| Empty Weight (lbf) | 38,122 |
| Fuel Weight (lbf) | 22,639 |

# 6 Wing and Powerplant Sizing

In this chapter, the methods and analysis performed to create the Performance Sizing Chart are presented. This chart will be used to create and predict the design of the ground attack aircraft using the design point chosen on the chart.

For the creation of the sizing chart is done through the use of the RFP and the FAA regulations. The conditions for performance include the take-off, landing, climb, and an instantaneous maneuver. The method followed for the performance sizing chart is seen in Chapter 3 of Ref. 2. Calculations for the sizing lines are shown in Appendix A.

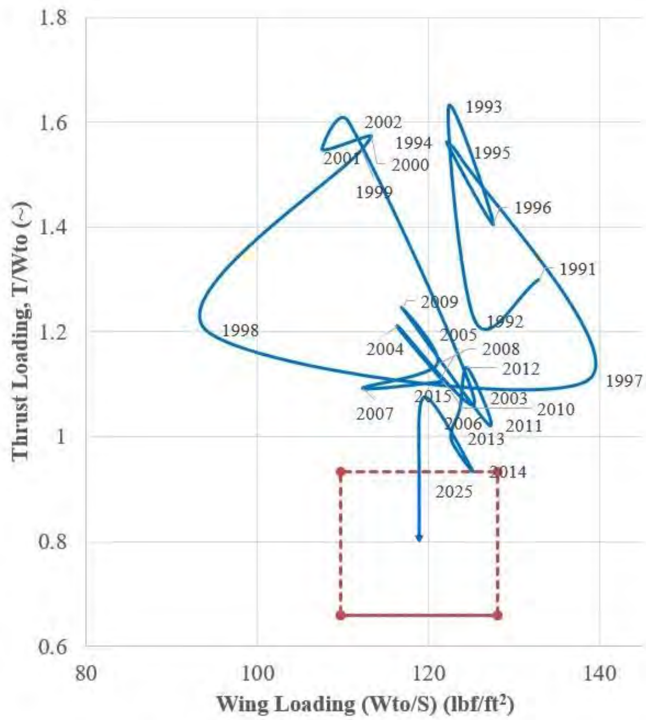


**Figure 6.1:** STAMPED Wing and Power Loading for fighters and multi-role fighter Market over Time

## 6.1 Discussion of Performance Constraints

The sizing of the aircraft is done on the sizing chart where the performance requirements are plotted for the take-off, landing, climb, and instantaneous maneuver. Once the performance sizing chart is made and plotted a design point is chosen which gives the preliminary wing loading and thrust to weight loading.

For the Performance and sizing of the ground attack aircraft for the time some values had to be inferred or estimated using graphs and charts. The initial sizing was done using methods in *Airplane Design Part I* Reference 2. The aspect ratio chosen was 5.34, and the zero lift drag coefficient and density would be 0.02 and 0.00197 slugs/ft$^3$ respectively. Due to the unpaved runways this craft would be stations on the friction coefficient was chosen to be 0.1 as per Reference 2. Drag polars for the external stores for each condition are shown in Table VI.

**Table VI:** Drag Polars for External Stores

| Flight Condition | Drag Polar |
|---|---|
| Cruise, Gears Up | $0.040 + 0.072CL^2$ |
| Cruise, Gears Down | $0.060 + 0.072CL^2$ |
| Take-Off, Gears Up | $0.055 + 0.077CL^2$ |
| Take-Off, Gears Down | $0.075 + 0.077CL^2$ |
| Landing, Gears Up | $0.105 + 0.082CL^2$ |
| Landing, Gears Down | $0.125 + 0.082CL^2$ |

The Climb Requirements where set from the FAR 25 certifications, which could be seen in Reference 2. Contains explanations of each of the FAR 25 climb requirements. Each of the requirements has a different climb gradient requirement (CGR) for five different one engine inoperable (OEI) situations and one all engines operable (AEO). All values used for CGR can be found in Reference 2. All calculations for the performance chart are shown 6.2 can be seen in Appendix A.

## 6.2 Sizing Chart Analysis

Through interpreting Figures 6.1 and 6.2, the STAMPED data collected and examined could logically be ignored. This is due to most of the attack aircraft examined were also in the range of fighters. Viewing the A-10 on the graph shows that the STAMPED data collected is not near the aircraft to be replaced. Due to the success of the A-10 a design point was chosen between the STAMPED data and the A-10.

**Table VII:** Design Point Values

| | |
|---|---|
| **Wing Loading, W/S (lbf/ft$^2$)** | 96.9 |
| **Thrust Loading, T/W (~)** | 0.42 |
| | |
| **Wing Area, S (ft$^2$)** | 803 |
| **Total Takeoff Thrust (lbf)** | 32676 |
| | |
| **CL Max, Clean** | 1.60 |
| **CL Max, Landing** | 1.84 |
| **CL Max, TO** | 1.76 |

Following the design point leads to values that could achieve the goal of an entry into service data of 2025 and be competitive in the market at that time.

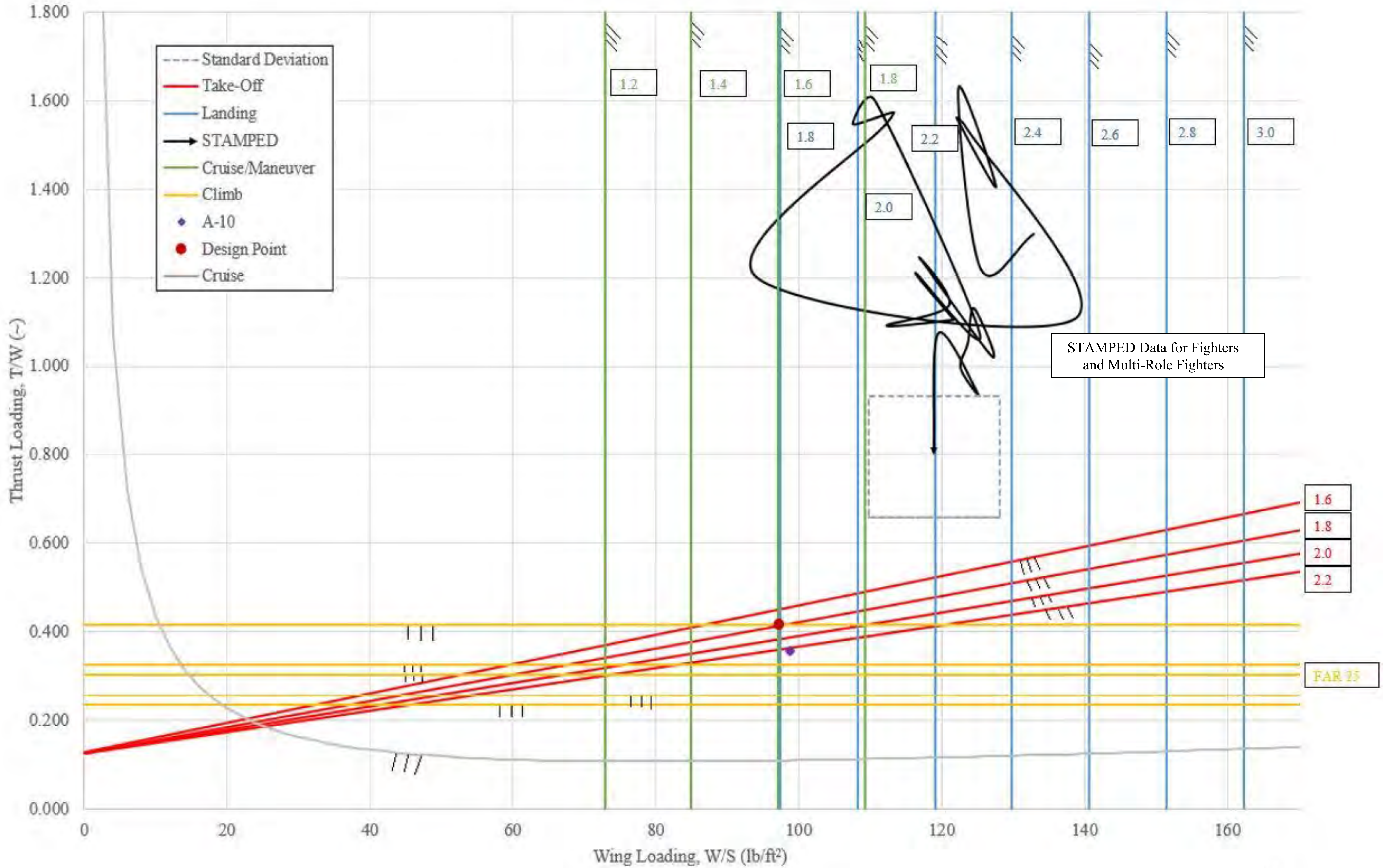

**Figure 6.2:** Sizing Constraints and STAMPED Design Point

# 7 Class I Configuration Matrix and Initial Downselection

The primary objective of this section is to describe the process for selecting the configuration chosen for the replacement of the A-10.

## 7.1 Impact of Design Factors

Many factors were considered in the initial configurations for the design of the A-21. The major factors that went into the configurations were: long range and loiter time, large payload and gun, load factor, and the protection of the pilot. Additionally, cost was taken into consideration for the overall design. The primary focus was on the ability to fulfill the long range and loiter time requirement. In addition, it was important to consider the gas exhaust created from the cannon, because of the impact on the engines.

## 7.2 Comparative Study of Airplanes with Similar Performance

Aircraft of similar mission specifications were reviewed and studied. Initial studies included attack and fighter aircraft sold and used in the path, which inevitably included the A-10 Thunderbolt II. Further investigations into similar aircraft showed that due to the long range and loiter time compared to the attack aircraft used in the past, bombers and cargo aircraft would be good sources of study.

The attack aircraft studied for their configurations are the A-10 Thunderbolt II, A-6 Intruder, and Sukhoi Su-25. These aircraft where chosen for their similar payloads and mission objectives. For aircraft with similar ranges and loiter times, bombers like the B-1 Lancer, B-2 Spirit, and cargo aircraft like the C-130 Hercules were studied. The attack aircraft studied do not have the required loiter time, and bombers and cargo aircraft studied do not have the speed or maneuverability to meet the RFP. Fighters similar to the F-35 Lightning and Eurofighter Typhoon were examined, which would not be able to meet the loiter time due to the specific fuel consumption of their engines. Information on aircraft studied for STAMPED analysis are shown in Table II.

The Su-25, A-6, and A-10 would be able to complete the given mission if not for their insufficient loiter time. Due to their ability to complete a similar mission, their configurations will be taken into account and improved upon. Improvements can be made to their weaknesses such as gun gas ingestion, low thrust to weight, and other factors. Most of the aircraft studied are multi-roll fighters which are more complex and would not suit the mission directive as well as the attack aircraft.

### 7.3 Configuration Sweep and Selection

Through the methods outlined in *Airplane Design Part II* (Ref 3), the concepts created based on research done can be compared and contrasted to find the best configuration for the A-21.

#### 7.3.1 Concept of Operations

For the concepts of this ground attack aircraft, the configuration that would be chosen had to fulfill all the specifications (Fig. 7.1). The aircraft would have an array of systems onboard to supply information on the battlefield where it would be operating. These systems include: the functionality of observations, detection of enemy combatants, and the ability to provide targeting imagery of enemy positons for strikes by other supporting aircraft. This aircraft will have the ability to provide four hours of airborne armed overmatch in a 500 nm radius around the base it would be stationed. Operating from unpaved runways, the aircraft will provide bombing and strafing runs with its 14,000 lbs. of stores and 35mm cannon. The conditions the aircraft would operate under puts the pilot at risk of enemy fire, so space has been provided to accommodate a titanium bathtub to surround the pilot for protection.

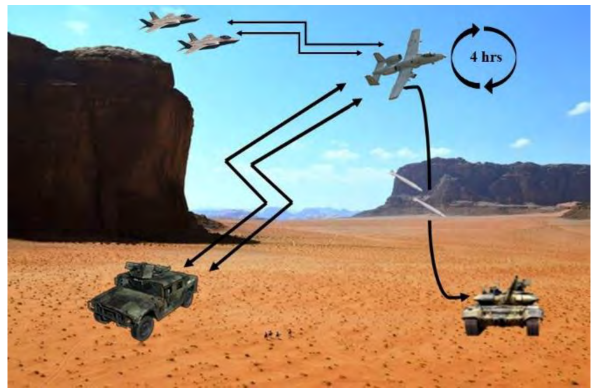


**Figure 7.1:** Concept of Operations

#### 7.3.2 Selection of the Overall Configuration

Using *Airplane Design Part II* (Ref 3), *Section 3.2* outlines 12 different categories of aircraft. A ground attack aircraft similar to the A-10 does not fall specifically into one of categories provided, but instead falls between two of them as it would fulfill similar rolls to that of a fighter and a bomber aircraft.

For a comparison of aircraft studied for their configuration, see Section 7.2. Historical information on similar aircraft used in the past and data on aircraft studied for STAMPED analysis are shown in Section 2.

Creation of the CAD models used in the configuration selection process was done using OpenVSP. Throughout the down selection process, many configurations for the aircraft were eliminated due to being a "show stopper" or having qualities that may not suit the mission objective. During the process of deciding on a configuration to base the design, many factors were researched and considered. These factors included gun gas ingestion of the engines, maneuverability, and many other factors. Most of the designs that were ruled out were due to major gun gas ingestion, maneuverability problems, or logical design problem. The three configurations chosen to be viable could be built in a way to avoid major design problems in supplementary design sections. The down selection matrix are shown in Figure 7.2. The aircraft chosen is due to the advantage of the gun gas ingestion and ability to complete the mission spec. Due to the time available, not all viable options could be flown against each other. A Forthcoming section will outline the design of the tail.

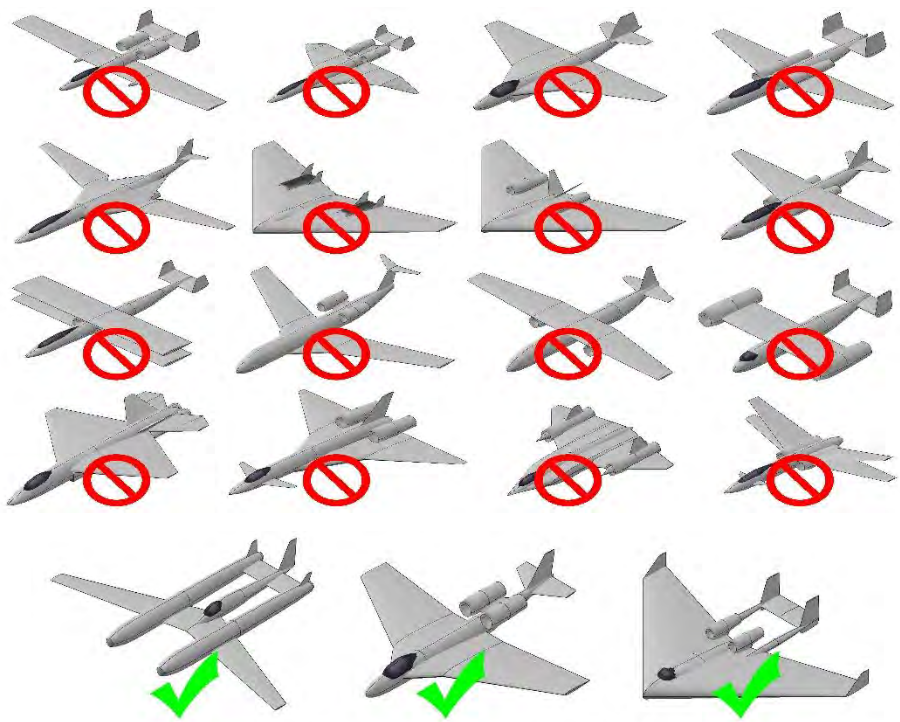

**Figure 7.2:** Configuration Down selection Matrix

## 7.4 Configuration Summary and Recommendations

The major findings in this chapter are the chosen configuration for the A-21, which is shown in Figure 7.3. This configuration was selected for the resistance it would have to gun gas ingestion of the engines. In addition, this choice will yield a good center of gravity placement and gives efficient space for the fuel, gun, and payload required by the RFP.

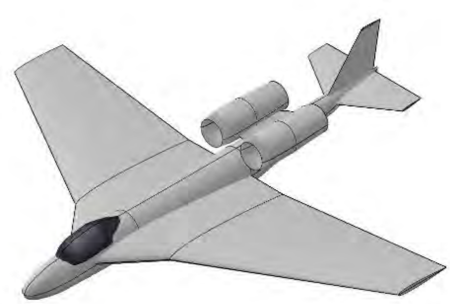

**Figure 7.3:** Configuration for the A-21 Valkyrie II

This author recommends for the configuration chosen, to move the horizontal tail to prevent exhaust gas of the engine from coming in contact with it, and moving of the wing to provide increased stability.

# 8 Layout of the Cockpit and the Fuselage

The purpose for this section is to display the preliminary Class I design process for the cockpit layout and fuselage of the A-21 Valkyrie II with the integration of components throughout. The methodology used is from *Airplane Design Part II*, Reference 3.

## 8.1 Layout Design of the Cockpit

Minimal space is used for the cockpit due to the military nature of the A-21. There is console space in the front and on either side of the pilot. Any extra information can be displayed on the canopy or in the helmet. Ample room is given for the head of the pilot to account for glass and helmet space. The sizing of the cockpit can accommodate up to a 95$^{th}$ percentile male. Space near the pilot is provided to account for the avionics and targeting systems. Additionally, there is space allowance for a titanium bathtub below the pilot to serve as protection from enemy fire. As per FAR 25, the pilot has more than 15 degrees of vision. A dimensioned three view of the cockpit is shown in Figure 8.1. A visibility chart for the pilot, with respect to his left eye is provided in Figure 8.2.

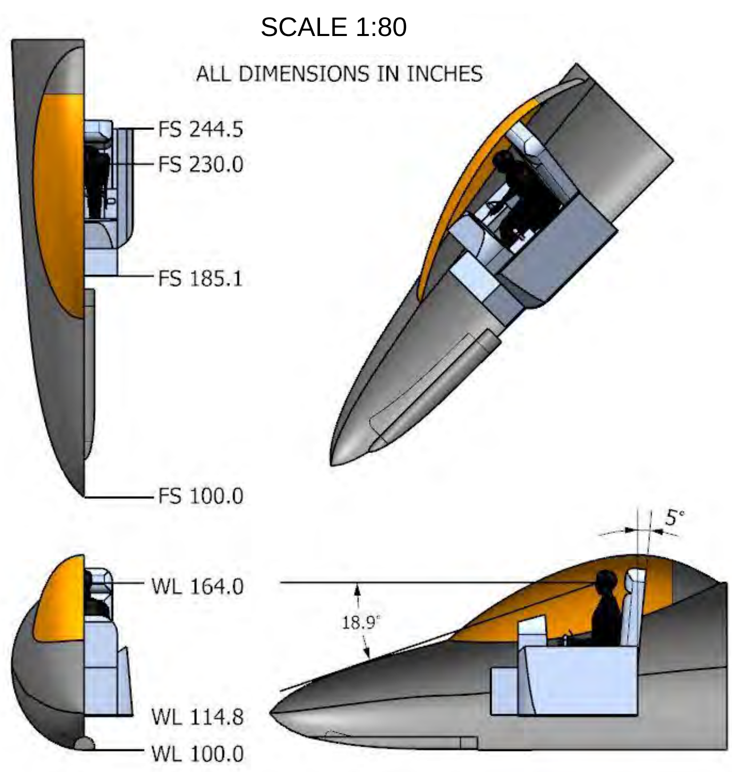


**Figure 8.1:** Cockpit of the A-21

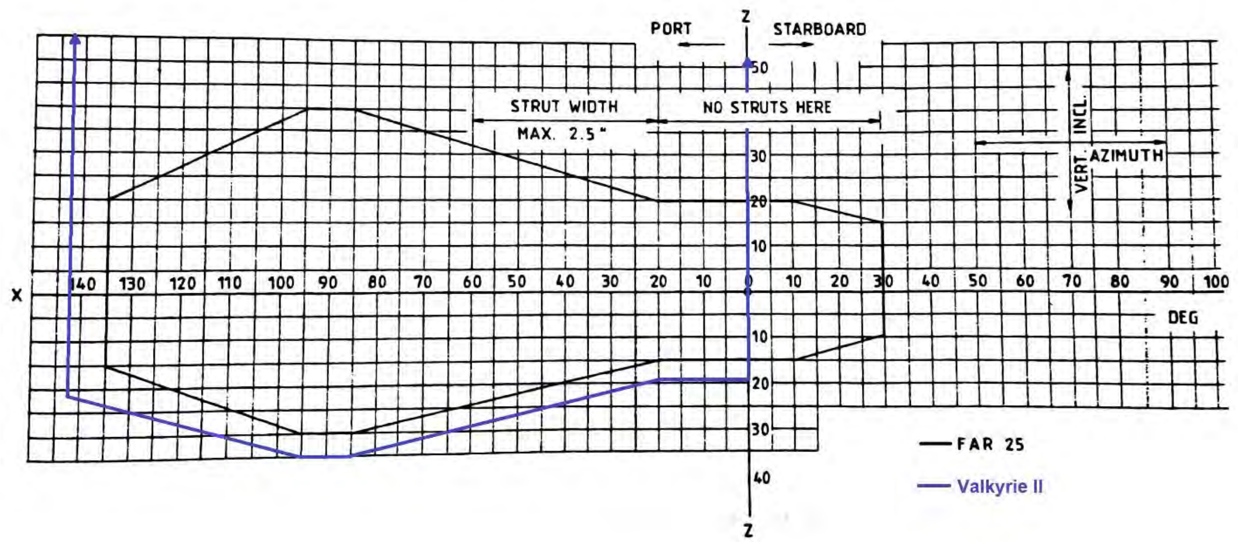


**Figure 8.2:** Visibility Chart of the A-21 Valkyrie II

## 8.2 <u>Layout Design of the Fuselage</u>

Initial Class I design of the fuselage is done by wrapping it around the components that need to be internally stored. The fuselage stores the cockpit, Bushmaster III, 35mm ammo, and internal Mark 82 stores. A notch is cut in the fuselage around the gun in an attempt to reduce gun gas ingestion into the engine. The area around the gun will have to be reinforced with a quarter inch thick stainless steel sheet to protect the aircraft from the impact damage from the shock waves created by the gun. Spacing has been provided for 2-2.5 inches ring frame for structure. The fuselage is done in an attempt to minimize wetted area for future design of the stability and controls of the A-21. A layout and dimensioned tree view of the fuselage layout are shown in Figure 8.3.

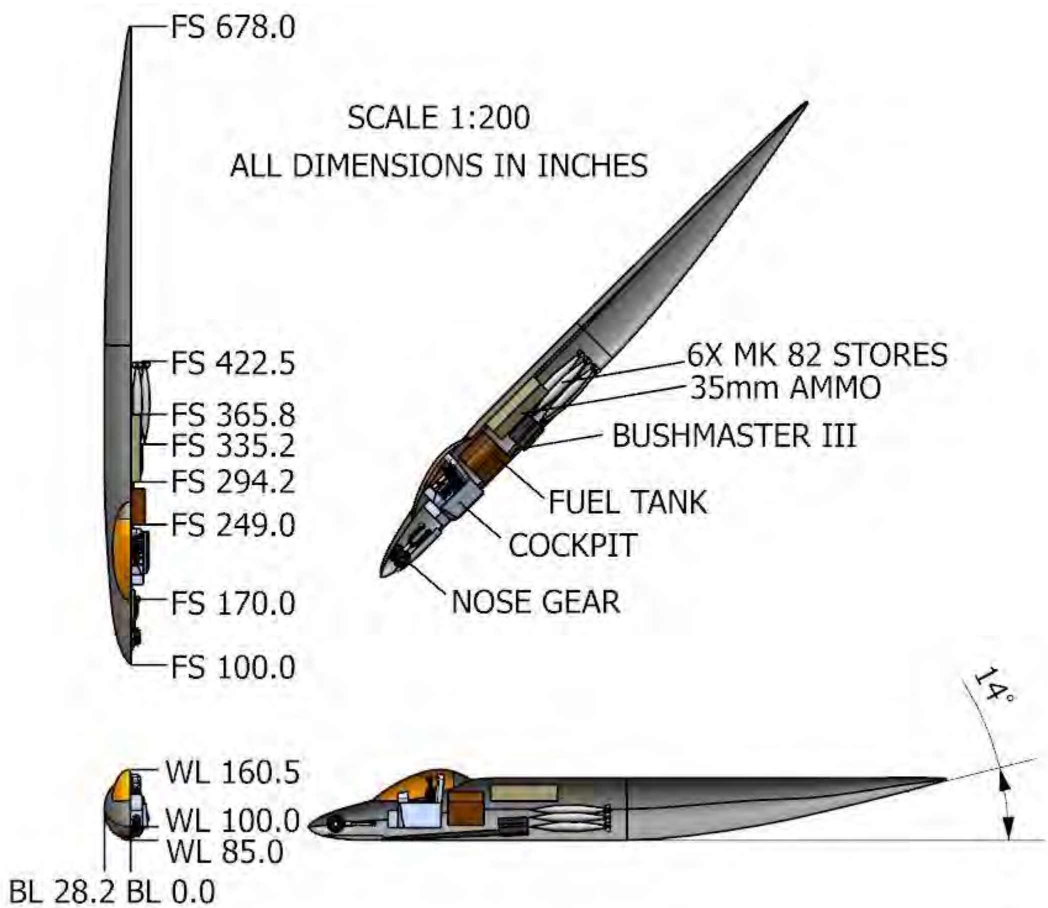


**Figure 8.3:** Fuselage Layout of the A-21

## 8.3 Cockpit and Fuselage Summary and Recommendations

Cockpit design is minimal and provides essential parts to achieve the mission objective. Ample room is left near the cockpit to store computing parts and protection for the pilot. The fuselage stores the essential weaponry for the specified mission and provides room for internal structure. The major findings of this chapter are shown below

i. Fuselage length: 56.5 ft;
ii. Maximum fuselage height: 5.5 ft;
iii. Maximum fuselage width: 4.7 ft;
iv. The cockpit visibility is greater than the FAR 25 requirements.

Changes to the cockpit could be made to downsize the canopy due to the excess vision available, lowering needed structure. The fuselage could be tighter around the internal objects to ensure excess materials are not used and to decrease cost.

# 9 Layout Design of the Propulsion Installation

This section has the purpose of describing and portraying the methodology for choosing the engine and installation of said engine. The methodology used in from *Airplane Design Part II* (Ref 3).

## 9.1 Selection and Layout of the Propulsion Installation

For the selection of the type of engine to be used on the A-21, many factors where considered. Some of these factors were the cruise speed, maximum speed, required range, loiter time, and the noise output (for a stealth option). Due to the cruise and maximum speed requirements in the RFP, a jet engine was selected for a preliminary concept. Further studying and calculations of the range and loiter times required by the mission specifications drove the size of the aircraft. An efficient engine had to be selected to reduce the weight. The use of an efficient engine would decrease the weight of the fuel. Thus, a turbofan jet engine was chosen.

Through studying aircraft with similar mission specifications, the number of engines needed could be determined. A two engine jet propelled ground attack aircraft was most commonly found. By choosing two engines, the center of gravity would not be displaced to far aft on the aircraft. For these reasons, two engines would be used. With the number and type of engine chosen and using the design point that was picked to be 0.42 thrust to maximum take-off weight, a thrust of 16,338 lbf per engine could be determined. The candidate engine that would meet the requirements of thrust and efficiency is the PW 1200G (Ref. 35); which has a maximum thrust of 17,000 lbf, and a specific fuel consumption of 0.35 lbm/lbf hr.

In the mid-wing configuration and as seen from the studies done in Section 2 and 7, aircraft of similar configuration and mission specification have their engines mounted to the fuselage. Similarly, the engines are mounted behind the wing, and high to avoid the gas exhaust produced by the gun. The engine will be connected to the fuselage with pylons. Figure 9.1 shows a three view of the engines on the fuselage with dimensions.

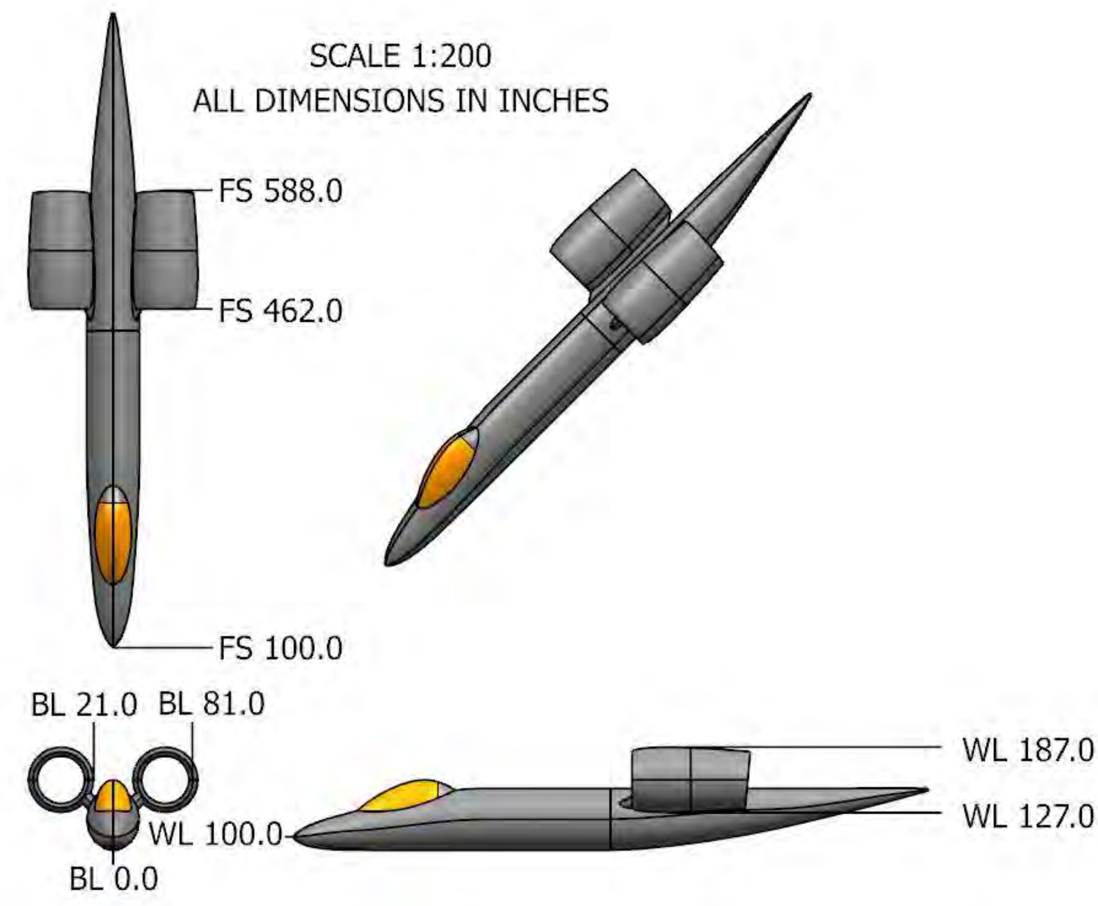


**Figure 9.1:** Turbofan engines on the A-21

## 9.2 Propulsion System Summary and Recommendations

The propulsion system major findings are the choosing of a PW 1200G, which is a turbofan jet engine. The engine chosen produces a maximum thrust of 17,000 lbf while the A-21 needs a thrust from each engine of 16,338 lbf. Pylons are used to mount the engines on the fuselage. Furthermore, the engines are placed high and away from the nose to prevent ingestion of the gun gasses. The engine has a diameter of 56 in and a length of 100 in.

This author recommends:

i) Further integration of the engine may require a small tow-up angle, or to move the engine vertically to avoided exhaust gasses on the horizontal tail;

ii) The engine could be moved horizontally aft to insure ease of axis and avoid collision on the wing during maintenance.

# 10 Class I Layout of the Wing

The directive of this section is to provide a layout of the sizing for wing planform design as per the configuration chosen in the Section 7. The procedure used in from *Airplane Design Part II* (Ref 3).

## 10.1 Wing Design Layout

For the design of the wing planform on the A-21, a cantilever mid-wing is used. This configuration for the wing provides low interference drag and moderate lateral stability. Due to the lateral placement of the wings, the mid-wing design does not prevent visibility from the cockpit. The type of wing used is a two planform section wing. The selection of a NASA MS airfoil provides advantage to its NACA series counterpart due to the lift needed. Spars are placed in the wing 10% of the chord from the leading edge and 0.5% of the chord away from the flaps and ailerons. The amount of fuel needed for the mission specification is 3310 gallons where the volume of the wing is 3830 U.S. gallons. Thus, all the fuel needed can be stored in the wings. The Torenbeek equation was used, however due to it not factoring in flaps or dry bays, it is not valid in this situation. All calculations for fuel can be seen in Appendix B. A diagram with dimensions is shown in Figure 10.1.

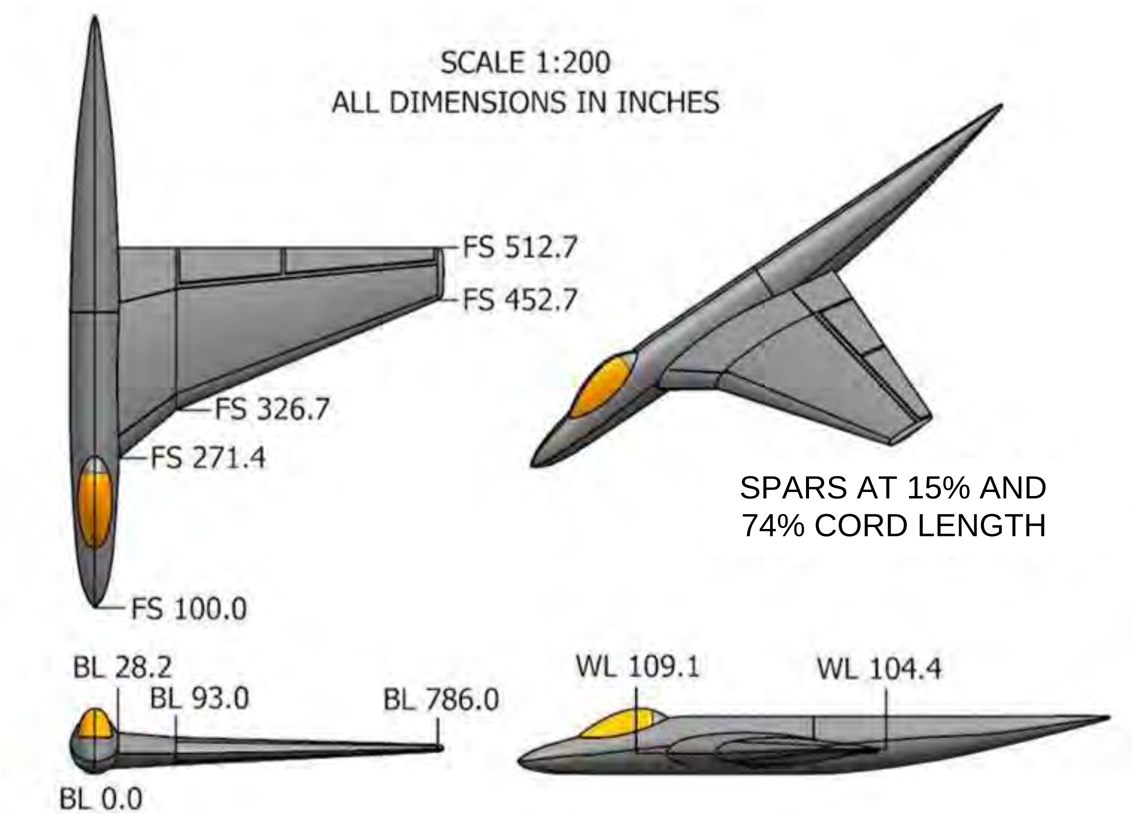


**Figure 10.1:** Wing Layout of the A-21

## 10.2 Wing Planform Summary and Recommendations

The cantilever mid-two planform cranked wing is a design that provides advantages for the conditions the aircraft would experience. Additionally, the size and volume of the wing chosen provides ample room for the storage of fuel, and provides plenty of space under the wing for weapon stores. Values and airfoils used for the wing designed are shown in Table VIII.

This author recommends that a beneficial improvement to the wing would be to add an incidence angle to the wing. This would further increase the aircraft's take-off capabilities and allow for a nose down approach during strafing runs without the loss of significant altitude.

**Table VIII:** Wing Dimensions for the A-21

| Total Wing | |
|---|---|
| b (ft) | 65.5 |
| S ($ft^2$) | 803.1 |
| A | 5.34 |
| **Root Wing Section** | |
| b (ft) | 15.5 |
| $c_r$ (ft) | 22 |
| $c_t$ (ft) | 15.5 |
| dihedral | 0 |
| i (deg.) | 0 |
| twist (deg.) | 0 |
| Airfoil | NASA MS(1)-317 |
| **Tip Wing Section** | |
| b (ft) | 50 |
| $c_r$ (ft) | 15.5 |
| $c_t$ (ft) | 5 |
| dihedral | 1 |
| i (deg.) | 0 |
| twist (deg.) | 0 |
| Airfoil | NASA MS(1)-313 |

# 11 Class I Design of the High Lift Devices

The purpose of the following section is to show the methodology for the sizing of the high lift devices for the take-off and landing conditions using *Airplane Design Part II* (Ref. 3). The preliminary sizing of the ailerons is included.

## 11.1 Design of High Lift Devices

Sizing of the high lift devices was performed using AAA (Advanced Aircraft Analysis). Calculations in AAA were utilized due to the cranked wing design used. This was done to compute the equivalent area of a single planform wing. Geometry inputs of the wing are shown in Figure 11.1 and the geometry of the single planform wing calculated in AAA are shown in Figure 11.2.

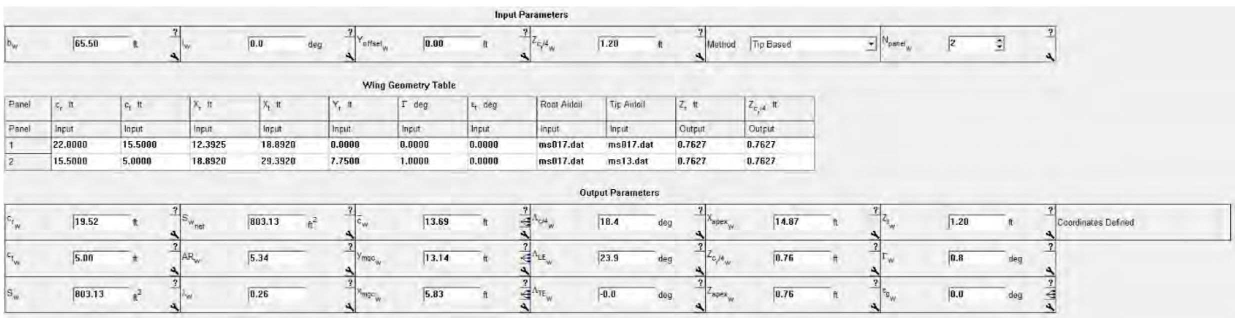


**Figure 11.1:** AAA Geometry Imputes

Using the new geometry, the required coefficients of lift for take-off and landing are entered into AAA, and the sizing of a plane flap can be calculated (Appendix B). Plane flaps are used on the A-21 due to the susceptibility this plane has to damage from enemy fire. AAA gives a plot of the ailerons and high lift on the single planform wing, this is shown in Figure 11.3. Ailerons are placed on the outboard side of the flaps similarly to the A-10. Calculations for the high lift devices can be seen in Appendix B. A three view of the high lift devices can be seen in Figure 11.4.

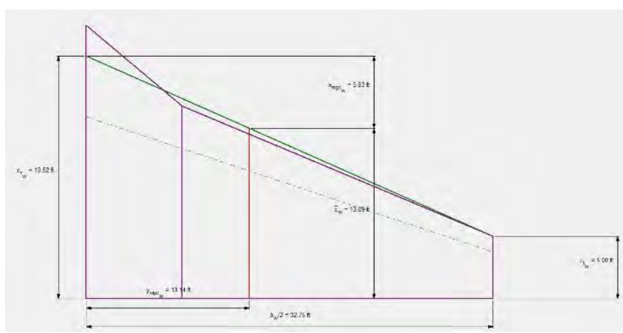

**Figure 11.2:** AAA Equivalent Area Wing

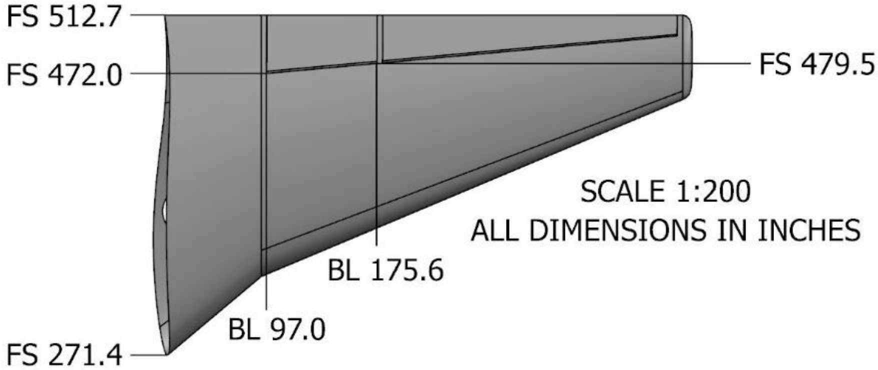


**Figure 11.3:** Dimensions for High Lift Devices on the A-21

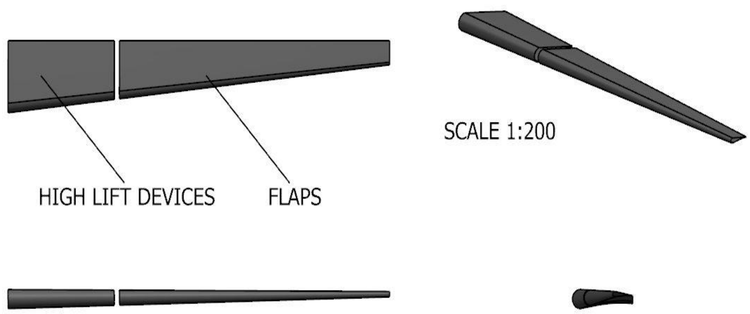


**Figure 11.4:** High Lift Devices three View for the A-21

## 11.2 High Lift Devices Summary and Recommendations

The high lift devices used are plain flaps because of the non-complexity needed for the flaps in the hazardous conditions of operation. The plain flaps used provide the needed lift increase for the take-off and landing conditions. The values for the high lift devices of the aircraft are shown in Table IX.

A recommendation to consider for the high lift devices would be a more complex flap that would decease flap area, thus increasing the storage volume in the wing.

**Table IX:** High Lift Devices Values

| High Lift Devices | |
|---|---|
| $c_f/c$ | 0.25 |
| $\eta_i$ (%) | 24.7 |
| $\eta_o$ (%) | 45.7 |
| $\xi_{TO}$ (deg) | 20 |
| $\xi_L$ (deg) | 60 |
| $S_{whd}/S_w$ | 0.247 |

# 12 Class I Design of the Empennage

The purpose of this section is to outline the decisions and processes that went into the Class I sizing of the chosen empennage. The methods used for the Class I design of the empennage are from *Airplane Design Part II*, Reference 3.

## 12.1 Empennage Design Procedure

The empennage configuration for the A-21 is a conventional cruciform tail, chosen for its simplicity and the position of the surfaces. Furthermore, use of the cruciform tail keeps the empennage surfaces away from the engine exhaust gas. For the preliminary sizing of the vertical and horizontal tails the $\bar{V}$-method is used. A volume coefficient for the vertical and horizontal tails are chosen to be 0.058 and 0.38 respectively. The preliminary design of the empennage with dimensions is shown in Figure 12.1 below. Calculations for the sizing of the empennage are shown in Appendix C.

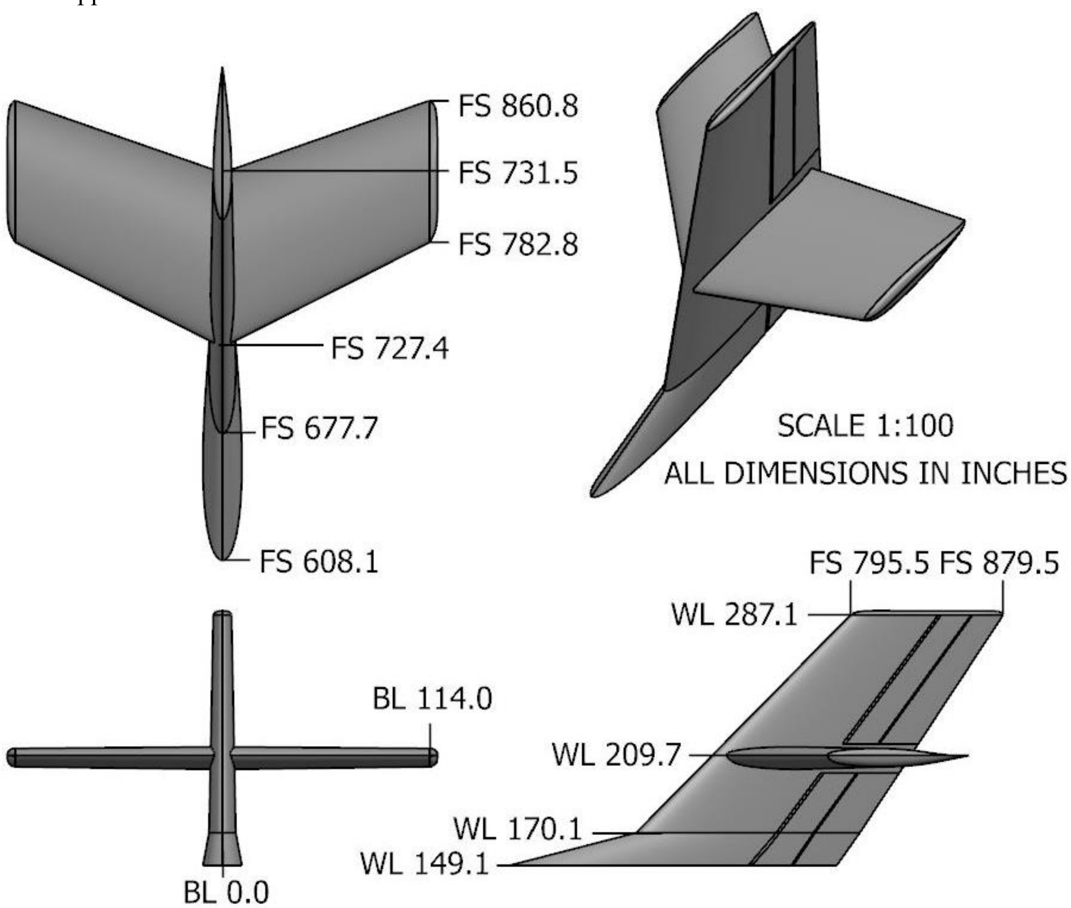


**Figure 12.1:** Preliminary Design of the A-21 Empennage

### 12.1.1 Horizontal Stabilizer

Cruciform tail designs place the horizontal tail in the middle of the vertical, this is done to allow the increase of the volume coefficient for both surfaces of the tail. A major factor in the design of the horizontal tail is to design for a favorable pitch break, where in the event of a stall the horizontal tail would stall after the wing. A favorable pitch break can be achieved by increasing the critical Mach number of the horizontal tail (Ref. 3). To increase the critical Mach number of the horizontal tail a sweep angle that is larger than that of the wing is used. Compared to the wing, the thickness to chord ratio is decreased (Ref. 3). The airfoil used for the horizontal tail is the inverse of the wing tip airfoil. This is done to ensure the tail would produce negative lift. Furthermore, the horizontal surface of the tail will be a stabilator to increase maneuverability and to have a lower tail volume coefficient. All values used for the horizontal tail are within the ranges for fighter aircraft per Reference 3.

### 12.1.2 Vertical Stabilizer

The vertical tail used is cranked to increase the volume coefficient while having a relatively smaller tail. Similarly, a large sweep angle is used for the tail to increase the volume coefficient and decrease tail size. A symmetrical airfoil is used to ensure lateral stability of the overall aircraft. Calculations for the cranked tail were done using AAA. All the values used for the sizing of the vertical tail fall within the expected ranges for fighters, as per Reference 3.

## 12.2 Summary and Recommendations of Empennage

The major findings in this chapter are that the empennage was sized for a small volume coefficient for the expectation of stabilator use in Class II design. The horizontal tail was sized to ensure a stable pitch break and maneuverability. Values for both the horizontal and vertical tail can be seen in Table X.

**Table X:** Class I Empennage Sizes

| Horizontal Tail | |
|---|---|
| $b_h$ (ft) | 19 |
| $S_h$ ($ft^2$) | 138 |
| $A_h$ | 2.62 |
| λ | 0.81 |
| $\Lambda_{c/4}$ (deg) | 25 |
| Airfoil | NASA MS(1)-0313 |
| **Vertical Tail** | |
| $b_v$ (ft) | 11.5 |
| $S_v$ ($ft^2$) | 106 |
| $A_v$ | 1.25 |
| λ | 0.61 |
| $\Lambda_{c/4}$ (deg) | 44 |
| Airfoil | NACA 0012 |

The author recommends that:

i) In Class II design of the empennage, the size of the overall empennage should be decreased to reduce aft weight;

ii) The horizontal tail should be moved for better integration of rudder panels.

# 13 Class I Design of the Landing Gear

This chapter will detail the Class I sizing procedure for the landing gear on the A-21. The methods used for the Class one sizing are from *Airplane Design Part II & IV* (Ref. 3 & 4). All calculations for landing gear values are shown in Appendix C.

## 13.1 Landing Gear Design Procedure

Retractable landing gear will be used due to the 300 kts cruise speed of the A-21, and a conventional tricycle landing gear arrangement will be utilized for its ease of integration and wide spread use. For the initial sizing of the landing gear, an estimated center of gravity range for the airplane is obtained. From the estimated center of gravities, the main landing gear is placed at a 15 degree angle back from the mast aft center of gravity per the longitudinal tip-over criteria. Additionally, a 55 degree cone is used to show that the lateral tip-over criteria is met. To ensure adequate ground clearance, the tail end of the plane must be able to rotate 15 degrees laterally, and a 5 degree lateral clearance must be met. Finally, the landing gear wheels can be sized by the weight of the aircraft and their spacing. Type III tires will be utilized for the ruff field conditions the aircraft will be operating in. These values for clearance and placement of the landing gears can be seen in Figure 13.1, and Figure 13.2 and 13.3 show the nose and main landing gear storage processes respectively.

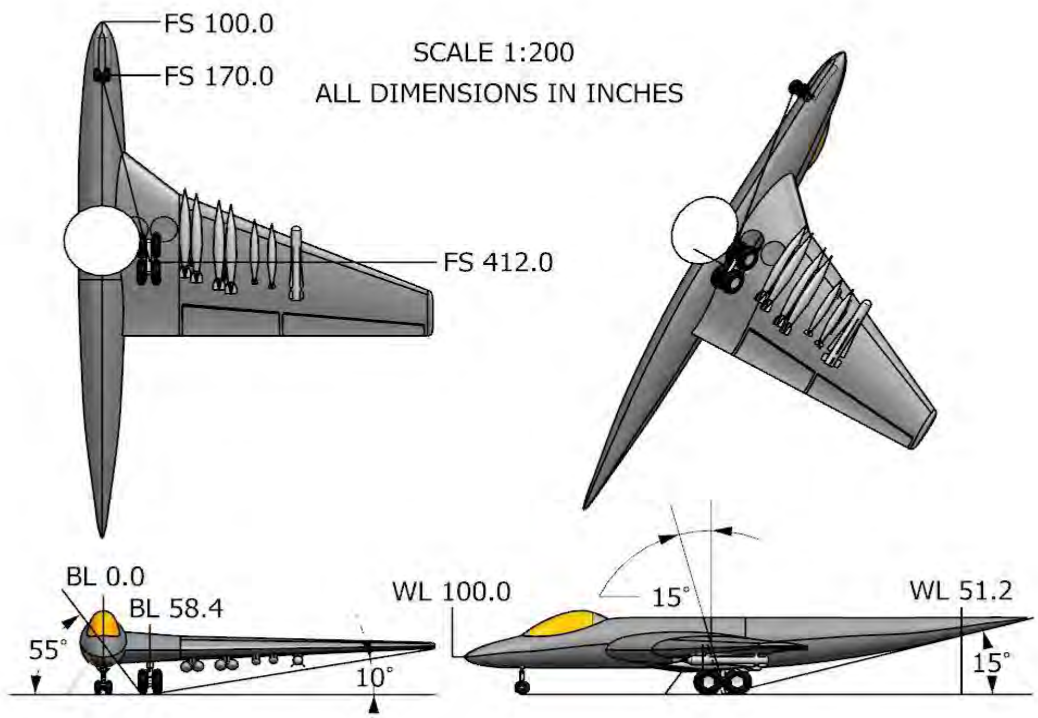


**Figure 13.1:** Fuselage Dimensions for the A-21

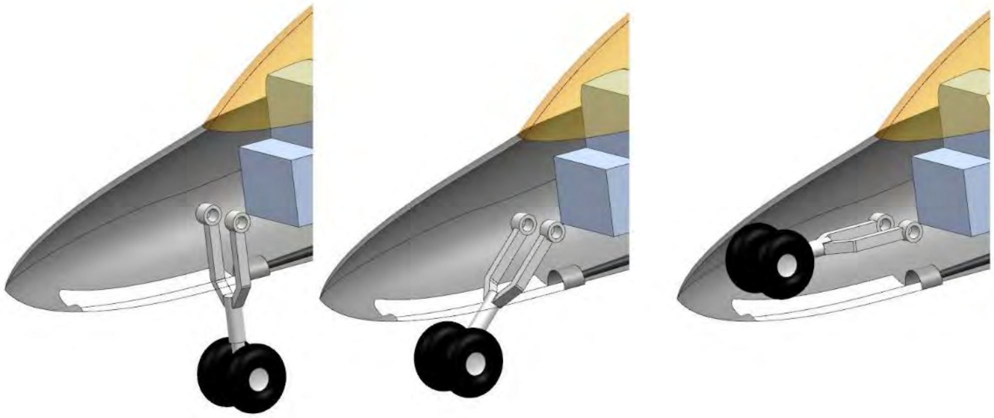

**Figure 13.2:** Nose Landing Gear Retraction Process (NTS)

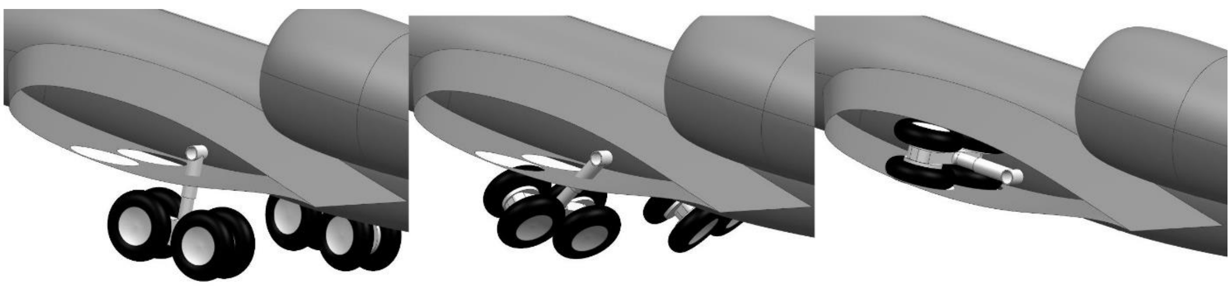

**Figure 13.3:** Main Landing Gear Retraction Process (NTS)

## 13.2 Summary and Recommendations of Landing Gear

The major findings in this section are that the A-21 meets the tip-over criteria, and the loads taken by the nose and main gear. Values for the loads and tire sizes can be seen in Table XI.

**Table XI:** Landing Gear Characteristics

| Nose Gear Tire | |
|---|---|
| $P_n$/Wto | 7.66% |
| D (in) | 18.75 |
| W (in) | 7 |
| P (psi) | 60 |
| W (lbs) | 3180 |
| **Main Gear Tire** | |
| $P_m$/Wto | 76.60% |
| D (in) | 33.36 |
| W (in) | 9.7 |
| P (psi) | 90 |
| W (lbs) | 9250 |

The Author Recommends that:

i) The number of tires on the main gear be reduced to 2 or less for ease of storage;

ii) A decrease in the length of the landing gear struts for storage and weight;

iii) The addition of a strike plate to the underside of the aft fuselage in the event of an over rotation.

# 14 Class I Weight and Balance Analysis

This section outlines the weight and balance aspects of the A-21 Class I design, and the center of gravity placement. The methodology used for the Class I weight and balance calculations is from *Airplane Design Part II & V,* Reference 3 and 6.

## 14.1 Preliminary Three-View

Figure 14.1 shows the three view of the Class I preliminary design for the A-21 Valkyrie II. Dimensions for the center of gravity of each component and the aircraft can be seen in Section 14.3 Figure 14.2.

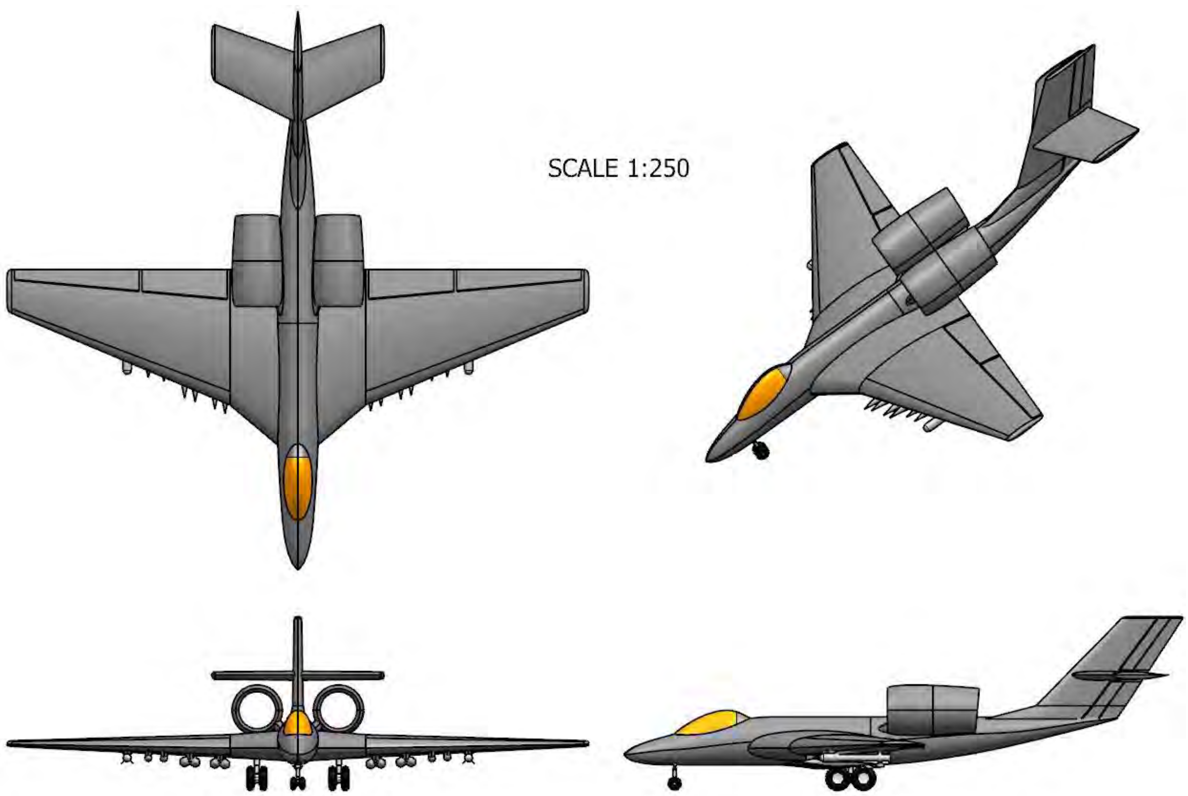


**Figure 14.1:** Preliminary Three-View of the A-21

## 14.2 Class I Weight Breakdown

Through using the initial weight estimation values found in Section 5, the weight of the structures in the aircraft can be estimated using weight fractions found in Reference 6. When choosing weight fraction estimations most of the weight allocation went into the fuselage and wings due to the structure needed to support the landing gear, munitions, engines, and all other components of the aircraft. Additionally, the weight estimates of the fixed equipment is low to account for the predicted improvements in technology. Generally, the weight fractions for engine structure, landing gear, and the empennage are within range to similar fighter aircrafts found in Reference 6. The weights and weight fractions used for each component are shown in Table XII.

**Table XII:** Weight and Weight Fractions for Each Components

| | Z Arm (ft) | X Arm (ft) | W (lbf) | W Fraction |
|---|---|---|---|---|
| Fuselage | 18.9 | 203.4 | 8558.0 | 0.110 |
| Wing | 10.2 | 311 | 8869.2 | 0.114 |
| H Empennage | 103 | 662.2347 | 855.8 | 0.011 |
| V Empennage | 97 | 641 | 933.6 | 0.012 |
| Engine Section | 59 | 410.4 | 155.6 | 0.002 |
| Engine | 59 | 416.7 | 8380 | 0.108 |
| Nose Landing Gear | -20 | 70 | 227.7 | 0.003 |
| Main Landing Gear | -16.5 | 312 | 2884.3 | 0.037 |
| Fixed | 14 | 120 | 6613.0 | 0.085 |
| Bushmaster III | -4 | 175 | 470 | 0.006 |
| **WE** | | | **37947** | **0.488** |
| Trapped Fuel and Oil | 14 | 300 | 389.00 | 0.005 |
| Crew | 29 | 125 | 200 | 0.003 |
| **WOE** | | | **38536** | **0.496** |
| Fuel Wing | 14 | 308 | 21505.91 | 0.276 |
| Fuel FL | 19 | 164 | 1133.16 | 0.015 |
| Bomb Bay | 20 | 275 | 3000 | 0.039 |
| Ex Bombs | -7 | 298 | 11000 | 0.141 |
| Ammo | 14 | 230 | 2625 | 0.034 |
| **WTO** | | | **77800** | **1.000** |

## 14.3 Class I Weight and Balance Calculations

Using the weights of each component calculated and shown in Table XII, the center of gravity for each individual component can be estimated. The estimations for the center of gravity are performed using References 3 and 6, as well as the visual representations in the CAD model. Positioning of the external stores was performed to position their center of gravity close to the operating empty weight center of gravity, this is done per Reference 3. The center of gravity of each component is estimated to be on BL 0.0 due to the symmetry of the A-21. Figure 14.2 shows the center of gravity for each component when the landing gear is down.

| Num | Section | WL (in) | FS (in) | W (lbf) |
|---|---|---|---|---|
| 1 | Fuselage | 118.9 | 303.4 | 8169 |
| 2 | Wing | 110.2 | 411.0 | 8636 |
| 3 | H Empennage | 203.0 | 762.2 | 856 |
| 4 | V Empennage | 197.0 | 741.0 | 934 |
| 5 | Engine Section | 159.0 | 510.4 | 156 |
| 6 | Engine | 159.0 | 516.7 | 8380 |
| 7 | Nose Landing Gear | 80.0 | 170.0 | 239 |
| 8 | Main Landing Gear | 83.5 | 412.0 | 2873 |
| 9 | Fixed | 114.0 | 220.0 | 6224 |
| 10 | Bushmaster III | 96.0 | 275.0 | 470 |
| | **WE** | | | **37947** |
| 11 | Trapped Fuel and Oil | 114.0 | 400.0 | 389 |
| 12 | Crew | 129.0 | 225.0 | 200 |
| | **WOE** | | | **38536** |
| 13 | Fuel in Wing | 114.0 | 408.0 | 22639 |
| 14 | Fuel in FL | 119.0 | 264.0 | 1133 |
| 15 | Int. Bomb | 120.0 | 375.0 | 3000 |
| 16 | Ex. Bombs | 93.0 | 398.0 | 11000 |
| 17 | Ammo | 114.0 | 330.0 | 2625 |
| | **WTO** | | | **77800** |


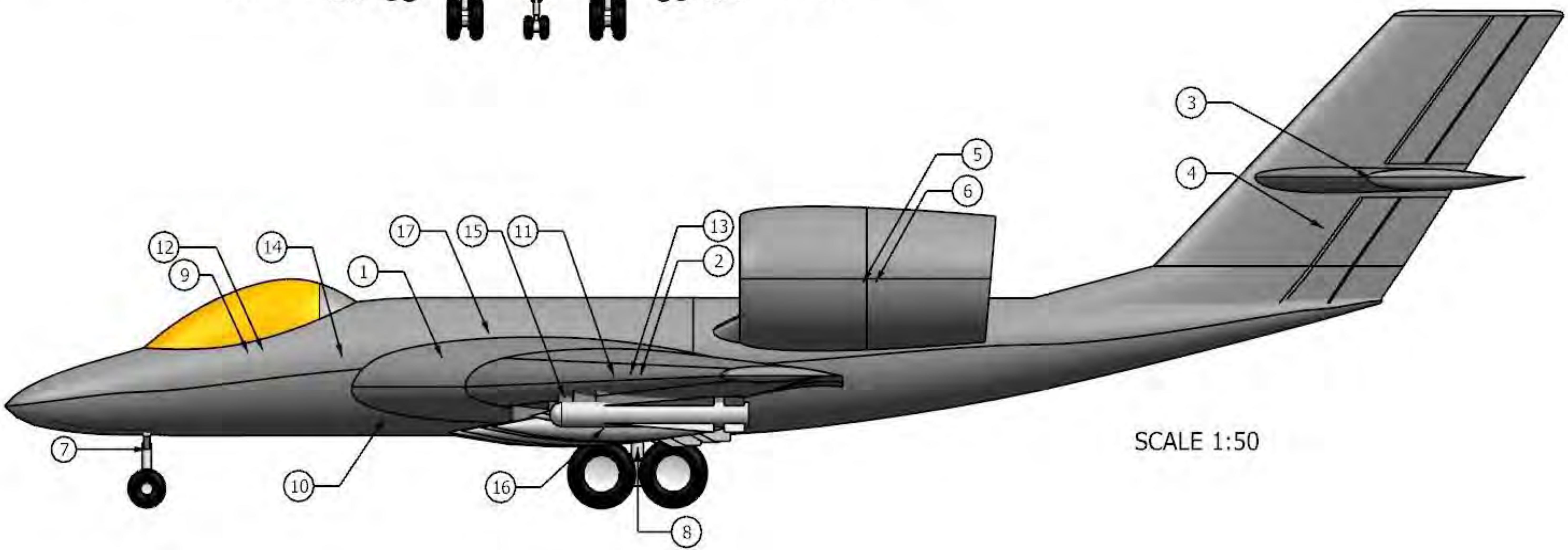


**Figure 14.2:** Component C.G. Location on the A-21

Utilizing the preliminary center of gravity locations shown above in Figure 14.2, the center of gravity of the aircraft at different ground and flight condition is found. The center of gravity of the A-21 is calculated when the aircraft is at empty weight, operating empty weight, and take-off weight. As well, the center of gravity for the aircraft is found when there are no munitions but full fuel, and vice versa. These calculations are also performed when the landing gear are fully deployed and stowed away. The movement of the center of gravity can be seen when the landing gear is deployed and stowed in Figure 14.3, case 1 and 2 respectively. Figure 14.3 shows that the center of gravity for the aircraft shifts a maximum of 3.72% of the mean geometric cord when the landing gear is down and 3.77% when the landing gear is stowed. The center of gravity shifts that result are within the allowable range for aircraft of this class. Landing gear are then shifted to the new calculated center of gravity. The center of gravity of this aircraft could be moved forward if necessary in Class II sizing by moving the internal stores to the wings, with the remainder of the ordnance or between the spars of the wing. Calculations for the center of gravity are shown in Appendix C.

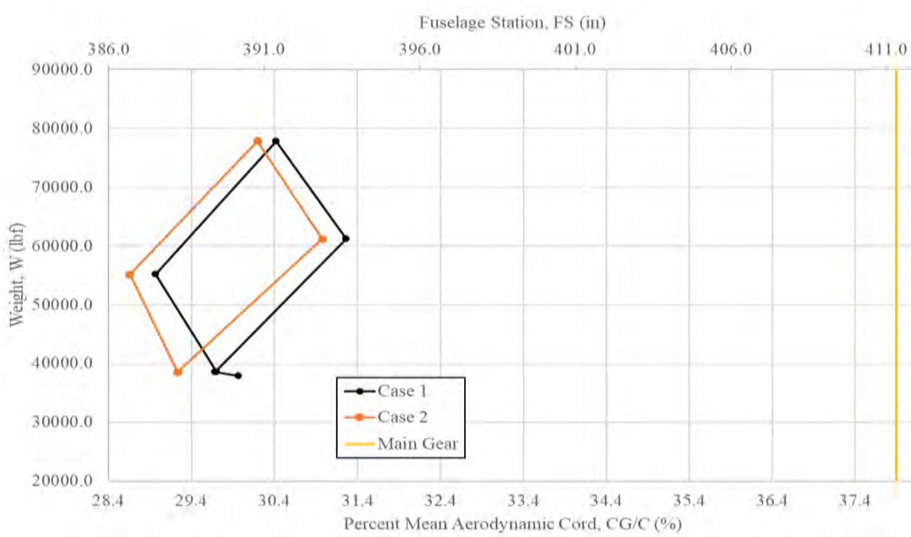


**Figure 14.3:** C.G. Excursion Diagram for the A-21

## 14.4 Summary and Recommendations of Weight and Balance

The major findings in this chapter are that the center of gravity shift is 6.1 inches when gears are down and 6.2 inches when gears are up. This correlates to 3.72% and 3.77% sift along the mean geometric cord of the wing. The center of gravity shift is within a reasonable margin for this class of aircraft.

This author recommends that:

i) The internal stores be moved forward to decrease the center of gravity shift along the aerodynamic cord;

ii) The aerodynamic center be compared with the center of gravity to ensure longitudinal stability.

# 15 V-n Diagram

This chapter displays the process and results of the V-n diagram for the A-21 military aircraft. The methodology used for the construction of the V-n diagram are from *Airplane Design Part II & V,* Reference 3 and 6.

## 15.1 V-n Calculations

A V-n diagram is used to determine the design limits and ultimate load factors at corresponding speeds to be used for the design of the aircraft structures (Ref. 6). A maximum level speed for the V-n diagrams is the cruise speed of the A-21, and the maximum dive speed is 1.25 times the level speed (Ref. 6). The gust lines are per FAR 25 regulations, but for military aircraft are usually not critical above a load factor of 3. Calculations for the FAR 25 gust lines are shown in Appendix C.

## 15.2 Presentation of the V-n Diagram

This V-n diagram shows the plane under the clean condition, as well, at a maximum level speed, $V_H$, of 300 kts and a maximum dive speed, $V_L$, of 375 kts. A positive limit load factor of 8 is used, as per the RFP, and a negative limit load factor of 3 is used for its use in many other attack aircraft (Ref. 6). Figure 15.1 shows the military V-n diagram for the A-21.

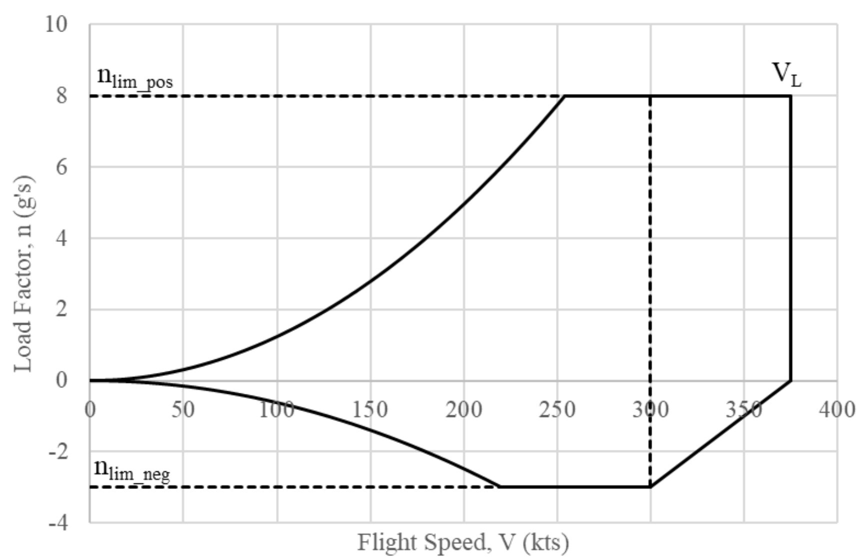


**Figure 15.1:** V-n Diagram for the A-21

# 16 Class I Stability and Control Analysis

This section details the analysis of the Class I longitudinal and lateral stability and control of the A-21 Valkyrie II using the methods found in *Airplane Design II &VI* (Ref. 3 and 7), Chapter 11 and Chapter 8 respectively. This includes the calculation of the static margin and associated gain, as well as the calculations for the rudder in the event of a one engine out condition. Lateral and longitudinal coefficients for the rudder and elevator/stabilator will be shown.

## 16.1 Stability and Control Analysis

This section will outline the static longitudinal stability, static directional stability, and minimum control speed with one engine of the A-21 inoperative. The analysis performed demonstrates that the size of the empennage would have to be increased to achieve a favorable stability condition.

### 16.1.1 Static Longitudinal Stability

A longitudinal X-plot for the A-21 is created by determining the rate at which the aerodynamic center moves aft as a function of horizontal tail area. The center of gravity is plotted similarly with an increasing tail shifting the center of gravity aft. The line of increasing center of gravity is found by reducing the weight fraction of the horizontal tail to zero and plotting a linear correlation. Calculation of the aerodynamic center shows that it is in front of the center of gravity when the horizontal tail area is reduced to zero, therefore a horizontal tail is required. The preliminary wing area proved to be inefficient, and a greater horizontal tail was created. The aerodynamic centers used for the wing and horizontal tail were found using AAA. Similarly, the aerodynamic center shift due to the fuselage and nacelles are calculated Multhop integration (Fig.16.1) in AAA, and the inputs and outputs can be seen with calculations for the aerodynamic center line in Appendix D. Figure 16.2 shows the longitudinal X-plot for this aircraft. Table XIII shows the values of aerodynamic centers and

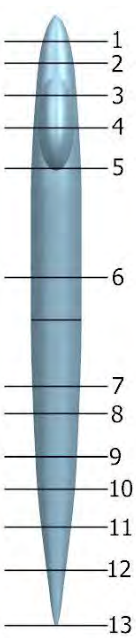


**Figure 16.1:** Multhopp Integration Sectioning

**Table XIII:** AC and Coefficients of Lift Curve Slope

| Aerodynamic Center | |
|---|---|
| $\bar{x}_{ac\,w}$ | 0.257 |
| $\bar{x}_{ac\,h}$ | 2.480 |
| $\Delta\bar{x}_{ac\,f}$ | -0.059 |
| $\bar{x}_{ac\,wf}$ | 0.197 |
| **Coefficients of Lift Curve Slope** | |
| $C_{L\alpha w}$ (1/deg) | 0.091 |
| $C_{L\alpha h}$ (1/deg) | 0.059 |
| $C_{L\alpha wf}$ (1/deg) | 0.091 |
| $C_{L\alpha}$ (1/deg) | 0.096 |

coefficients of lift curve slopes from the Polhamus equations in Reference 7, which are used for the calculation of the longitudinal X-plot and feedback gain.

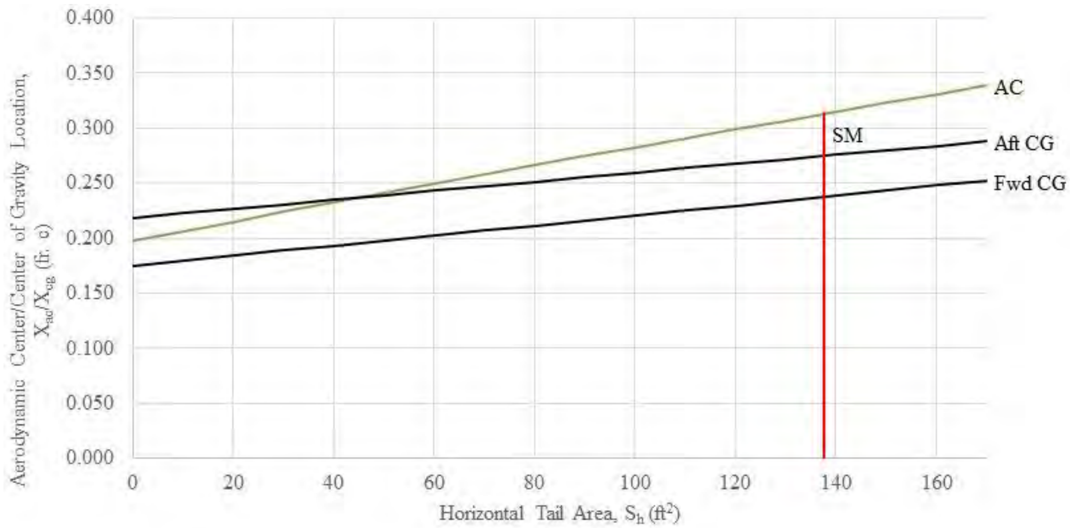


**Figure 16.2:** Longitudinal X-Plot for the A-21

The horizontal tail size was increased from previous iterations to produce a more desirable static margin. From the longitudinal X-plot with a horizontal tail area of 137.75 ft$^2$ a static margin of 3.83% is achieved. As Reference 3 demonstrates, the A-21 falls in the category of aircraft which desire a static margin of 10%. Thus, this aircraft is de-facto stable and a feedback augmentation system is required to bring the static margin to its desired value. Calculations for a feedback gain are calculated to achieve a static margin increase of 6.18%. The gain found for the feedback augmentation system is 1.92 deg/deg, and calculation for feedback gain is shown in Appendix C and falls in the appropriate range of less than 5 deg/deg.

### 16.1.2 Static Directional Stability

To determine the lateral stability of the A-21, an X-plot of the directional stability is constructed with the methods found in Reference 3. The X-plot is made by graphing the yawing moment due to sideslip angle with respect to the vertical tail area. With the calculations performed using the preliminary vertical tail area, a yawing moment coefficient due to sideslip of 0.001 /deg was overshot. Therefore the vertical tail was resized to be 82.8 ft$^2$. With the new tail dimensions,

**Table XIV:** Lateral Coefficients

| Lateral Coefficients | |
|---|---|
| $C_{L\alpha v}$ (1/deg) | 0.034 |
| $C_{n\beta wf}$ (1/deg) | -0.0004 |
| $C_{y\delta r}$ (1/deg) | 0.0016 |
| $C_{n\delta r}$ (1/deg) | -0.0010 |

a yawing moment coefficient due to sideslip of 0.0011 /deg was achieved. Furthermore, as a result to the yawing moment coefficient due to sideslip being greater than 0.001 /deg the aircraft is de-facto stable. A sideslip to rudder feedback augmentation system is required. The gain calculated for the feedback loop is 0.086 deg/deg which falls in the appropriate range of less than 5 deg/deg. Table XIV shows the lift curve slope and yawing coefficients used for the directional stability X-plot as well as the feedback gain. Figure 16.3 shows the X-plot for the directional stability.

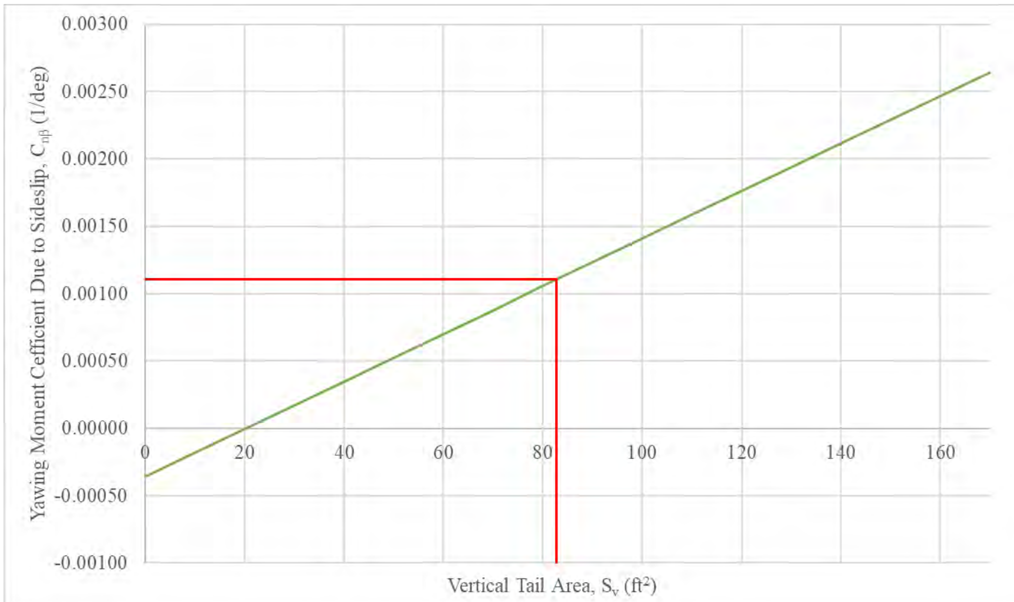


**Figure 16.3:** Static Directional Stability X-plot for the A-21

### 16.1.3 One Engine Out

**Table XV:** OEO Moments

| OEO Yawing Moment | |
|---|---|
| $N_{tcrit}$ (ftlbs) | 75950 |
| $N_D$ (ftlbs) | 18988 |

In the event of an engine out event which typically would occur during take-off, the rudder must be sized to provide the moment needed to counter act the effects of one engine being inoperable. The moment created by this event is calculated by adding the moments created by the thrust of one engine and the induced drag by the other. This calculation will determine the critical engine out yawing moment needed for the rudder sizing. Additionally, the minimum control speed at which this would occur is found to be about 1.2 times the landing stall speed, as per Reference 3. To achieve a favorable maximum rudder deflection, the rudder extends 88% of the vertical tail and cuts 45% inboard. Furthermore, the rudder used is a two hinged system to provide more yawing moment due to the rudder. Finally, the maximum rudder deflection angle is found to be 30 degrees, which falls within an allowable range if a two hinged rudder is used. All Calculations for the one engine out condition are done using AAA, and this can be seen in Appendix D. Table XV shows the yawing moments found for the critical and induced drag of the engines.

## 16.2 Class I Stability and Control Analysis Conclusions and Recommendations

The major findings in this chapter are the static margin found in the longitudinal X-plot, yawing coefficient due to sideslip, and their associated gains. Additional, the moments created by a one engine out condition and its accompanying rudder deflection angle calculations. All values calculated can be seen in Table XVI.

**Table XVI:** Class I Stability and Control Results

| | |
|---|---|
| SM | 3.83% |
| $k_\alpha$ | 1.920 |
| $C_{\eta\beta}$ (1/deg) | 0.001 |
| $k_\beta$ | 0.086 |
| $\delta_r$ (deg) | 19.2 |
| $S_h$ ($ft^2$) | 138 |
| $S_v$ ($ft^2$) | 83 |

This author recommends that:

i) More iterations be performed on the size of the tail to decrease tail size and wetted area;

ii) The center of gravity should be moved forward with more iterations to increase the static margin. this is to achieve inherent stability of the aircraft and decrease complexity;

iii) The tail should be moved forward to decrease the overall length of the plane.

# 17 Class I Drag Polar and Performance Analysis

The purpose of this chapter is to present the Class I performance and drag polar analysis of the A-21 using methods and charts found in *Airplane Design I, II, & VI* (Ref. 2, 3, and 7). The following will show the Wetted Area Breakdown and presentation of the drag polars results. Calculations for the wetted area of planforms and the fuselage can be seen in Appendix D.

## 17.1 Drag Polar Analysis with Wetted Area Breakdown

The wetted area of the airplane is in the integral of the airplane perimeter for the distance from the nose to the tail, as per Reference 3. This is simplified using a CAD program. The wetted area for each component of the aircraft is found using CAD and a calculation to verify the values found is performed using the methods in Reference 3. Each component has their wetted area calculated and added together to determine the full wetted area of the aircraft. This method is used to account for the friction coefficient and further for the parasite area. Table XVII shows the wetted area for each component of the aircraft along with the total wetted area of the aircraft. Wetted area of planforms does not include the area in which it intersects the fuselage. For the fuselage wetted area, a perimeter plot can be seen in Figure 17.1 which shows the perimeter of the fuselage with respect to fuselage stations.

**Table XVII:** Wetted Area

| Component | Swet (ft2) |
|---|---|
| Wing | 1491 |
| Horizontal Tail | 269 |
| Vertical Tail | 165 |
| Fuselage | 562 |
| Nacelle | 181 |
| Canopy | 40 |
| Pylons | 127 |
| Stores | 332 |
| **Total** | **3166** |

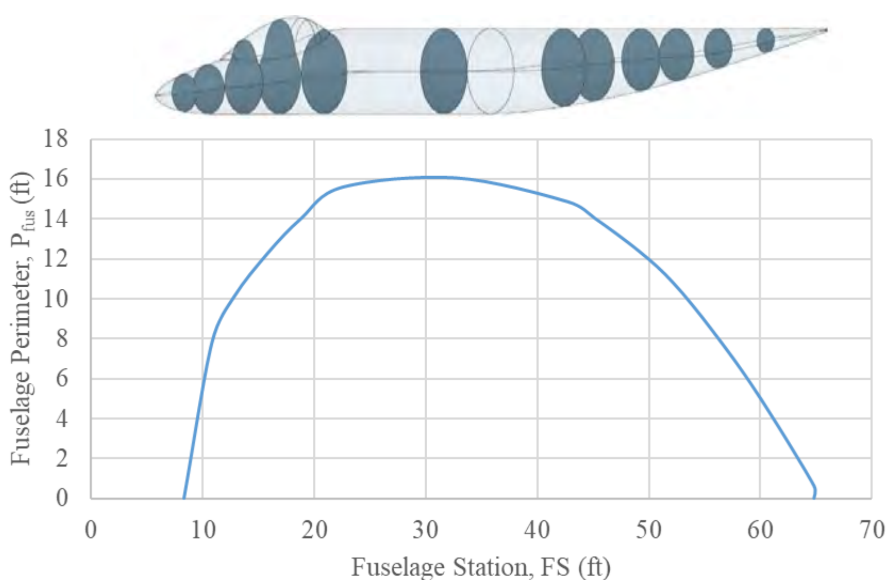


**Figure 17.1:** Fuselage Perimeter Plot

From the wetted area of the fuselage in Reference 2 a skin friction coefficient can be determined to be 0.01 due to the conditions this aircraft would Experience during service. This skin friction coefficient corresponds to a parasite area of 19 $ft^2$ through charts in Reference 2. From the parasite area and the total wing area the zero lift drag coefficient can be calculated, to be 0.024. Due to the slow speed of this aircraft the compressibility drag increment is zero. For take-off flaps, landing flaps, and landing gear, the increase in drag coefficient is 0.015, 0.065, and 0.02 respectively. The original and newly calculated drag polar equations of the airplane in each conditions where bombs are external, shown below and graphed in Figure 17.2.

| Flight Condition | Part I | Part II |
|---|---|---|
| | A = 5.34, e = 0.825 | A = 5.34, e = 0.800 |
| Cruise, Gears Up | $0.040 + 0.072C_L^2$ | $0.024 + 0.075C_L^2$ |
| Cruise, Gears Down | $0.060 + 0.072C_L^2$ | $0.044 + 0.075C_L^2$ |
| Take-Off, Gears Up | $0.055 + 0.077C_L^2$ | $0.039 + 0.077C_L^2$ |
| Take-Off, Gears Down | $0.075 + 0.077C_L^2$ | $0.059 + 0.077C_L^2$ |
| Landing, Gears Up | $0.105 + 0.082C_L^2$ | $0.089 + 0.082C_L^2$ |
| Landing, Gears Down | $0.125 + 0.082C_L^2$ | $0.109 + 0.082C_L^2$ |

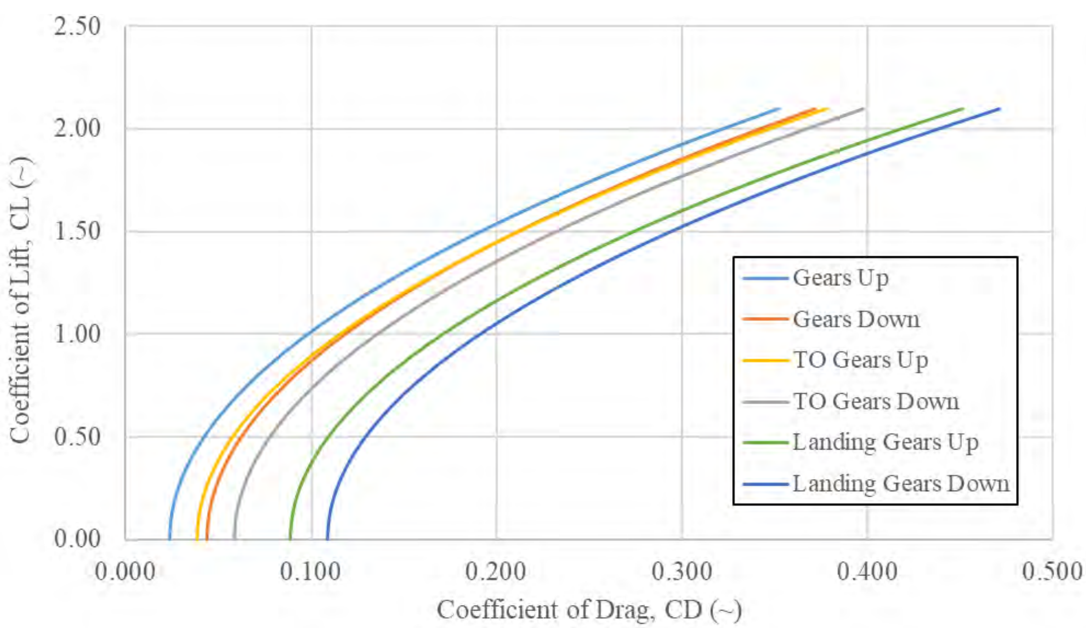


**Figure 17.2:** Drag Polars for External Bombs

As seen in the drag polars, the zero lift drag coefficient has decreased due to a very conservative approach in the wetted area of 5,000 $ft^2$ when the final wetted area came to be 3220 $ft^2$. The Oswald Efficiency Factor was lowered to account for the lift to drag estimations. The lift to drag ratios are calculated and adjusted for the velocity and altitude to produce lift to drag ratios similar to what was predicted in part I of the design. The critical lift to drag ratios in each condition of the mission profile with their corresponding altitude and velocity are shown in Table XIX in Section 18. The lift to drag ratios predicted in part I are easily achieved by the aircraft. This can be seen in the drag polars. Additionally, the lift to drag ratios calculated are for an external bombs condition. Therefore this aircraft should be able to achieve a more favorable flight mission when the external bombs are removed.

## 17.2 Conclusions and Recommendations

The major findings of this chapter are the drag polars referenced above and the lift to drag ratios calculated for each leg of the mission profile. The calculated lift to drag ratios for each of the flight phases are shown in Table XVIII. The lift to drag ratios found show that the mission specification can be met by the A-21 Valkyrie II.

**Table XVIII:** L/Ds during Mission Profile

| Mission Leg | L/D |
|---|---|
| Cruise 1 | 11.7 |
| 4hr Loiter | 11.8 |
| Cruise 2 | 11.9 |
| Dash | 8.0 |
| TE | 9.1 |

The author recommends that iterations be performed by placing the lift to drag ratios calculated into the part I weight calculations to more accurately calculate the lift to drag ratios for the A-21. Due to time constraints, these iterations were not performed.

# 18 Analysis of Weight and Balance, Stability and Control, and L/D Results

Through this chapter the weight and balance, stability and control, and L/D of the A-21 will be discussed in terms of results. The methodology used in *Airplane Design Part II* (Ref. 3) will be referenced as a guide. Applying the values calculated prior to this section, an analysis of them will be performed.

## 18.1 Impact of Weight and Balance and Stability and Control Results on the Design

The preceding subsection will discuss the methods found in Reference 3 of weight and balance and stability and control. The weight and balance results are from the center of gravity excursion diagram in Section 14. The maximum center of gravity excursion is 3.77% which is well within the allowable values of similar aircraft. For the longitudinal stability of the aircraft a static margin of 3.83% is seen which falls within the accepted range of de-facto stable and a gain is found to be 0.366 deg/deg which falls below the allowable value of 5 deg/deg. Furthermore, for longitudinal stability, the yawing moment coefficient due to sideslip is 0.00168 /deg which is above the required value of 0.001 /deg, and a gain is calculated for the de-facto stable condition of 0.406 deg/deg which falls below the allowable value of 5 deg/deg. Therefore, A-21 is in the acceptable ranges of values.

## 18.2 Analysis of Critical L/D Results

The analysis of the critical lift to drag ratios will show that the A-21 is within the accepted ranges of weight change due to the new lift to drag ratios. Table XX shows the lift to drag ratios calculated at each of the critical flight phases in the mission profile. The values for lift to drag to are found with external stores attached so the airplane is able to go beyond when the external stores are removed. After the new lift to drag calculations are performed the new lift to drag calculations are used to find a new weight. The percent differences in the weight of the new to the old values are seen in Table XIX. The percent change in the weights of the total, fuel, and empty fall within the 5% acceptable range. Therefore, the lift to drag ratios found for the A-21 are within the acceptable range.

**Table XX:** Lift to Drag Ratios at Conditions

| Mission Leg | Altitude (ft) | Velocity (kts) | L/D |
|---|---|---|---|
| Cruise 1 | 25,000 | 300 | 11.7 |
| 4hr Loiter | 10,000 | 230 | 11.8 |
| Cruise 2 | 25,000 | 300 | 11.9 |
| Dash | 5,000 | 350 | 8.0 |
| TE | 0 | 138 | 9.1 |

**Table XIX:** Change in Weight Due to New L/Ds

| Change in Aircraft Weights Due to L/D Change | |
|---|---|
| Take-off Weight | 2.31% |
| Empty Weight | 4.43% |
| Fuel Weight | 2.31% |

## 18.3 Design Iterations Performed

Throughout the process of Class I design the design has changed by a couple of factors. Originally, the aerodynamic center was found to be in front of the center of gravity. Therefore the internal stores and ammo were moved forward while the wing was moved aft by one foot. This resulted in the center of gravity shifting forward and aerodynamic center shifting aft. As well, in the center of gravity excursion shifting from 5.3% to 3.64%. When the static margin was calculated, it became necessary to achieve a better static margin and decrease the longitudinal feedback gain. Thus the horizontal tail size was increased to 138 $ft^2$. During the calculations of one engine out condition, the maximum rudder deflection was out of acceptable range, and thus the vertical tail and rudder size was increased. This resulted in an aircraft with favorable values that fall within the acceptable ranges.

## 18.4 Summary and Recommendations

This chapter demonstrates that with the design iterations done the design of the A-21 falls within the acceptable ranges for similar aircraft. Therefore, the aircraft design processes of the A-21 may proceed forward from Class I to Class II design.

# 19 Preliminary Three-View

This section will finalize the preliminary design of the A-21 Valkyrie II. The proceeding section will show the design of the A-21 after the Class I design, per References 2 through 7 has been performed. Based on the acceptable values that were calculated the design may proceed.

## 19.1 CAD Figures of Class I Aircraft

Figure 19.1 shows the three-view of the finalized preliminary design for the A-21 Valkyrie II after Class I design has been performed.

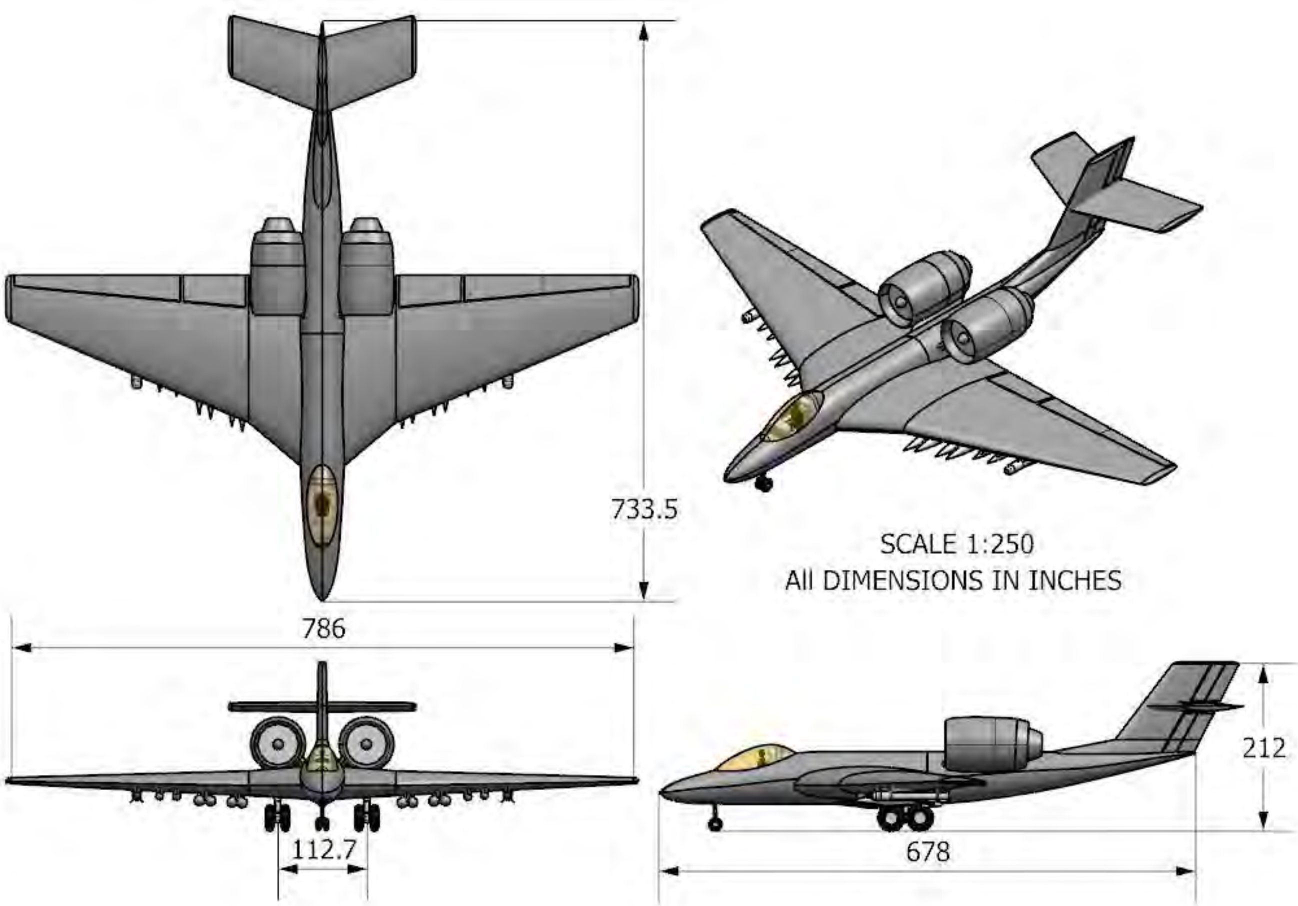


**Figure 19.1:** Dimensioned Three-View of the A-21

## 19.2 Table of Class I Aircraft Characteristics

Table XXI shows the major characteristics of the Class I design of the A-21 Valkyrie II. For the planforms and the fuselage.

**Table XXI:** Class I Aircraft Characteristics

| | Wing | Horizontal Tail | Vertical Tail |
|---|---|---|---|
| Area | 803 ft | 138 ft | 82.8ft |
| Span | 65.5 ft | 19 ft | 9.5 ft |
| MGC | 13.7 ft | 7.28 ft | 8.82 ft |
| MGC L.E. : F.S. | 26.5 ft | 61.7 ft | 55.3 ft |
| | | | |
| Aspect Ratio | 5.34 | 2.62 | 1.09 |
| Sweep Angle | 18.4 deg | 25 deg | 38.1 deg |
| Taper Rato | 0.26 | 0.81 | 0.67 |
| Thickness Ratio at Ro | 0.17 | 0.13 | 0.12 |
| Thickness Ratio at Tip | 0.13 | 0.13 | 0.12 |
| Airfoil: Root | NASA(1)-0317 | NASA(1)-0313 | NACA 0012 |
| Airfoil: Tip | NASA(1)-0313 | NASA(1)-0313 | NACA 0012 |
| Dihedral Angle | 0.8 deg | 0 deg | 90 deg |
| Incidence Angle | 0 deg | 0 deg | 0 deg |
| | | | |
| Aileron Chord Ratio | 0.25 | Elevator Cord Ratio 1 | Rudder Cord Ratio 0.45 |
| Aileron Span Ratio | 0.467 - 0.990 | Elevator Span Ratio 1 | Rudder Span Ratio 0.88 |
| Flap Cord Rato | 0.25 | | |
| Flap Span Ratio | 0.247 - 0.457 | | |

| | Fuselage | Overall |
|---|---|---|
| Length | 56.5 ft | 64 ft |
| Maximum Heigh | 5.5 ft | 19.9 ft |
| Maximum Width | 4.7 ft | 65.5 ft |

## 19.3 Class I Aircraft Description

The A-21 Valkyrie II is an exceptional plane to meet the mission specifications provided by the RFP because of the internal and external division of the stores, as well as the implementation of a 35mm cannon. The very efficient and new engines provide the ability to meet the long range and loiter time. The A-21 is the appropriate aircraft to fulfill the mission specification now and in the future.

# 20 Description of Major Systems with Ghost Views

The purpose of this section is to describe the major systems used and needed for flight operations of the A-21 Valkyrie II. All methods used for the implementation of the aircraft systems are from *Airplane Design II*, Reference 3.

## 20.1 List of Major Systems

The major systems used for the flight operations of this aircraft can be seen in Figure 12.1 and include the following:

- Flight Control System
- Fuel System
- Environmental Control System
- Electrical System
- Hydraulics System

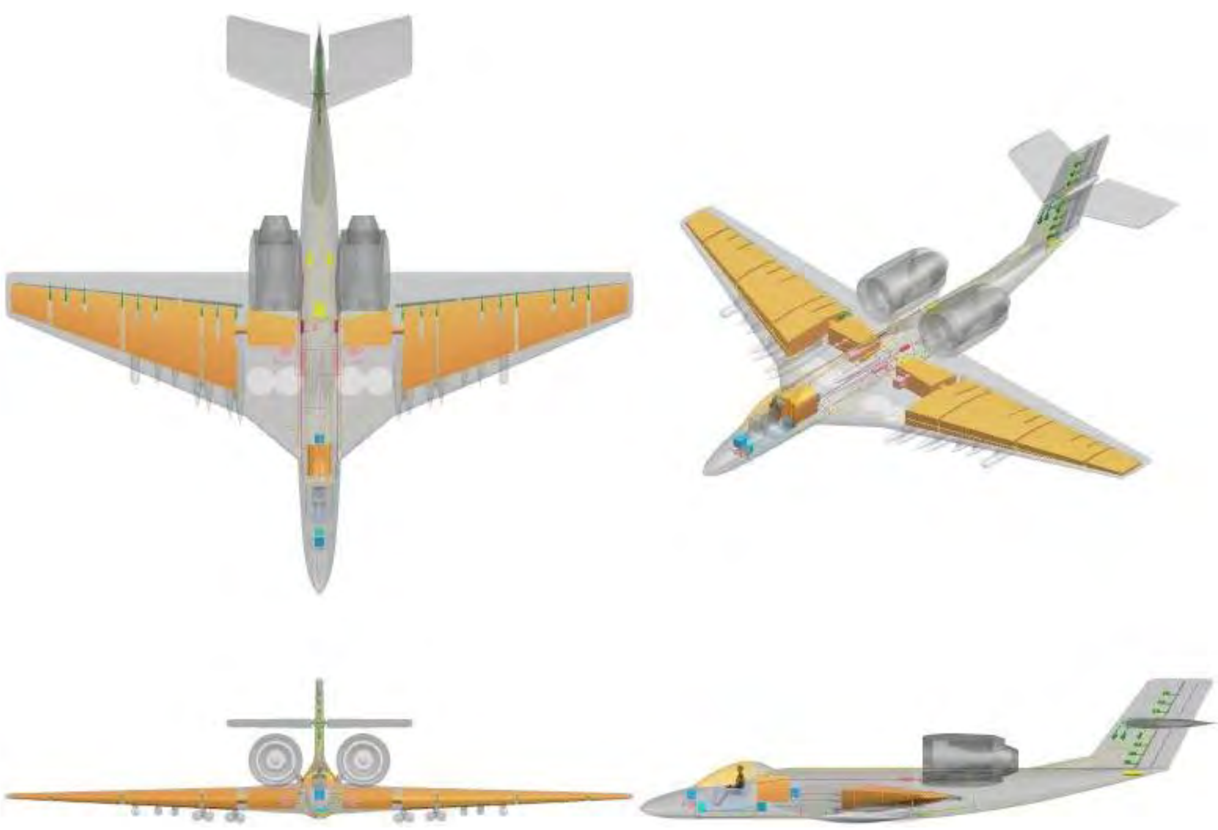

**Figure 20.1:** Systems Three-View (1:250)

## 20.2 Description of the Flight Control System

The A-21 Valkyrie uses a triply redundant controls for both the primary and secondary flight control systems. Primary flight controls include the ailerons, rudder, and stabilator. The only secondary flight control surfaces are the flaps. The flight controls for all surfaces utilize an irreversible optics based, fly-by-light design. Through the use of a fly-by-light design, the A-21 is less susceptible to interference that this aircraft would experience during service. Irreversible flight controls are used to decrease the complexity of a mechanical reversible control system. For computations, three computers are connected to a voting network which send and receive flight commands. A ghosted three-view of the control systems are shown in Figures 20.2, and a close-up of the actuators and computers with labeling can be seen in Figures 20.3 and 20.4 respectively. Actuators are sized to only require two per control surface in the event of a failure. All actuators used are from the Thomson T series (Ref. 36). These are used for their wide range of stroke length and to reduce complexity by utilizing the same actuator throughout the aircraft. Furthermore, this actuator was chosen based on its ability to achieve the standard speed of 100 to 300 deg/s for stable fighter aircraft, and its ability to apply the necessary force required of 2982 lbf per actuator. Valises for the chosen actuator can be seen in Table XXII. The CAD used for the actuator is provided by Reference 37. Actuators are sized based on the hinge moments found using AAA and calculations which can be seen in Appendix E. Furthermore, the forces needed for each control surface are shown in Table XXIII.

**Table XXII:** Actuator Dimensions (Ref. 36)

| | |
|---|---|
| Length (in) | 22.05 |
| Diameter (in) | 1.57 |
| Load (lbf) | 3372 |
| Maximum, Linear Speed (in/s) | 78.7 |
| Weight (lbm) | 58.4 |

**Table XXIII:** Force Required for Each Control Surface

| Surface | Force Required (lbf) | Stroke Length (in) |
|---|---|---|
| Alleron | 5479 | 40 |
| High Lift Devices | 5750 | 40 |
| Stabolator | 5964 | 40 |
| Rudder | 5396 | 40 |

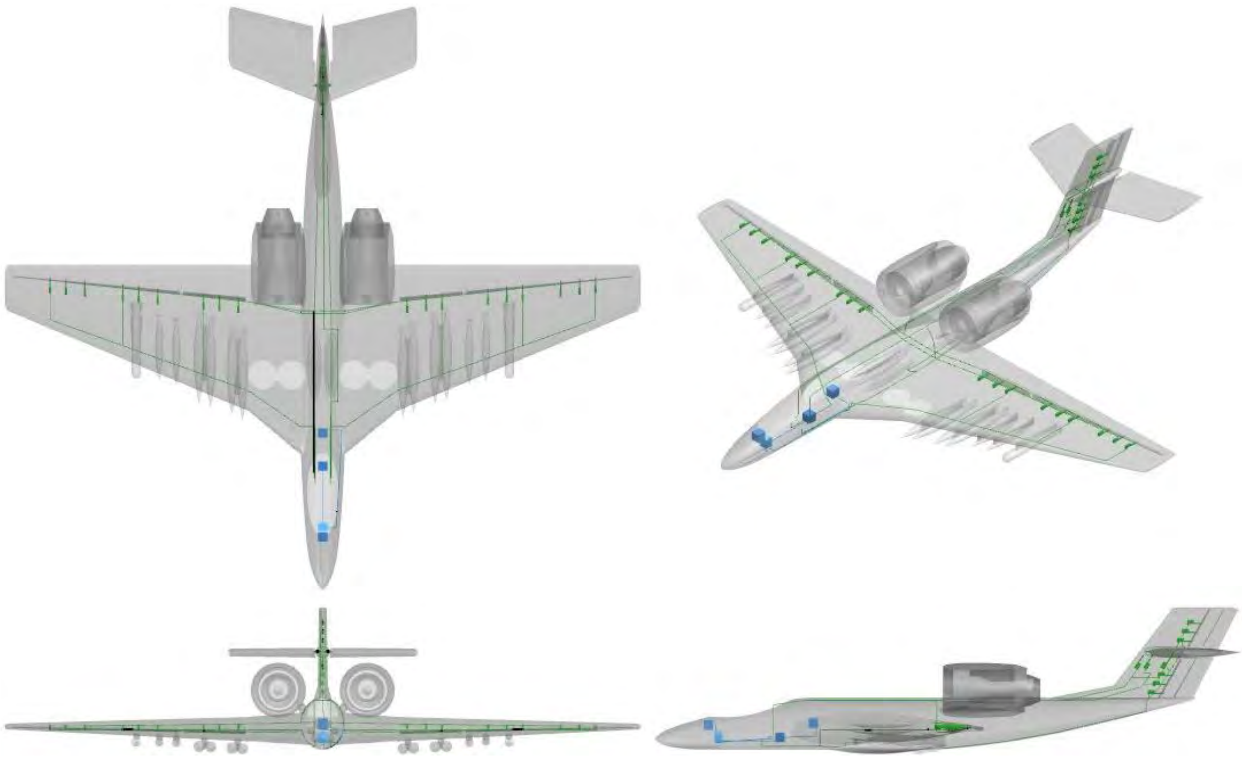

**Figure 20.2:** Flight Control System Three-View (1:250)

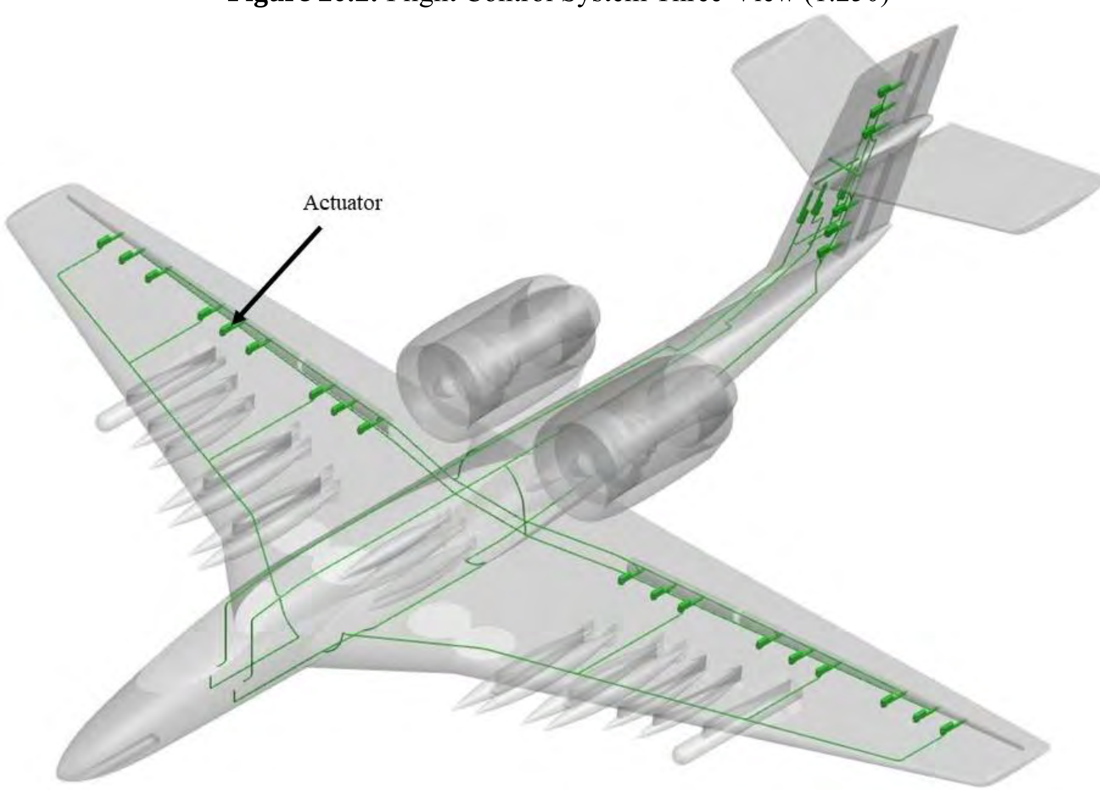


**Figure 20.3:** Actuator Optic lines (NTS)

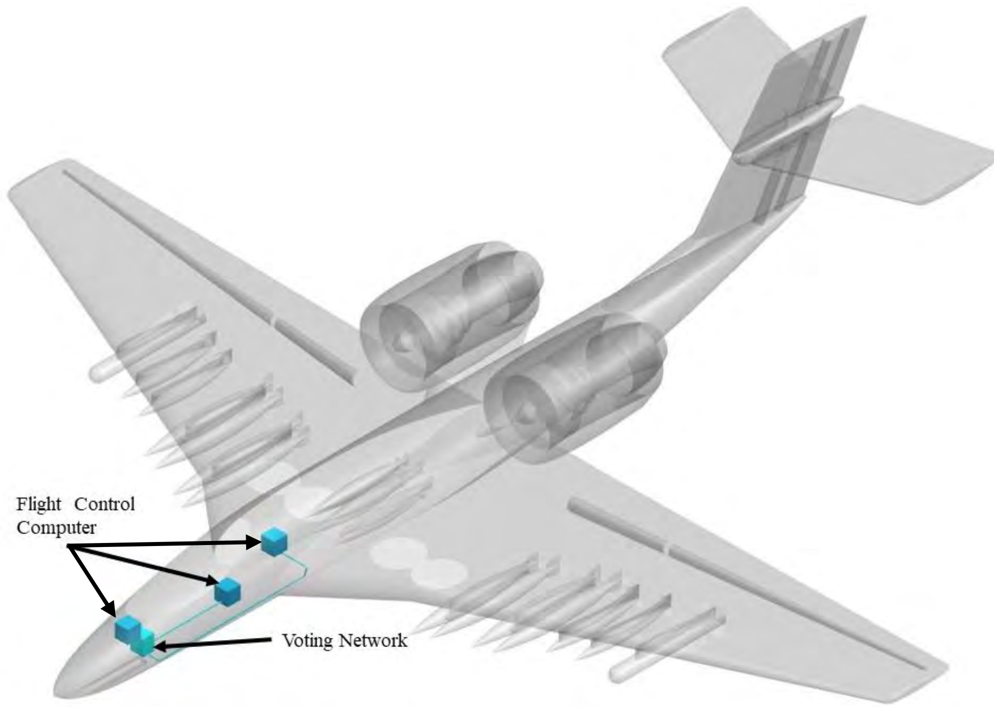


**Figure 20.4:** Computer Voting Network (NTS)

## 20.3 Description of the Fuel System

The A-21 Valkyrie II stores most of the fuel needed for its missions in the wing tanks, but a final tank is placed in the front section of the fuselage to assist with the center of gravity location. Each of the wing tanks are lined with a self-sealing bladder in the event of a puncture and are shielded in the event of a lightning strike. All fuel tanks are connected by fuel lines, pumps, and check valves to provide safety and maneuverability during operations. A fuel port on the underside of the wing is located away from bombs for ease of access. Furthermore, fuel sumps are placed at the lowest point of the tanks. These can be accessed from the aft of the aircraft. A fuel bleed/vents system is placed at the outboard sections of the wings for safe operations during operations. Slots are placed in the tanks to give room for the actuators. Each wing will have a surge tank at the wing tips for ground maneuvers. The pumps should be sized to pump 13070.4 lbm/hr. calculations for the fuel flow are shown in Appendix E. Figure 20.5 shows the fuel system layout and placement of pumps, sumps, and vents. Figure 20.6 shows a close up view for clarity.

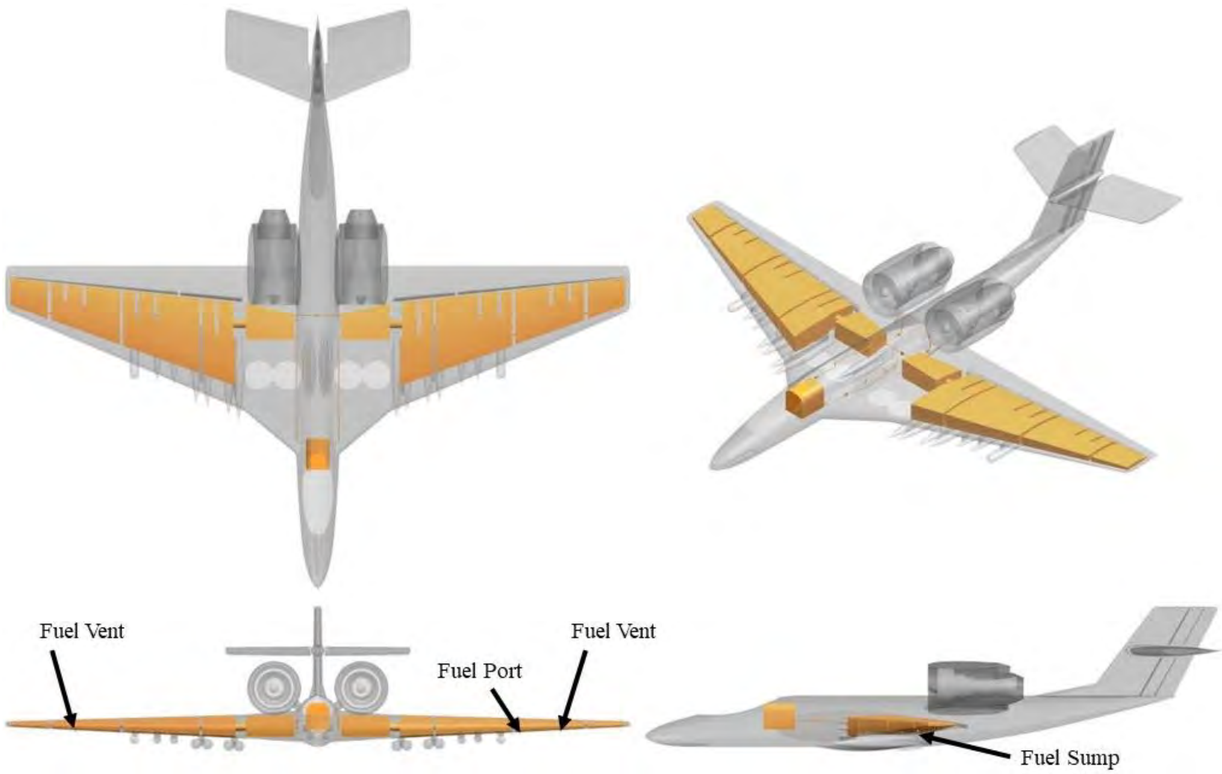


**Figure 20.5:** Fuel System Three-View (1:250)

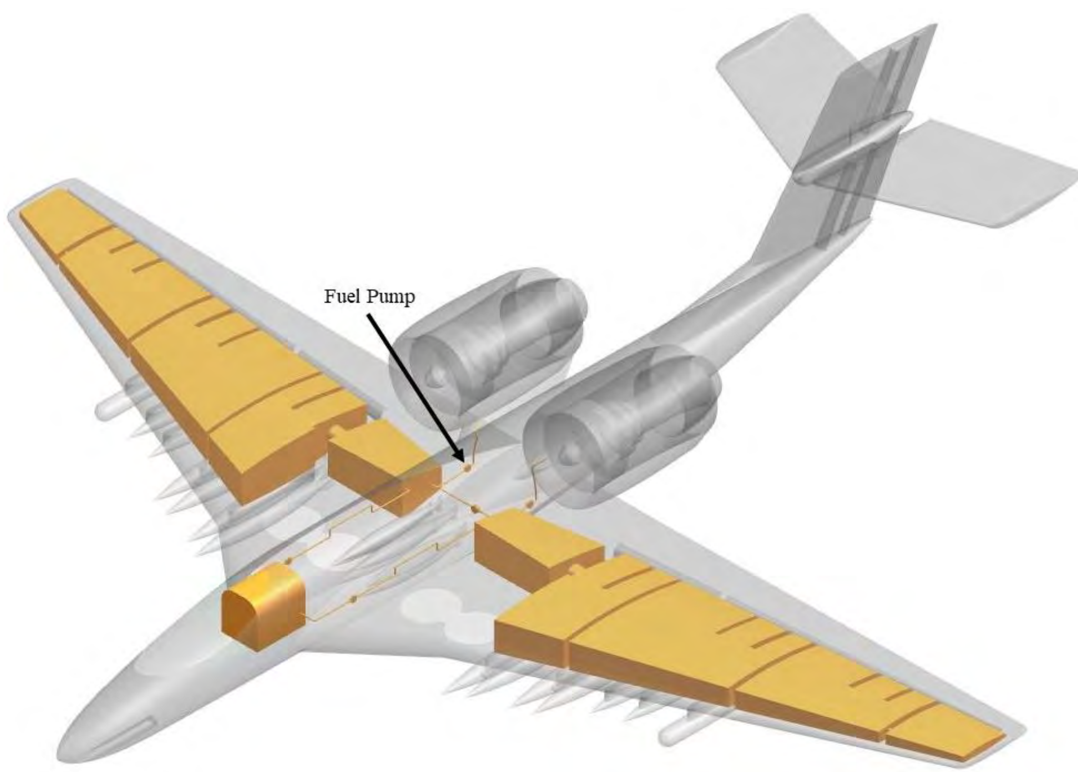


**Figure 20.6:** Fuel System Close-up (NTS)

## 20.4 Description of the Electrical System

The A-21 Valkyrie II has a triply redundant electrical system that provides power to all of the systems on the aircraft. The electrical system also provides power to external stores, lights, pumps, and cockpit. An auxiliary power unit (APU) is placed in the tail of the aircraft to provide environmental controls and other functions during engine start up. A battery is placed at the aft end of the plane to provide effective cooling and safety. Furthermore, power is also provided by the two generators near the engines which pull power off the engines while in use. Due to the use of optic control lines, the electrical lines are able to run with them. Table XXIV shows the estimated power consumed by each control surface. Figure 20.7 shows the basic layout of the electrical system, and Figure 20.8 shows a close-up of the system, with labels for the APU, battery, and generators.

Table XXIV: Estimated Power Used by Control Surfaces

| | |
|---|---|
| Alleron | 5368 W |
| High Lift Devices | 4226 W |
| Stabolator | 16801 W |
| Rudder | 3965 W |
| **Total** | **30360 W** |

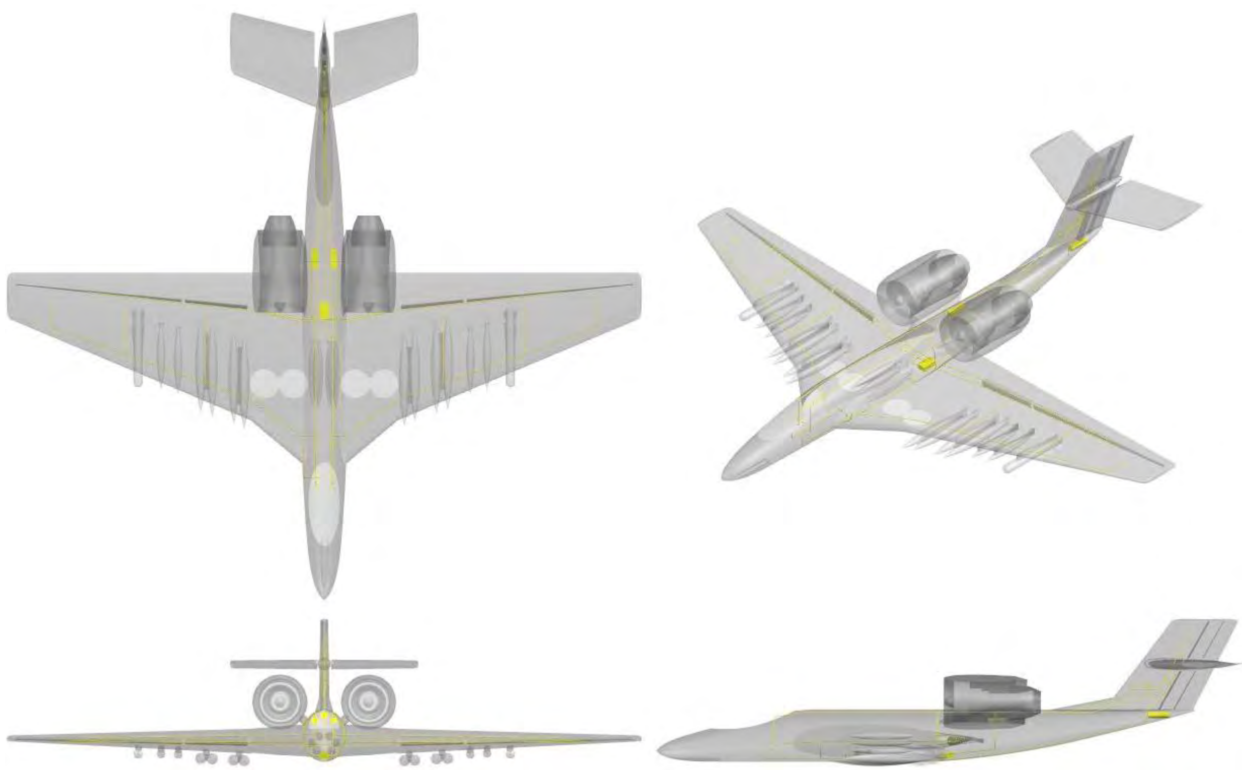

**Figure 20.7:** Electrical System Three-View

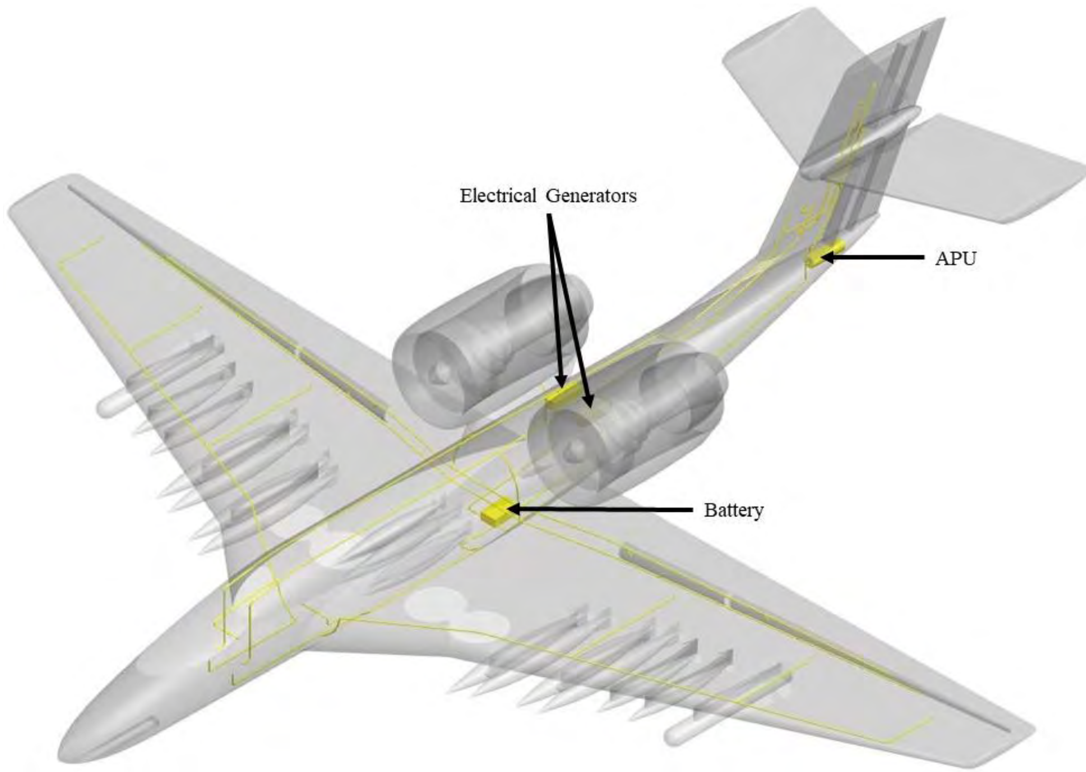


**Figure 20.8:** Electrical System Close-up (NTS)

## 20.5 Description of the Hydraulic System

The A-21 Valkyrie II implements a triply redundant hydraulic system which is used to actuate the landing gear and bomb doors. To ensure redundancy, two hydraulic reservoirs are placed above the bomb bay and can be drained easily when bombs are not loaded. Furthermore, each landing gear has two pumps to provide hydraulic fluid to the respective rotary actuators. A hydraulic accumulator is placed aft of the bomb door for ease of access. The maximum hydraulic pressure needed for this system is calculated to be 1225 psi for the main landing gear, these calculation are shown in Appendix E. A direct comparison is used to estimate the flow rate for this system to be 4 gpm, from reference 5. Figure 20.9 and 20.10 shows the placement of the hydraulic system in a three-view and a close-up labeled view respectively.

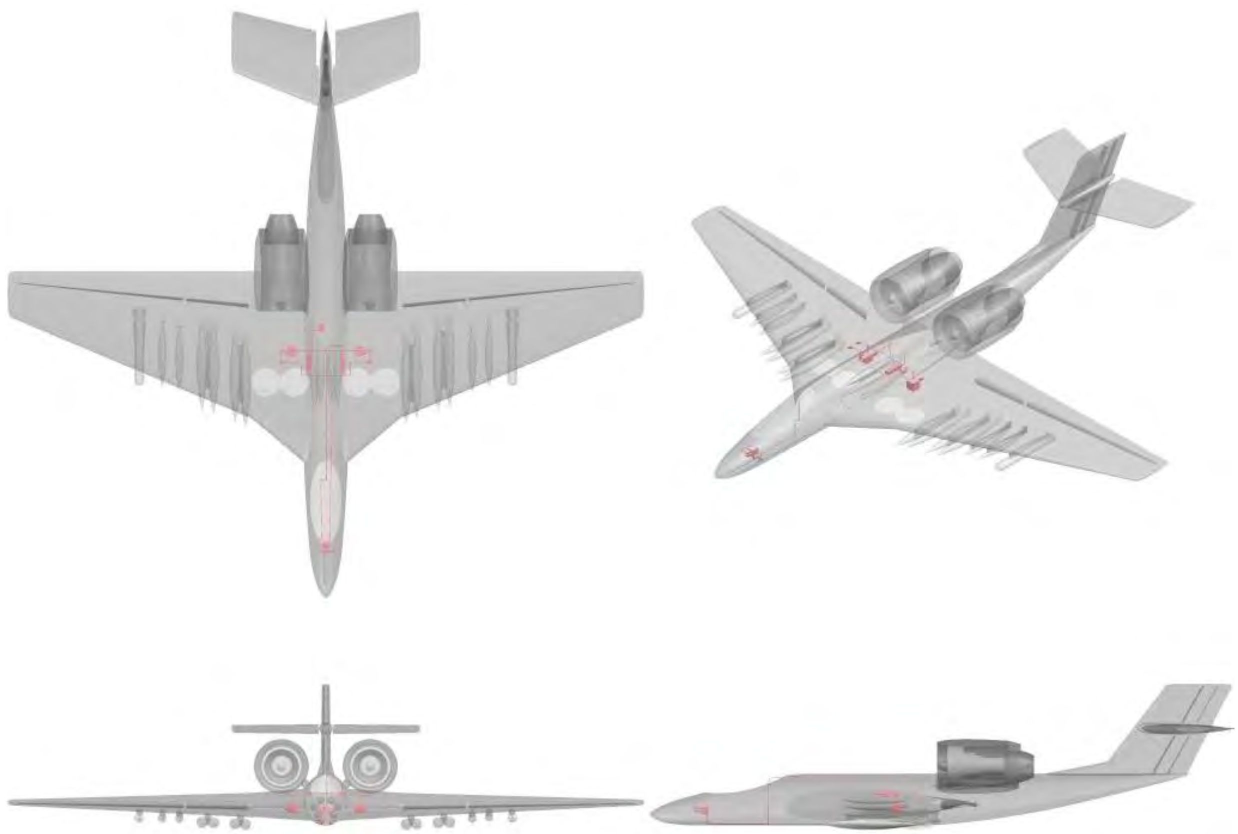

**Figure 20.9:** Hydraulic System Three-View (1:250)

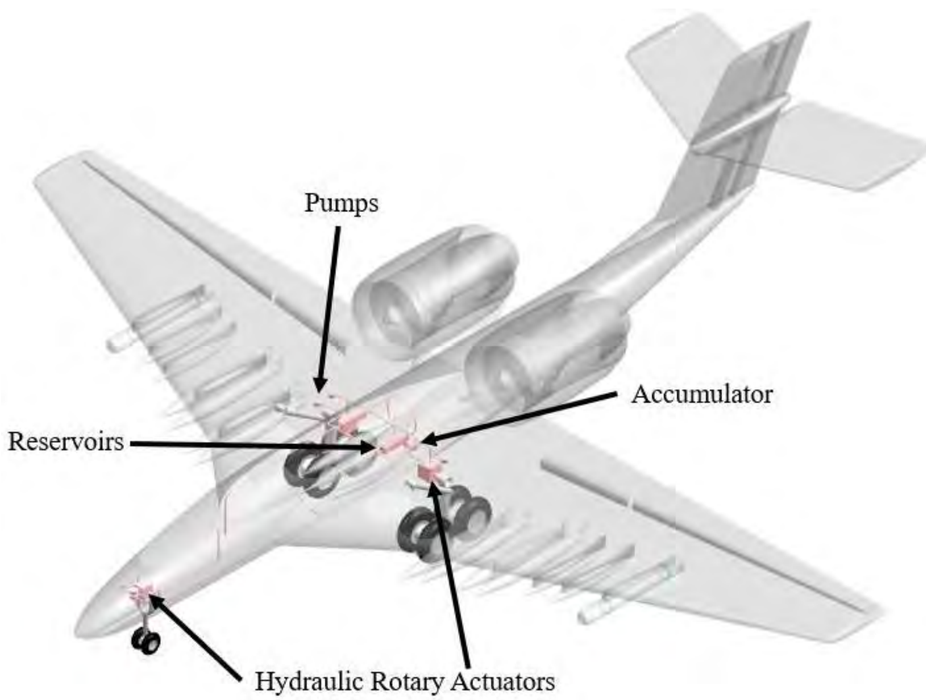


**Figure 20.10:** Hydraulic Close-up (NTS)

## 20.6 Description of the Environmental Control System

The A-21 Valkyrie II provides the ability to control the environment in the cockpit using doubly redundant bleed air taken off the engines. A heat exchanger is utilized to control the temperature of the air coming into the cockpit. This system is implemented due to the hot or frigid environments the pilots must endure during missions. The system implements a doubly redundant system by taking air from both engines and using two heat exchangers. This system allows for the pilot to control the temperature inside the cockpit doing missions. A three-view of this system can be seen in Figure 20.11, and a labeled close-up view can be seen in Figure 20.12.

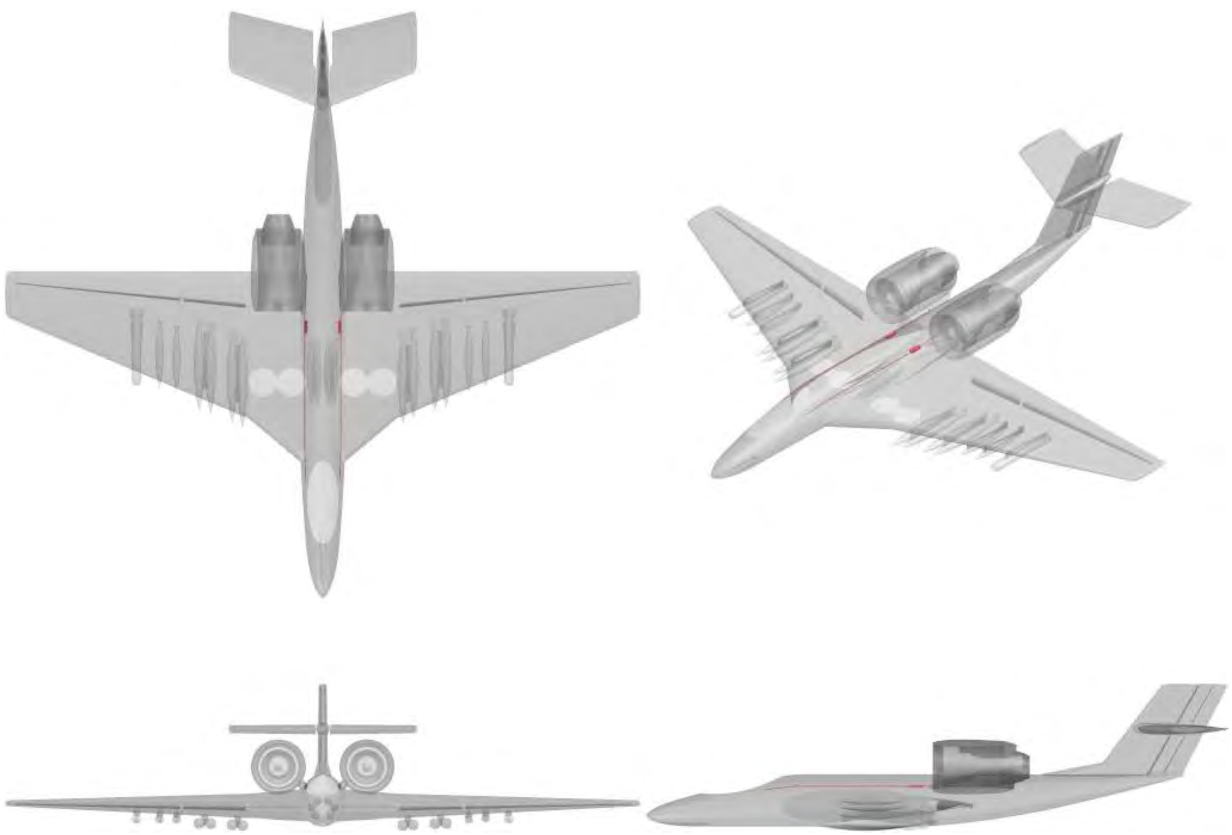

**Figure 20.11:** Environmental System Three-View (1:250)

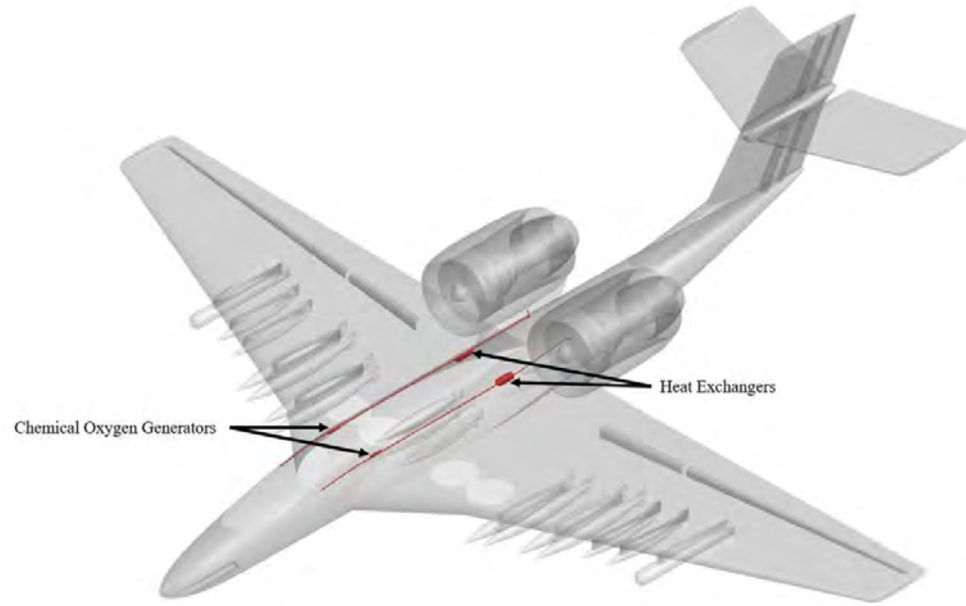


**Figure 20.12:** Environmental System Close-up (NTS)

## 20.7 Conflict Analysis

Due to the complexity of the systems there are some conflict locations that need to be addressed. The fuel tanks in the wings are placed within close proximity to the landing gear tires. This could cause a rupture in the fuel tank if the tires were to explode. Therefore, a system to deflate the tires when a maximum pressure is reached should be implemented. Due to the proximity of the electrical and optical cables that run throughout the wing, these cables should be shielded in this area.

## 20.8 Summary and Recommendations

The major findings of this chapter are that the A-21 Valkyrie is built to be robust and redundant. With a Triply redundant flight control and electrical systems, and While the environmental and the hydraulic systems are doubly redundant. Most systems are placed in easily accessible positions for maintenance and servicing. All the systems in the A-21 Valkyrie are shown in Figure 20.13 with the appropriate structure. See Tables XXII and XXIII for the actuator chosen and the required for on each control surface respectively. For the fuel system, the pumps need to pump 13070.4 lbm/hr. the electrical loads for the control surfaces are shown in Table XXIV. In the hydraulic system a maximum pressure of 1225 psi is needed and the pumps need to pump 4 gpm.

This author recommends

i. Wires should be shielded when running near or around fuel tanks;

ii. A Refueling port be added in the nose for longer unspecified missions, possibly in the future.

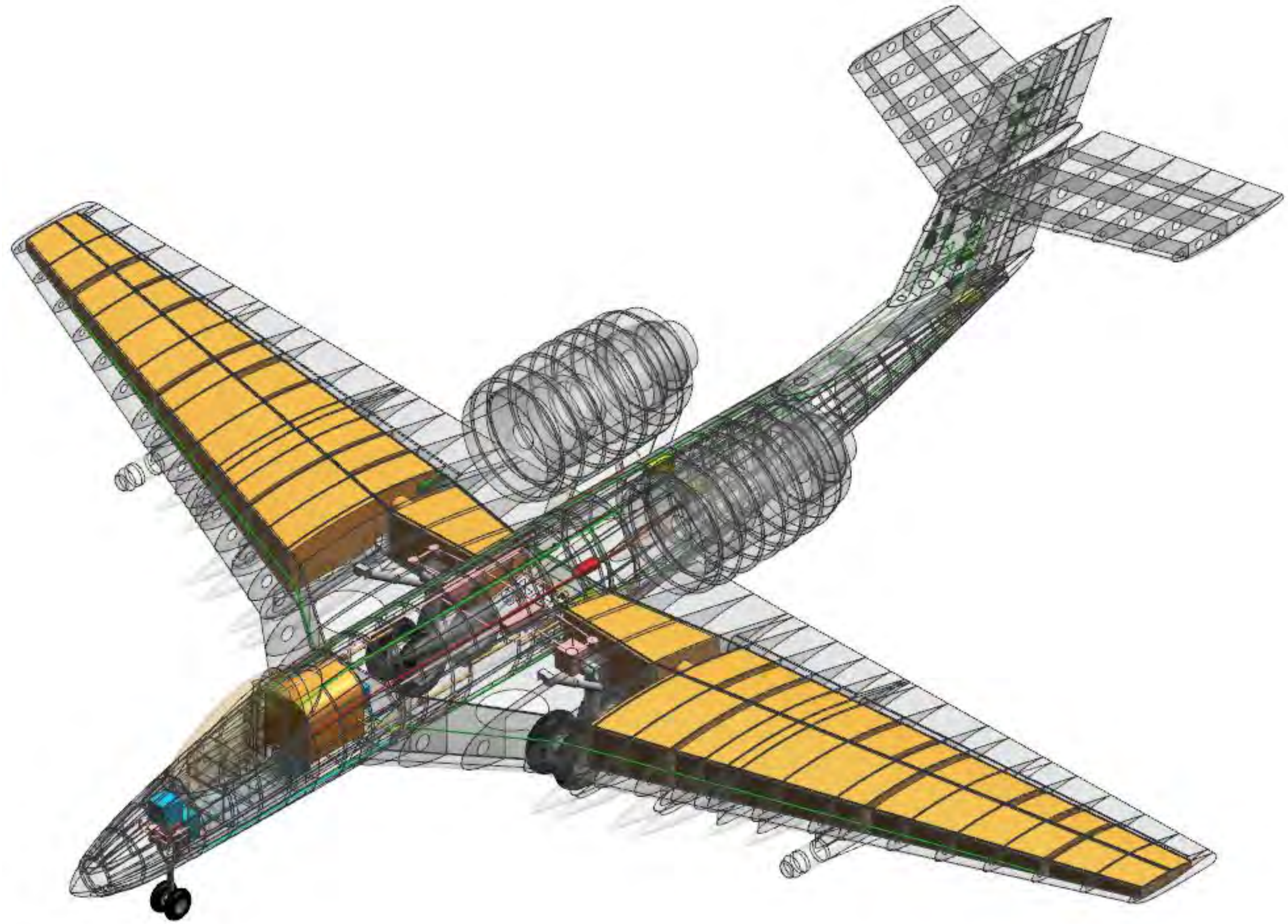



**Figure 20.13:** All Systems with Aircraft Structure (NTS)

# 21 Sizing of the Landing Gear Tires and Struts using Class II Methods

The purpose of this section is to derive the Class II analysis of the landing gear tires and struts. The methods used for Class II design in this section can be seen in *Airplane Design Part II and IV*, Reference 3 and 5. All calculations in this section can be found in Appendix E.

## 21.1 Description of Major Landing Gear Components and Disposition

The landing gear on the A-21 Valkyrie are sized to handle the worst case landing loads. As per Reference 5, United States Air Force aircraft are deigned to handle a vertical speed of 10 ft/s. To size the tire for Class II conditions the static load is found and multiplied by a factor of 1.07 for FAR 25 certification and a factor of 1.25 to allow for growth in the aircraft weight. Next, a dynamic loading is calculated and compared to the static load found earlier. This will result in the load needed to size the main and nose landing gear tires. These calculations can be seen in Appendix E. The resultant calculations demonstrate that both the nose and the main landing gear tires are sized by static loading. Tires in this aircraft are given a clearance of Tires 1.23 in radially and 2.75 in width wise on the nose gear, as well, 1.42 in radially and 3.4 in width wise on the main gear. The Tires chosen for the nose and main gear are shown in Table XXV. These tires are obtained from Goodyear in Reference 38.

**Table XXV:** Tire Dimensions (Ref. 38)

| | **W (in)** | **$D_0$ (in)** | **P (psi)** |
|---|---|---|---|
| Nose Gear Tire | 5.75 | 17.5 | 148 |
| Main Gear Tire | 10.45 | 34.45 | 95 |

Landing gear struts are then sized for diameter and stroke length for the appropriate landing loads, according to Reference 5. The struts use an oleo-pneumatic system to absorb the energy of landing with high efficiency. During landing, a load factor of 3 is used to find the worst possible strut stroke for a fighter type aircraft. Table XXVI shows the strut diameter and stroke length of the landing gear on the A-21 Valkyrie II. Calculations for the strut stroke length and diameter can be seen in Appendix E.

**Table XXVI:** Landing Gear Strut Dimensions

| | **Strut Diameter (in)** | **Strut Stroke (in)** |
|---|---|---|
| Nose Gear | 3.12 | 8.76 |
| Main Gear | 7.08 | 7.27 |

Mounting of the nose and main landing gear are done on the forward pressure bulk head and on the middle spar respectively. For the retraction of the landing gear, hydraulic rotary actuators are used to rotate and lock the gear into place. This can be seen in Section 20.5, Figure 20.10. As a locking mechanism, a rib mounted piston is used as a drag brace to prevent movement due to drag forces when extended. This system is shown on the main landing gear in Figure 21.1.

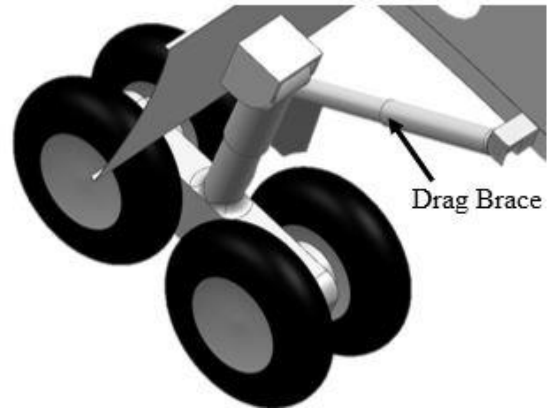


**Figure 21.1:** Drag Brace on the Main Gear

For the hydraulic rotary actuation of the landing gear, the torque required to retract the landing gear is shown in Figure 21.2. Therefore, a rotary actuator with a maximum torque of 10870 ft-lbs and 1418 ft-lbs for the main and nose gear respectively is required. The calculations used are seen in Appendix E.

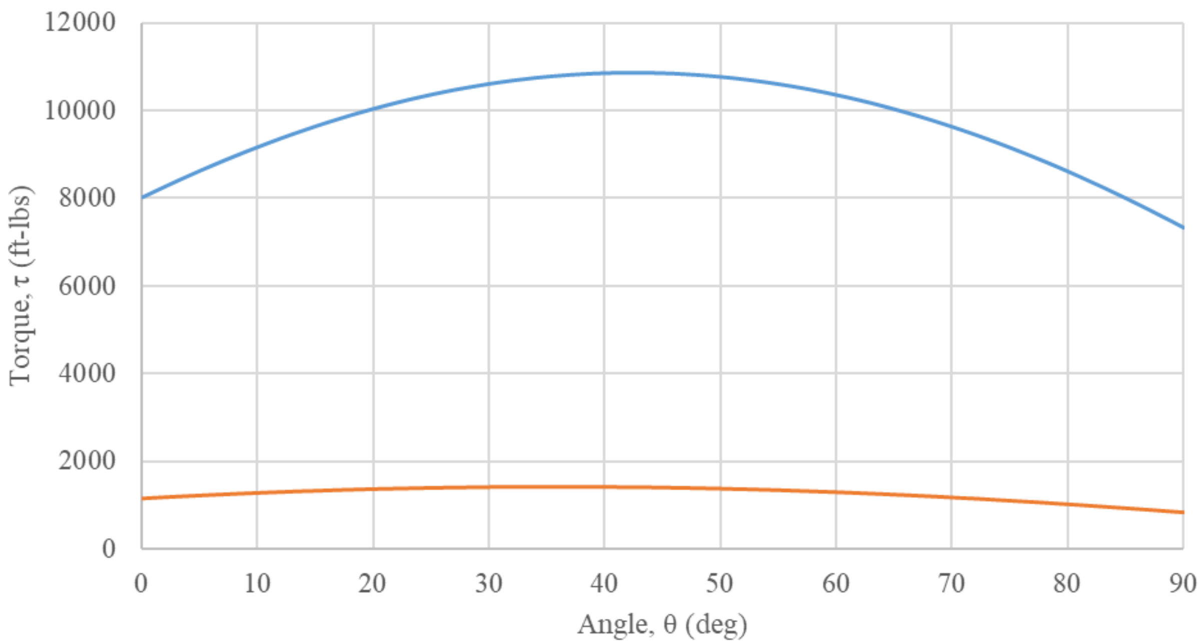


**Figure 21.2:** Landing Gear Retraction Torque

## 21.2 CAD Drawing of Landing Gear Components, Disposition and Integration into Airframe

A three view of the A-21 Valkyrie with the landing gear fully extended and fully retracted is shown in Figures 21.3 and 21.4 respectively.

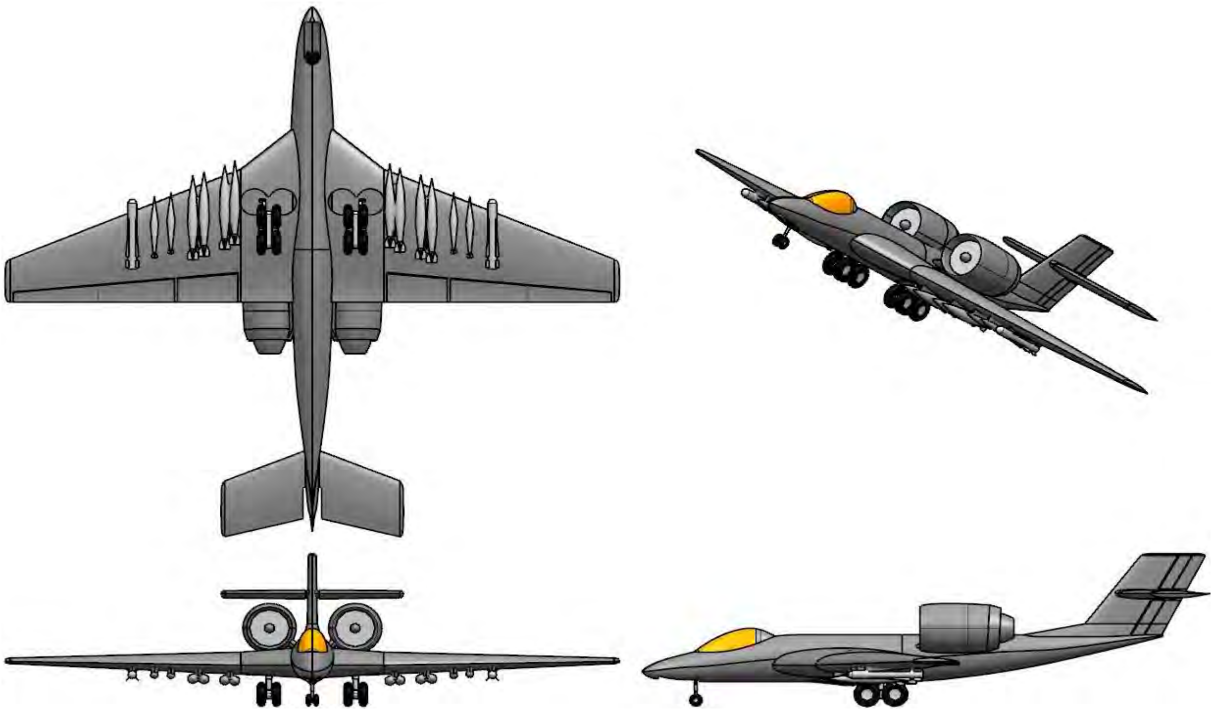

**Figure 21.3:** Landing Gear Fully Extended (1:250)

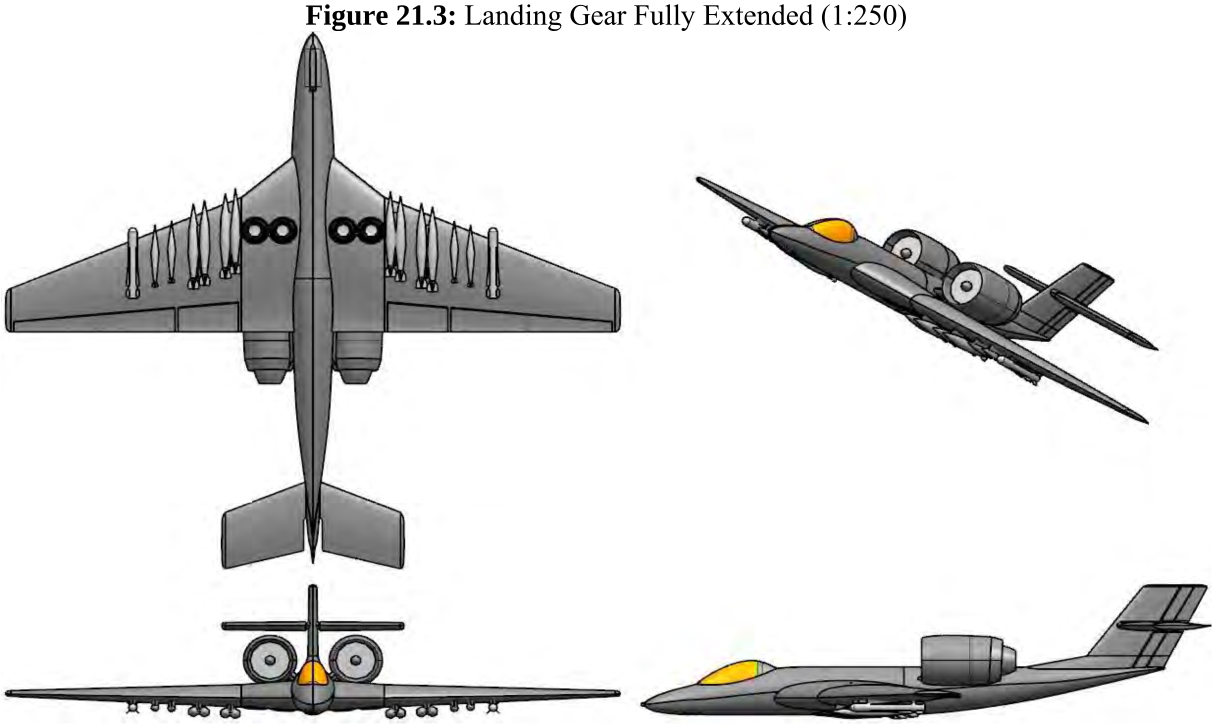

**Figure 21.4:** Landing Gear Fully Retracted (1:250)

## 21.3 Summary and Recommendations

The major findings in this section are the drag bracers used for the landing gear, the refining of the retraction of the landing gear, shown in Figure 21.3 and 21.4, and values calculated for the landing gear tires, struts, and actuators shown in Table XXVII.

**Table XXVII:** Landing Gear Tire and Strut Values

| | Main Gear | Nose Gear |
|---|---|---|
| Tire Width (in) | 10.45 | 5.75 |
| Tire Diameter (in) | 34.45 | 17.5 |
| Tire Pressure (psi) | 95 | 148 |
| Strut Diameter (in) | 7.08 | 3.12 |
| Strut Stroke (in) | 7.27 | 8.76 |
| Loads (lbf) | 96412 | 7646 |
| Retraction Torque (ft-lb) | 108070 | 1418 |

The author recommends that a finite element model be run with high fidelity using PATRAN/NASTRAN or similar finite element analysis software to verify the values calculated.

# 22 Initial Structural Arrangement

The purpose of this section is to demonstrate the preliminary layout of structures through the A-21 Valkyrie II. All method employed are from *Airplane Design Part II and III*, Reference 3 and 4.

## 22.1 Layout of Structural Components

For the loads the A-21 would experience during service, a preliminary structure is placed in this aircraft. This aircraft is most similar to that of a fighter, therefore estimating structure values will be from Reference 4. The A-21 Valkyrie will have a frame depth of 2 in. This value for frame depth is per similar fighter values in Reference 4. Furthermore, a ring frame spacing of 18.75 in is used as per Reference 4. This value is used due to it falling within the expected values for a fighter type aircraft. For similar reasons the longerons are given a spacing of 10 in. Frames are placed around landing gear and bomb doors for structural support and to carry load paths. Ring frames around the engines and spars are given an increased depth to incorporate the extra load. Two bulk head are placed forward and aft of the cockpit to support the landing gear and protect the pilot. A titanium bathtub will be built into the forward and aft bulk head for structural support and protection of the pilot.

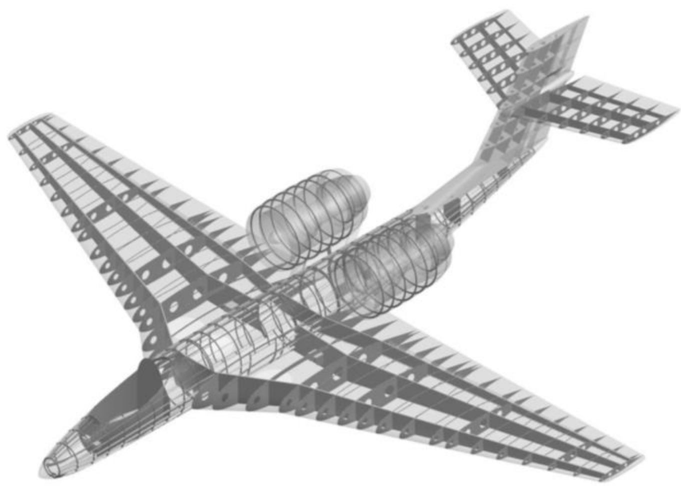

**Figure 22.1:** A-21 Preliminary Structure (NTS)

For the wings and empennage fighters have a wide variation in rib spacing. Therefore, ribs are placed at the necessary points on the wing such as the crack, external stores, and control surfaces. To fill the gaps without ribs, a 24 in rib spacing is used. This value is chosen for its similarity to some other aircraft. Throughout the ribs of the wing and empennage, lightening holes are used to decrease the weight of the overall structure. A three spars concept is used in the wings and empennage for extra structural support in the event of damage. Spars are placed at 15%, 45%, and 74% of the cord in the wing and empennage. The extra structure of the mid spar gives a favorable space to incorporate the main landing gear mounting point.

## 22.2 CAD Drawings of Structural Layout

A three-view of the internal structural layout of the A-21 Valkyrie II is shown below in Figure 22.2.

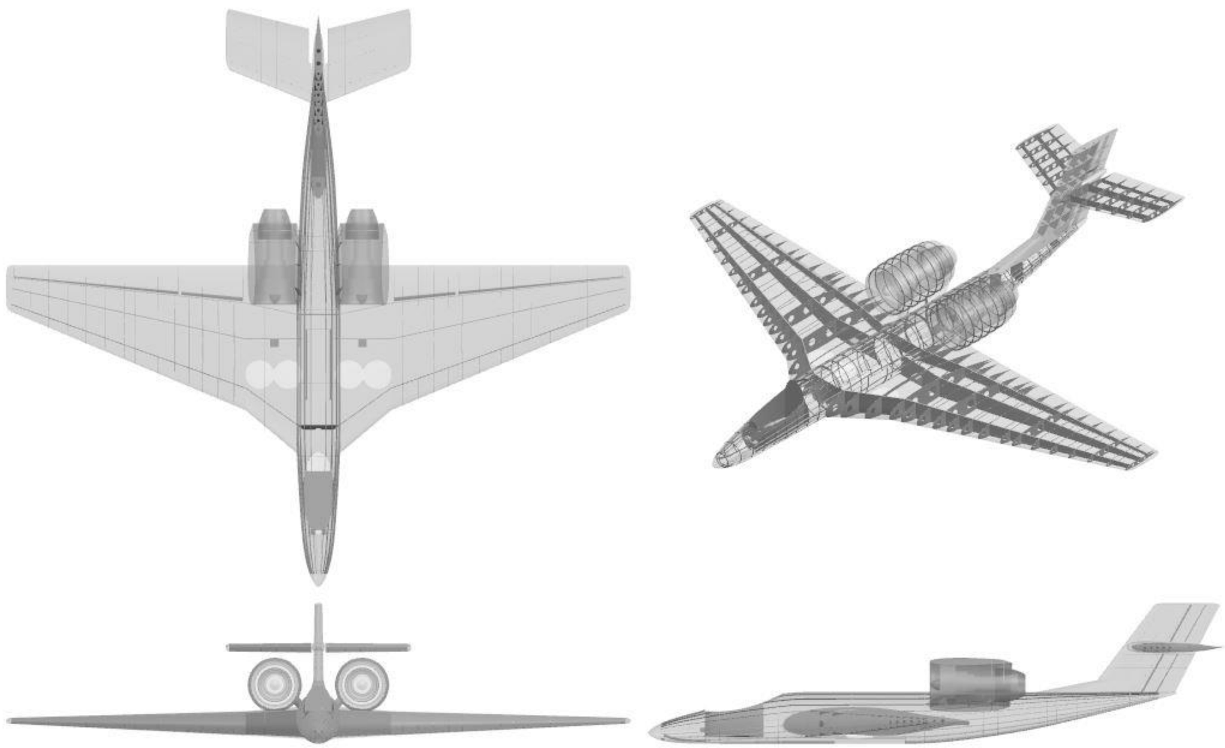

**Figure 22.2:** Structural Layout Three-View (1:250)

## 22.3 Summary and Recommendations

The major findings of this chapter are that the A-21 Valkyrie II has ring frame and longeron spacing of 18.75 in and 10 in respectively. The wings and empennage have ribs at structural points and a spacing of 24 in. Spars are placed at 15%, 45%, and 74% of the wing or empennage cord length.

This author recommends a finite element model be run with high fidelity using PATRAN/NASTRAN or similar finite element analysis software. This is to determine if more or less structure would be required to handle loads experienced in service.

# 23 Class II Weight and Balance

This section outlines the Class II weight and balance aspects and calculations made with the A-21 Valkyrie II. The methodology used for the Class II weight and balance calculations are derived from *Airplane Design Part II & V,* References 3 and 6.

## 23.1 Class II Weight & Balance Calculations

By using the Class I weight estimation values found in Section 14, the weight of the structures in the aircraft can be calculated using AAA and formulas found in Reference 6. The structural weights of the fuselage, wings, empennage, and nacelles can be calculated using AAA. Additionally, the weights associated with each of the aircraft systems, those in Section 20 and more, are calculated using AAA. Some values, which are associated with that of testing equipment, are estimated using the Appendix of Reference 6. All weights calculated were within the acceptable values for similar aircraft.

## 23.2 Class II CG Positions on the Aircraft, CG Excursion

Using the weights of each component calculated, the center of gravity for each individual component can be estimated. The estimations for the center of gravity are performed using References 3 and 6, as well as the visual representations in the CAD model. Positioning of the external stores was performed to position their center of gravity close to the operating empty weight center of gravity; this is done per Reference 3. Furthermore, the armor associated with the titanium bathtub and fuel tanks are estimated based on similar aircraft. The weights and their associated weight fractions for each structure, system, and removable item are shown in Table XXVIII. The center of gravity for each component is estimated to be on BL 0.0 due to the symmetry of the A-21. Figure 23.1 shows the center of gravity for each component and system when the landing gear is down.

**Table XXVIII:** A-21 Weights and Weight Fractions of All Components

| Number | | W (lbf) | W Fraction |
|---|---|---|---|
| 1 | Wing | 5809 | 0.076 |
| 2 | Fuselage | 4860 | 0.064 |
| 3 | Horizontal Tail | 916 | 0.012 |
| 4 | Vertical Tail | 467 | 0.006 |
| 5 | Necelle | 545 | 0.007 |
| 6 | Engines | 8400 | 0.110 |
| 7 | M Landing | 2084 | 0.027 |
| 8 | N Landing | 328 | 0.004 |
| 9 | Armor / Ti Bathtub | 3756 | 0.049 |
| | **Fixed Equipment** | | |
| 10 | Fuel System | 749 | 0.010 |
| 11 | Propulsion System | 448 | 0.006 |
| 12 | Flight Controlls | 1676 | 0.022 |
| 13 | Hydraulic System | 747 | 0.010 |
| 14 | Avionics | 1155 | 0.015 |
| 15 | Electrical System | 847 | 0.011 |
| 16 | APU | 311 | 0.004 |
| 17 | Air Systems / De-Iceing | 720 | 0.009 |
| 18 | Oxygen System | 17 | 0.000 |
| 19 | Furnishing | 192 | 0.003 |
| 20 | Armament System | 1500 | 0.020 |
| 21 | Other (Paint/testing) | 1373 | 0.018 |
| 22 | Bushmaster III | 550 | 0.007 |
| | **WE** | **37449** | **0.490** |
| 23 | Trapped Fuel and Oil | 382 | 0.005 |
| 24 | Crew | 200 | 0.003 |
| | **WOE** | **38031** | **0.498** |
| 25 | Fuel Wing | 20509 | 0.268 |
| 26 | Fuel FL | 1228 | 0.016 |
| 27 | Bomb Bay | 3000 | 0.039 |
| 28 | Ex Bombs | 11000 | 0.144 |
| 29 | Ammo | 2625 | 0.034 |
| | **WTO** | **76393** | **1.000** |

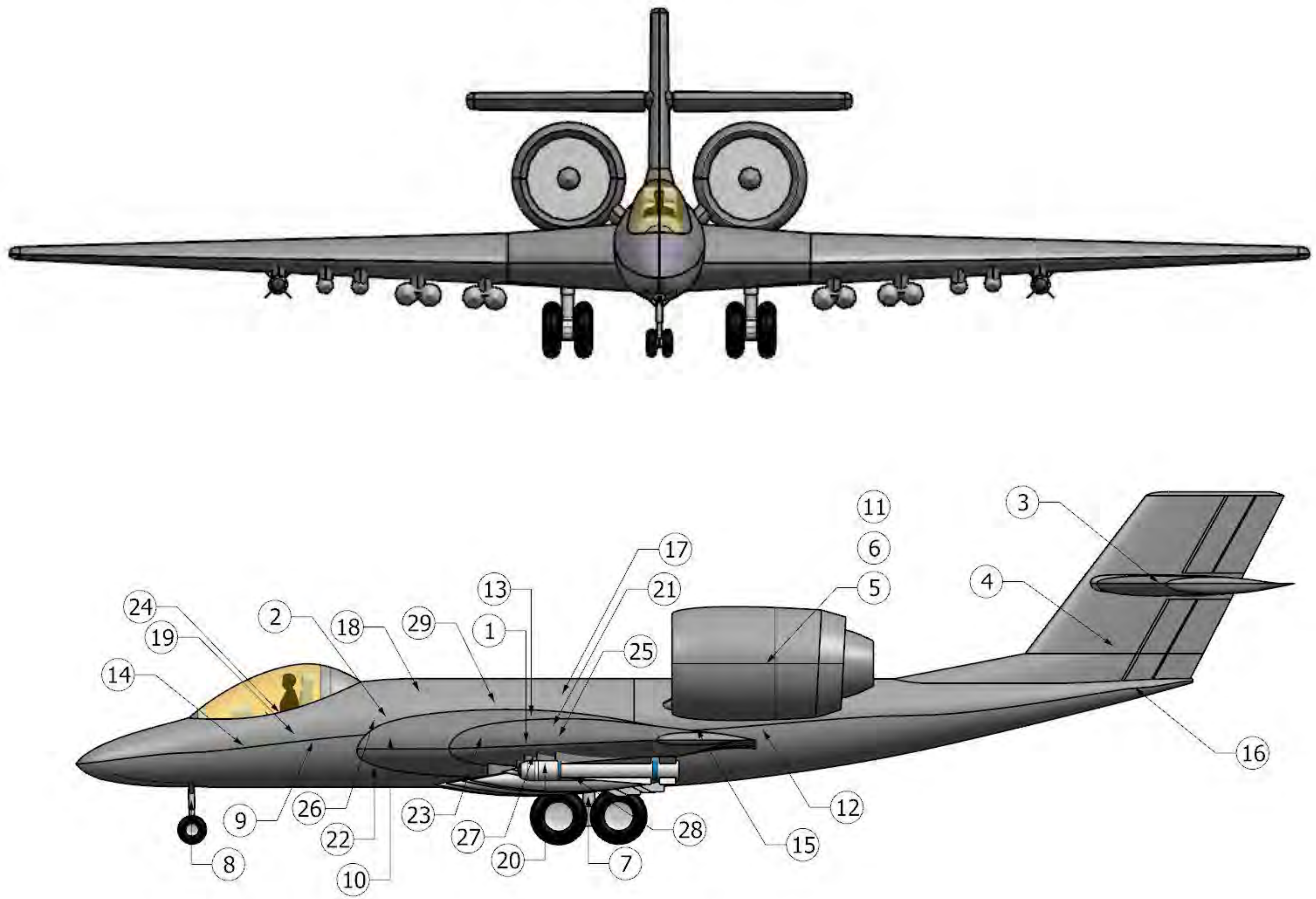


| Number | | WL (in) | FS (in) |
|---|---|---|---|
| 1 | Wing | 110 | 400 |
| 2 | Fuselage | 119 | 270 |
| 3 | Horizontal Tail | 203 | 760 |
| 4 | Vertical Tail | 197 | 740 |
| 5 | Necelle | 160 | 505 |
| 6 | Engines | 160 | 505 |
| 7 | M Landing | 84 | 412 |
| 8 | N Landing | 80 | 170 |
| 9 | Armor / Ti Bathtub | 120 | 260 |
| | **Fixed Equipment** | | |
| 10 | Fuel System | 121 | 370 |
| 11 | Propulsion System | 140 | 505 |
| 12 | Flight Controlls | 125 | 465 |
| 13 | Hydraulic System | 127 | 360 |
| 14 | Avionics | 105 | 200 |
| 15 | Electrical System | 118 | 450 |
| 16 | APU | 147 | 730 |
| 17 | Air Systems / De-Iceing | 135 | 350 |
| 18 | Oxygen System | 137 | 304 |
| 19 | Furnishing | 117 | 220 |
| 20 | Armament System | 95 | 350 |
| 21 | Other (Paint/testing) | 122 | 360 |
| 22 | Bushmaster III | 96 | 270 |
| | **WE** | | |
| 23 | Trapped Fuel and Oil | 114 | 400 |
| 24 | Crew | 129 | 225 |
| | **WOE** | | |
| 25 | Fuel Wing | 114 | 408 |
| 26 | Fuel FL | 119 | 264 |
| 27 | Bomb Bay | 120 | 375 |
| 28 | Ex Bombs | 93 | 385 |
| 29 | Ammo | 114 | 330 |
| | **WTO** | | |

**Figure 23.1:** Class II CG Locations (1:80)

Utilizing the preliminary center of gravity locations shown above in Figure 23.1, the center of gravity for the aircraft at different ground and flight conditions is found. The center of gravity for the A-21 is calculated when the aircraft is at empty weight, operating empty weight, and take-off weight. Additionally, the center of gravity for the aircraft is found when there are no munitions but full fuel, and vice versa. These calculations are also performed when the landing gear are fully deployed and stowed away. The movement of the center of gravity can be seen when the landing gear is deployed and stowed in Figure 23.2, case 1 and 2 respectively. Figure 23.2 shows that the center of gravity for the aircraft shifts a maximum of 4.91% of the mean geometric cord when the landing gear is down and 4.80% when the landing gear is stowed. The center of gravity shifts that result are within the allowable range for aircraft of this class.

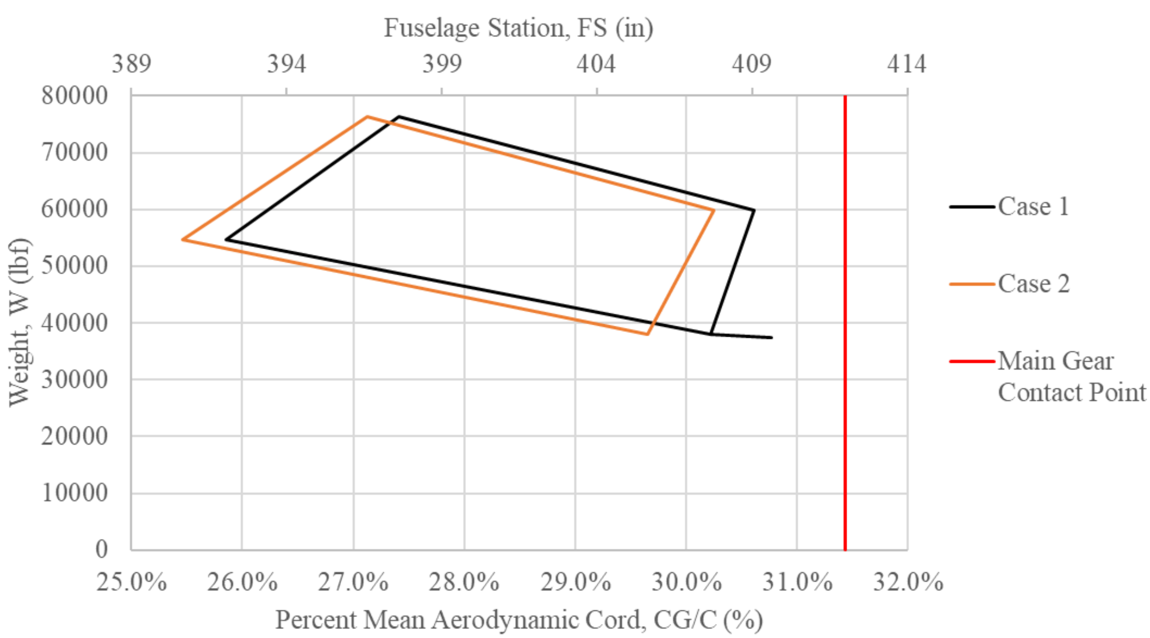


**Figure 23.2:** Class II C.G. Excursion Diagram for the A-21

Moments of inertia where calculated for each component and the entire airplane using Reference 6 and AAA, sown in Appendix F. Table XXIX shows the moments of inertia for the A-21 and all components.

**Table XXIX:** Moments of Inertia

| | Ixx (Slugs-ft$^2$) | Iyy (Slugs-ft$^2$) | Izz (Slugs-ft$^2$) | Ixy (Slugs-ft$^2$) | Iyz (Slugs-ft$^2$) | Izx (Slugs-ft$^2$) |
|---|---|---|---|---|---|---|
| Wing | 364040.7236 | 612930.8063 | 248890.0827 | 0 | 0 | -301008.5145 |
| Fuselage | 2982.855061 | 141353420.6 | 139617522.9 | 0 | 0 | 15567971.58 |
| Horizontal Tail | 6599244.027 | 408682823.1 | 398966040 | 0 | 0 | 62262882 |
| Vertical Tail | 2908443.227 | 195844806.6 | 191447040 | 0 | 0 | 29016192 |
| Necelle | 955876.6948 | 91338862.5 | 89377222.5 | 0 | 0 | 13241070 |
| Engines | 14735482.17 | 1408050000 | 1377810000 | 0 | 0 | 204120000 |
| M Landing | 2496908.062 | 203402980.1 | 202835692.8 | 0 | 0 | -10726887.6 |
| N Landing | 476251.0355 | 1737340 | 1606220 | 0 | 0 | -458920 |
| Armor / Ti Bathtub | 13323.91209 | 97654699.43 | 96152319.44 | 0 | 0 | 12019039.93 |
| **Fixed Equipment** | | | | | | |
| Fuel System | 6230.759666 | 54961745.4 | 54631260 | 0 | 0 | 4249098 |
| Propulsion System | 214540.8122 | 74200000 | 73483200 | 0 | 0 | 7257600 |
| Flight Controlls | 79402.74953 | 224305830 | 223258455 | 0 | 0 | 15291675 |
| Hydraulic System | 58942.23273 | 51034930.1 | 50490440 | 0 | 0 | 5243238 |
| Avionics | 198624.4165 | 11573862.5 | 11545000 | 0 | 0 | 577250 |
| Electrical System | 11.50666879 | 104056492.8 | 103782000 | 0 | 0 | 5337360 |
| APU | 259619.8933 | 124202720.8 | 123515280 | 0 | 0 | 9214632 |
| Air Systems / De-Iceing | 205350.8555 | 45907490 | 45025000 | 0 | 0 | 6303500 |
| Oxygen System | 6026.286373 | 726446.5 | 703310.4 | 0 | 0 | 127561.2 |
| Furnishing | 238.7364735 | 2812943.5 | 2757600 | 0 | 0 | 390660 |
| Armament System | 801561.7593 | 93787500 | 93750000 | 0 | 0 | -1875000 |
| Other (Paint/testing) | 20711.077 | 93499757.2 | 92835080 | 0 | 0 | 7855276 |
| Bushmaster III | 269027.7824 | 15903800 | 15895000 | 0 | 0 | -374000 |
| **WE** | **30672841.58** | **3445651382** | **3389732573** | **0** | **0** | **384339189.6** |
| Trapped Fuel and Oil | 6472.765703 | 34451814.43 | 34376949.08 | 0 | 0 | 1604257.624 |
| Crew | 23689.93235 | 3293200 | 3125000 | 0 | 0 | 725000 |
| **WOE** | **30703004.28** | **3483396396** | **3427234522** | **0** | **0** | **386668447.2** |
| Fuel Wing | 347542.8912 | 1949580418 | 1945560664 | 0 | 0 | 88434575.66 |
| Fuel FL | 958.7121499 | 33480682.51 | 33037254.17 | 0 | 0 | 3827486.763 |
| Bomb Bay | 10642.24404 | 228075000 | 226875000 | 0 | 0 | 16500000 |
| Ex Bombs | 6939247.408 | 894014000 | 893475000 | 0 | 0 | -21945000 |
| Ammo | 44483.03117 | 139377000 | 138862500 | 0 | 0 | 8452500 |
| **WTO** | **38045878.56** | **6727923497** | **6665044941** | **0** | **0** | **481938009.6** |

## 23.3 Summary and Recommendations of Class II Weight and Balance

The major findings in this chapter are that the center of gravity shift when gears are down and up are 4.91% and 4.80% sift along the mean geometric cord of the wing respectively. The center of gravity shift is within a reasonable margin for this class of aircraft.

This author recommends that additional iterations be performed to achieve a more accurate and favorable center of gravity placement.

# 24 Class II Weight and Balance Analysis

The Purpose of this section is to show the analysis of the A-21 Valkyrie II weight and balance found in Section 23. The methodology used is from *Airplane Design Part II & V,* References 3 and 6.

## 24.1 Class II Weight and Balance Analysis

Based on the calculations performed in Section 23, the A-21 Valkyrie II has an acceptable weight and balance. The A-21 satisfies all tip over requirements for an aircraft of this caliber. When calculated, the Class II CG is approximately 3 inches off from the Class I CG. Thus, the Class II CG is in an acceptable range. The CG excursion of this aircraft is within acceptable ranges according to Figure 23.2 and Reference 6.

## 24.2 Summary and Recommendations of Class II Weight and Balance Analysis

The author concludes that through weight and balance analysis, the current deign of the A-21 Valkyrie II meets all criteria for Class II weight and balance as specified by Reference 6. Furthermore, the A-21 has become marginally more unstable from the Class I analysis due to the more accurate determinate of weights and weight locations.

The author recommends the further iterations be performed on the weight and balance of the A-21 to achieve a more favorable stability.

# 25 Updated 3-View

This section displays the most accurate and recent three-view of the A-21 Valkyrie II. This section also shows the future variants of the A-21 family of aircraft.

## 25.1 Updated 3-View

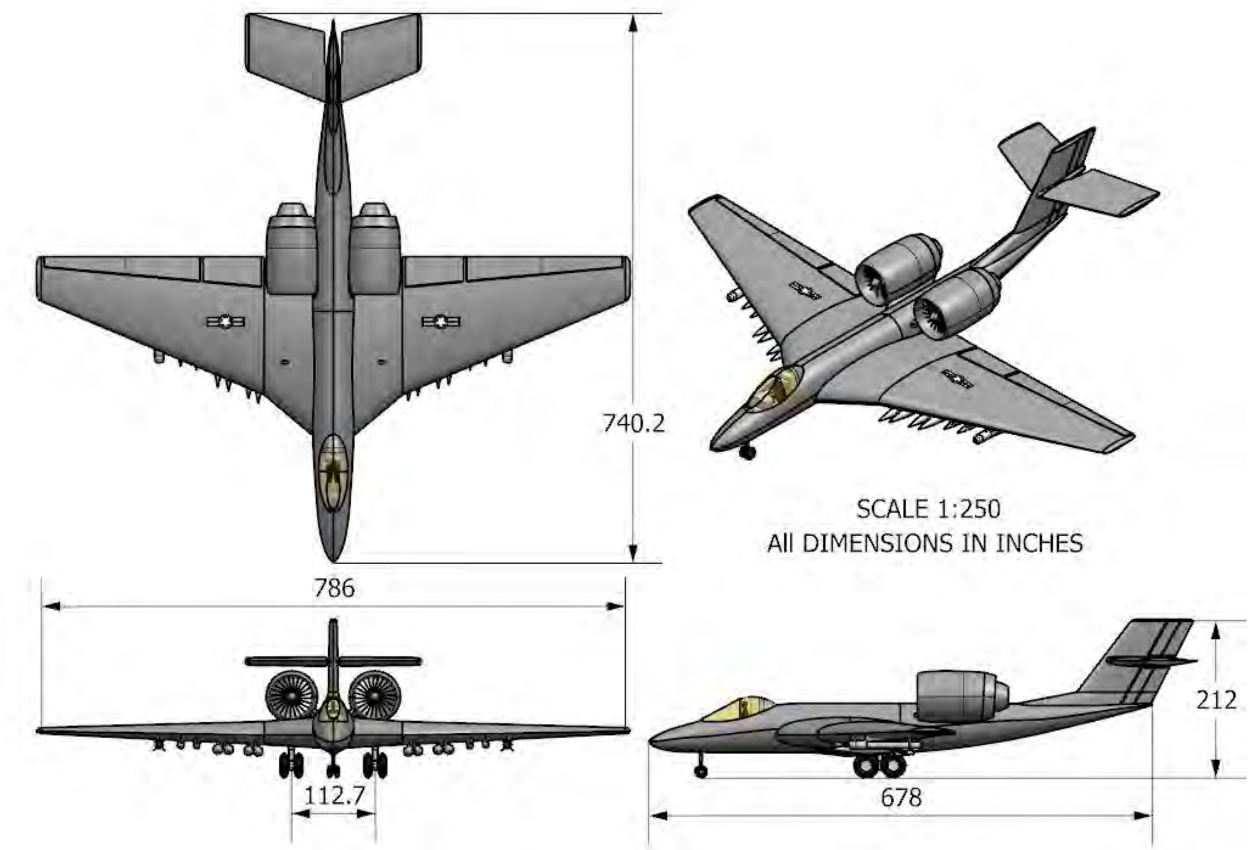


**Figure 25.1:** Updated Three-View (1:250)

The A-21 Valkyrie II is designed with future variants in mind. Therefore, the A-21 will have a 100 series where a new or improved engine may be installed in place of the current one to provide the aircraft with more thrust and better fuel economy. Also, winglets may be used for an even greater fuel economy boost. A 200 series engine with the addition of a fuselage plug to further expand the size and amount of internal stores will be offered. The final series offered will be piloted by an artificial intelligence once the technology is available for this usage. The cockpit and titanium bathtub will be substituted for an AI system and Kevlar shielding. Figure 25.2 shows how the A-21 will be changed for each variant in the family of aircraft.

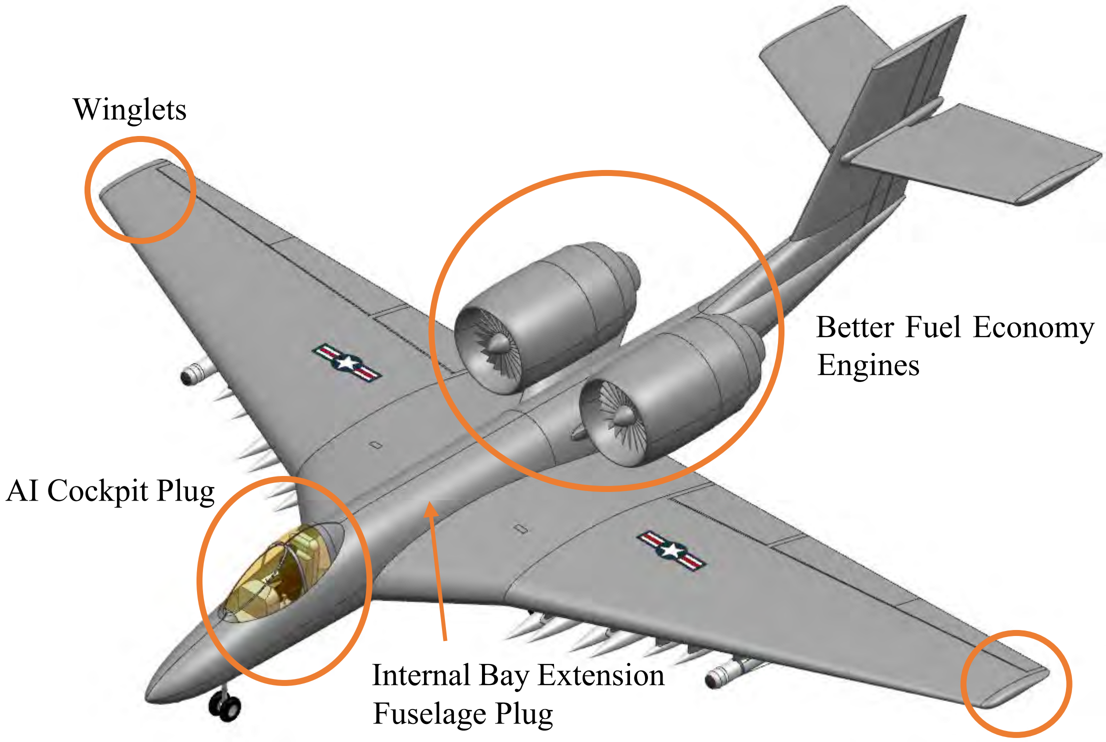


**Figure 25.2:** Display of Changes Made with Variances (NTS)

## 25.2 Summary and Recommendations

This displays the final three-view of the A-21 Valkyrie and the three variants in this family of aircraft are shown above.

The author recommends more research be conducted regarding the time frame for the recommended technologies.

# 26 Advanced Technologies

The A-21 Valkyrie II will encompass the most advanced technologies to stay ahead of the curve in both the market and the battlefield. Because the A-21 has a design fixed date of 2020, this allows time for the development and certification of new technology. Therefore, the possibility for the availability of guided ammunition could be achieved by the time of the design fix date or for a future upgrade. This technology of guided ammunitions is a new field of study for many research groups. The Defense Advanced Research Projects Agency (DARPA) has been doing research into the field of advanced ballistic technology through the EXACTO program. This program has shown that with the use of a self-steering bullet, an increase in the accuracy with difficult and long-distance shots, as well as the accuracy on moving targets is achieved, per Reference 39. Figure 26.1 shows the results of an EXACTO program ammunition test on a moving target. This technology of guided ammunition is currently being studied at the University of Kansas by graduate student Lauren Shumacher. This research at the University of Kansas shows that guided ammunition could be as effective, or  more effective than missiles at air-to-air combat (Reference 40).

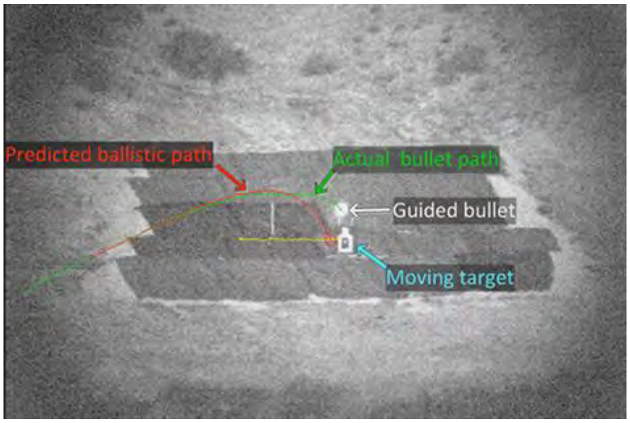


**Figure 26.1:** EXACTO Round Test (Ref. 39)

The current weapons system of the aircraft will also be equipped with a highly advanced targeting system. This will enable the aircraft to hit targets more accurately and at longer ranges. Furthermore, an advanced communications array will be installed to communicate and survey with other supporting aircraft to make the most optimal tactical decisions. Electronic warfare should be further researched for inclusion in the A-21 arsenal. This would increase the competitiveness of the A-21 in the market because of the trend seen in the fighter aircraft currently being sold.

# 27 Risk Mitigation

Many steps in the design process where taken to manage the risks that would be associated with this design. First, for center of gravity and volume constraints, a fuel tank is placed relatively close to the pilot. Thus, steps were taken to decrease and minimize the overall risk to the pilot of this aircraft. A titanium bulk head was placed between the pilot and the fuel tank in the case of a tank rupture during the operation of the aircraft. Further action was taken by designing the fuel tank with a self-sealing bladder for when the aircraft would take on ground fire. Figure 27.1 shows the fuel tank proximity and the aft bulkhead protection.

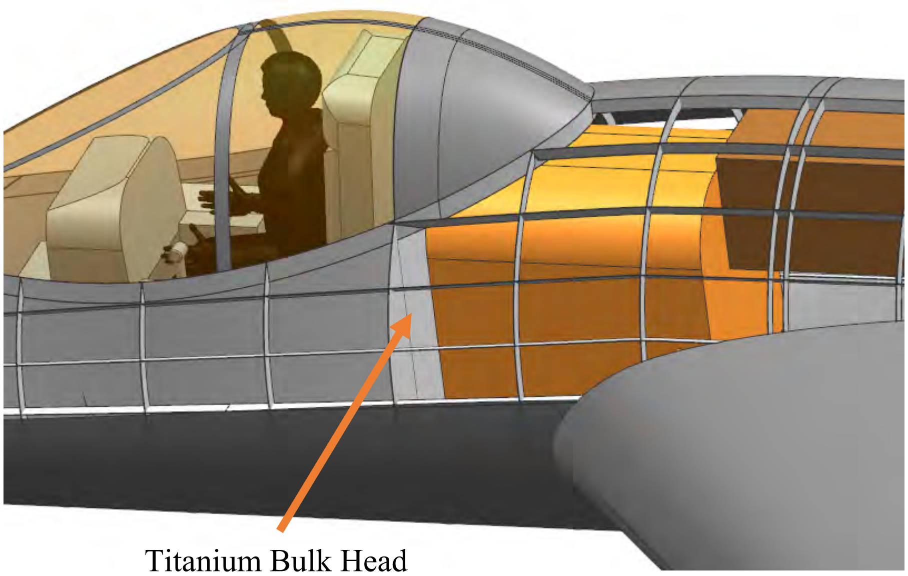


**Figure 27.1:** Protective Titanium Bulk Head

The titanium bulkhead used above is also part of the overall protective titanium "bathtub" surrounding the pilot, further mitigating the risk of enemy fire on the pilot. Further mitigation is taken in the wiring systems by shielding all vulnerable points in the wiring runs throughout the wings and forward fuselage. Due to the advancement of electronic warfare in recent history, a fly-by-light design was used in the control system to further prevent the risk of interference from an enemy opposition. Since technology advancements are not always predictable, guided ammunition may not be available or certified by the design fixed date of 2020. Therefore, the current bushmaster III will be used until guided ammunition is an available option. This will further minimize the budgetary and timing risks of technology advancements. To further mitigate the risk of guided munitions failures, the pilot must also be trained to fire conventional munitions as well as guided.

## 28 Manufacturing Plan

This section will outline the preliminary manufacturing design process for the production of the A-21 Valkyrie. Figure 28.1 shows the exploded view of the A-21 which depicts all parts and systems in the aircraft. This also shows where each part is incorporated in the manufacturing process.

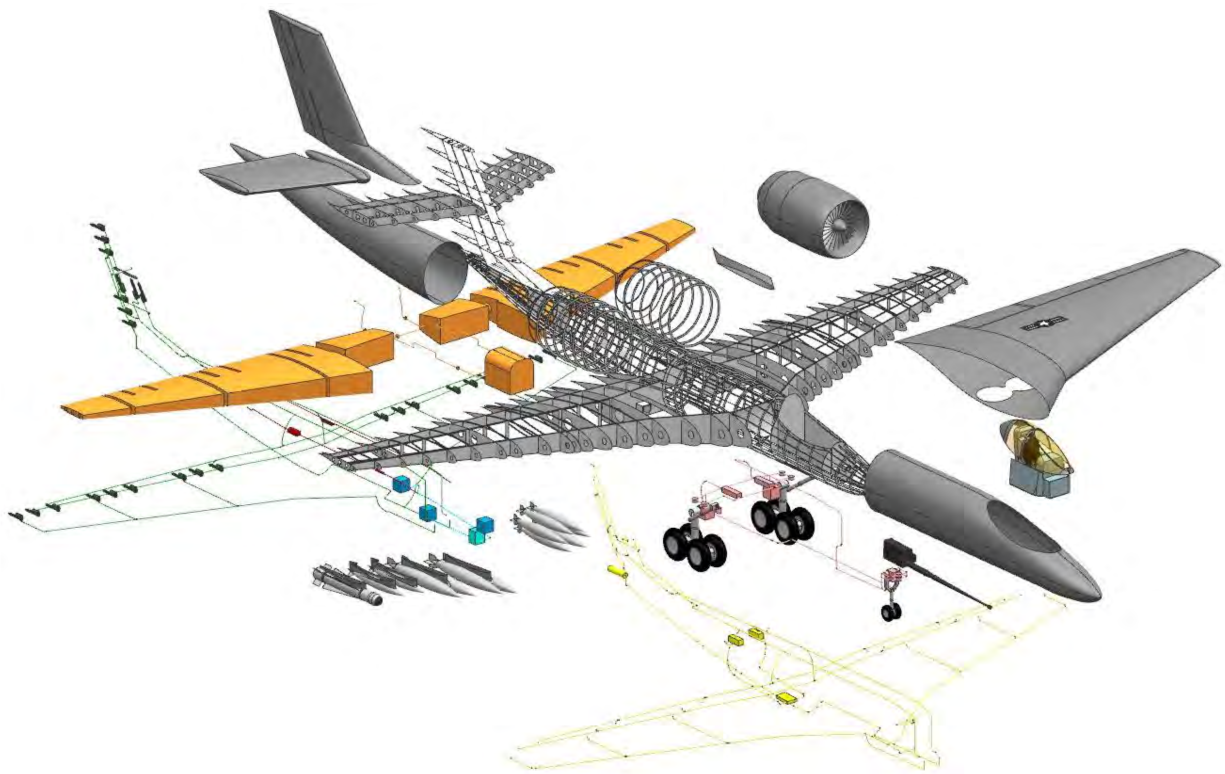

**Figure 28.1:** Exploded View (NTS)

In the preliminary design of the manufacturing process, a bill of materials is needed to determine the material and the manufacturing company used to supply each part. Each part of the A-21 will be outsourced to different companies around the United States. Parts will be delivered from all the outsourced companies to the manufacturing facility and assembled in-house. Table XXX shows the bill of materials for the A-21 Valkyrie II. As seen in the bill of materials, most of the parts for the aircraft are made of standard high strength aluminum.

**Table XXX:** Bill of Materials

| Part | Material | Manufacturer |
|---|---|---|
| Wing | Aluminum | Boeing |
| Fuselage | Aluminum | Spirit AeroSystems |
| Horizontal Tail | Aluminum | Cessna |
| Vertical Tail | Aluminum | Beechcraft |
| Necels | Aluminum | Prat & Whitney |
| Pylons | Aluminum | Cessna |
| Engines | - | Prat & Whitney |
| Landing Gear | - | Goodritch Corporation |
| Tires | - | Goodyear |
| Cockpit | - | Lockheed |
| Ejection Seat | - | Martin-Baker |
| Bushmaster III | - | Orbital ATK |
| Systems | - | Raytheon |
| Munitions | - | Orbital ATK |

The manufacturing process used for the A-21 Valkyrie II is an assembly line based design. The Aircraft will begin on a conveyer belt system starting with the wing. Due to the mid wing design of the A-21, the fuselage will be received in two parts and assembled around the wing. The process will continue as the aircraft moves down the belt system and more parts are assembled on the aircraft. Systems will be installed in the appropriate locations around the aircraft as the aircraft travels down the line. To ensure ethical and safety standards, the safety and concern for the workers will be a top priority during the assembly process.

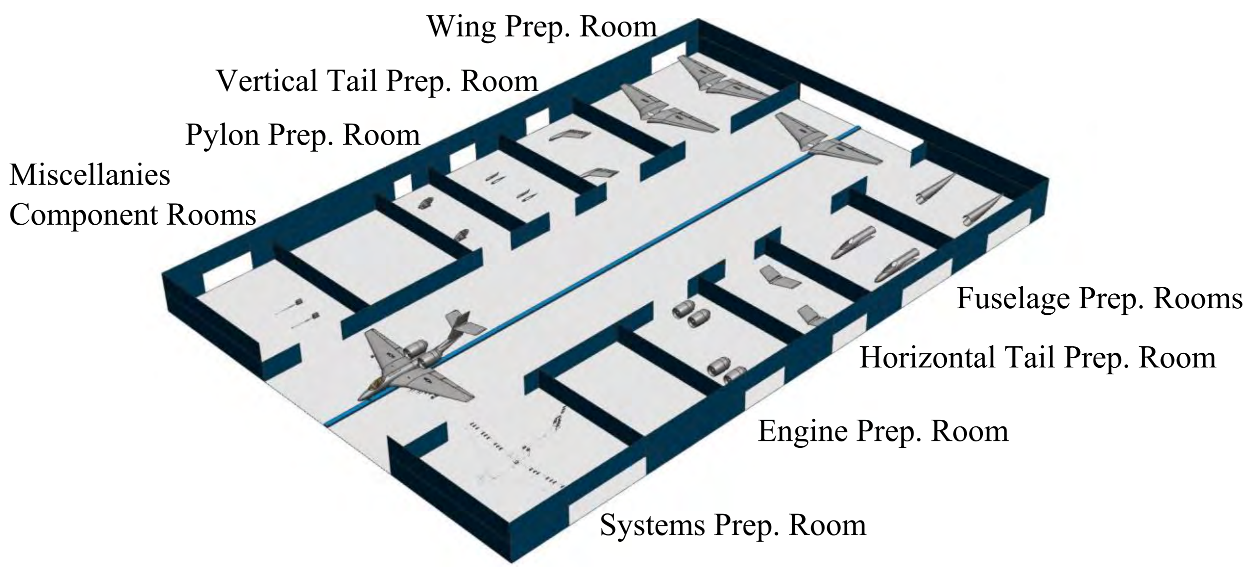


**Figure 28.2:** Manufacturing Facility Layout

Figure 28.3 shows the part flow diagram of the manufacturing process that will be utilized with the factory layout shown in Figure 28.2.

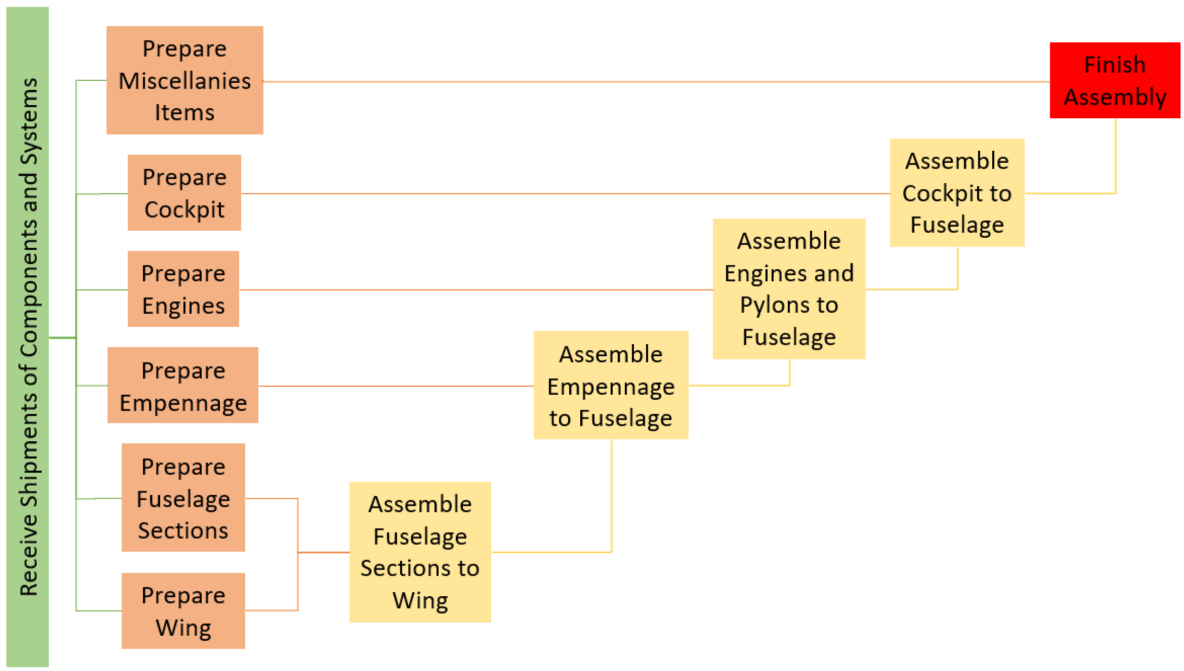


**Figure 28.3:** Manufacturing Part Flow Diagram

## 29 Cost Analysis

The Purpose of this section is to analyze the costs associated with the A-21 Valkyrie II. The methodology used for this section is per Reference 9. This cost analysis process is performed using AAA. AAA will calculate the flyaway and the operating costs as shown in Appendix F. Table XXXI shows the costs calculated using AAA at the production runs specified in the RFP.

**Table XXXI:** AAA Costs

| | |
|---|---|
| R.T.D.E. Cost | $385,104,000 |
| Direct Operating Cost | $3872.56/hr |
| Lifercycle Cost (500 Built) | $79,178,932,001 |
| Lifercycle Cost (1500 Built) | $108,198,307,825 |
| Flyaway Cost (500 Built) | $33,158,000 |
| Flyaway Cost (1500 Built) | $30,150,000 |

Figure 29.1 shows the acquisition cost as a function of the production run, as calculated using AAA. This shows that acquisition cost decreases to an asymptote of approximately 30 million dollars.

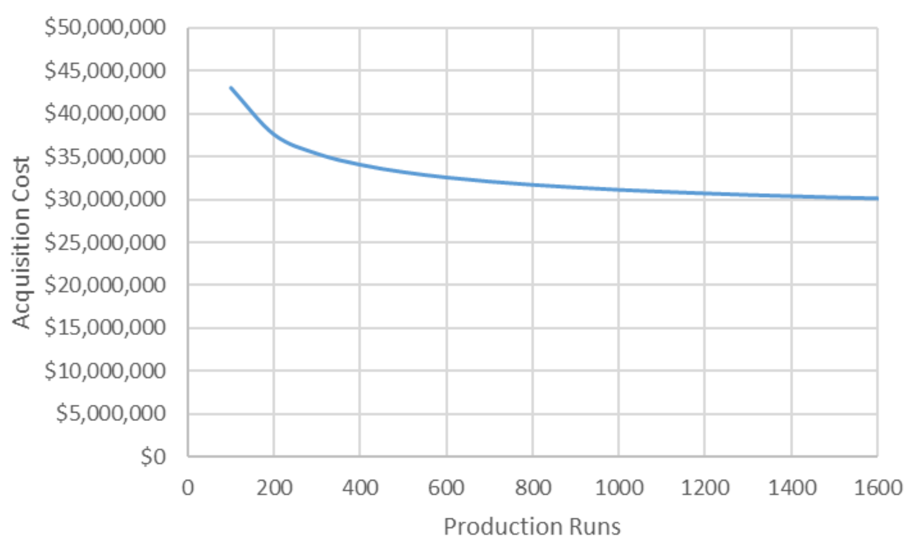


**Figure 29.1:** Acquisition Cost over Differing Production Runs

# 30 Specification Compliance

This section will display the compliance to the RFP the A-21 Valkyrie II has. Table XXXII shows the compliance with the RFP requirements.

**Table XXXII:** RFP Compliance

| Specification Requirements/ Aircraft Characteristics Objective/ Threshold Specifications | Aircraft Performance Predicted or Characteristic | Spec., or Requirement Threshold, Objective Met? | Page # |
|---|---|---|---|
| Operate from unimproved airstrips as short as 6,000 ft long ICAO hot day, 5,000-ft field elevation | <6,000ft | Yes | 13, 15 |
| 1x 35mm cannon with 750 rounds, and 14,000 lb of stores | Internal/ External Stores Mix and 35 mm Bushmaster III | Yes | 33 |
| Carry an electro-optical targeting system capable of providing Category 2 target coordinates | E-0 System Integration in family | Yes | 72 |
| Carry an advanced communications array, allowing it to more effectively integrate with ground forces and communicate with command and control elements | Coms Array integrated in to family | Yes | 72 |
| provide at least 4 hours of AAO at a 500 nautical mile radius from its operating airfield | 4 hour loiter within 500 nautical mile radius | Yes | 13, 15 |
| Crew of 1-2 pilots | 1 pilot | Yes | 33 |
| 300 knots true airspeed (KTAS) maximum speed | 350 kts maximum speed | Yes | 44 |
| At least 200 KTAS cruse speed | 300 kts cruse speed | Yes | 44 |
| 45,000 ft Ceiling | 45,000 ft ceiling | Yes | 44 |
| Maximum design load factor of 8 g | 8 g max load factor | Yes | 15 |
| Compliance with military specifications and requirements (MIL-SPECs) | Met military compliance | Yes | - |
| Fly-away and direct operating cost estimation | $30,150,000 | Yes | 77 |
| Technology development plans (including projected budgets and schedules) | Guided Munitions Integration | Yes | 72 |
| Risk reduction plans (in case technology development fails) | Appropriate risk mitigation | Yes | 73 |
| Weight and balance estimation | Found CG and excursion | Yes | 67, 68 |
| Aircraft sizing and configuration selection | Sized with sizing chart | Yes | 15 |
| Aerodynamic design | Drag polars calculated | Yes | 42 |
| Structural layout and sizing | Preliminary Structure | Yes | 63, 64 |
| Stability and handling qualities | Appropriate X-Plots made | Yes | 38, 39 |
| Propulsion integration | Integration of turbofan engines | Yes | 23 |

The objective function specified in the RFP can now be broken-down and properly calculated. The objective function, seen in Equation 1, is a way of quantifying the compliance with the RFP. Table XXXIII designates the A-21 inputs to the objective function and the weighting fractions displayed in Section 3. Table XXXIII also displays the weighted result of the objective function.

**Equation 1**

OF = [(Actual Range with 4 hrs AAO)/(500 nm)]^2 + [Actual Dash Speed/(300 KTAS)]^2 + [Actual Cruise Speed/(200 KTAS)]^2 + [$40M /(Actual Fly-Away Cost)]^2 + [$3000/hour /(Actual Direct Operating Cost)]^2 + [6,000 ft /(Fully Loaded Minimum Runway Length)]^2 + [(Max Positive Load Factor with 50% Internal Fuel, Gun, and Gun Ammo)/8]^2 + Observable (= 0 if missiles/sensor pod/ gun/fuel tanks are externally carried, 1 otherwise)

**Table XXXIII:** Objective Function Calculation

| | | |
|---|---|---|
| Range at Given Payload (nm) | 500 | 13% |
| Dash Speed (kts) | 350 | 15% |
| Cruise Speed (kts) | 300 | 15% |
| Acquisition Coast ($) | 30150000 | 7% |
| Life Cycle Coast ($/hr) | 3873 | 7% |
| Balance Field Length (ft) | 6000 | 20% |
| Max Load Factor (g) | 8 | 17% |
| Observables (0 = External, 1 = Internal) | 0 | 6.67% |
| Objective Function Weighted | 1.199017576 | |

# 31 Marketing Plan and Aircraft Design Summary

This section will define how the marketing of the A-21 Valkyrie II should be pursued. The A-21 should be initially sold exclusively to the United States and close allies of the United States. The A-21 may initially be marketed to the US Air Force, Army, Navy, and Marines. After a predetermined amount of time, the A-21 will be put up for a review to be offered for sale to ally/NATO countries. This plan would mitigate the risk of the A-21 harming the United States interests. This plan would maximize the profitability potential with the least amount of risk to the U.S. The brochure that may be used to market the A-21 Valkyrie I is displayed below. It showcases the advantages this design will have over the competition.


A-21 Valkyrie II
Span……65.5 ft / 20 ft
Length……61.7 ft / 18.8 ft
Wing Area……803.1 $ft^2$ / 74.6 $m^2$
Combat Radius……500 n.mi / 926 km
Loiter Time……4 hrs
Maximum g-rating……8.0
Maximum Speed……350 kts / Mach 0.54
Weapons Payload……16,625 lbf
Flyaway Cost: $30,150,000
Operating Cost: 3,872 $/hr
Variable Incidence Stabilator
11,000 $lb_f$ of External Stores
PW1217G
• 17,000 $lb_f$ Thrust
• Ultra High Bypass Ratio
35mm Bushmaster III
3,000 $lb_f$ of Internal Stores
Guided Munitions Implementation
A-21

## 32 References


1. Brandt., "Cloase Air Support (A-10 Replacement); Request for Proposal," 2017-2018 AIAA Foundation Undergraduate Individual Aircraft Competition, pp. [online RFP], URL: http://www.aiaa.org/designcompetitions/ [23 August 2017].
2. Roskam, Jan, *Airplane Design: Part I, Preliminary Sizing of Airplanes,* DARcorporation, Lawrence, KS, 2005.
3. Roskam, Jan, Airplane Design: Part II, *Preliminary Configuration Design and Integration of the Propulsion System*, DARcorporation, Lawrence, KS, 2005.
4. Roskam, Jan, A*irplane Design: Part III, Layout Design of Cockpit, Fuselage, Wing,and Empennage: Cutaways and Inboard Profiles, DARcorporation,* Lawrence, KS, 1989.
5. Roskam, Jan, *Airplane Design: Part IV, Layout of Landing Gear and Systems,* DARcorporation, Lawrence, KS, 2010.
6. Roskam, Jan, Airplane Design: Part V, *Component Weight Estimation,* DARcorporation, Lawrence, KS, 1999.
7. Roskam, Jan, *Airplane Design: Part VI, Preliminary Calculation of Aerodynamic Thrust and Power Characteristics,* DARcorporation, Lawrence, KS, 2008.
8. Roskam, Jan, *Airplane Design: Part VII, Determination of Stability, Control and Performance Characteristics: Far and Military Requirements,* DARcorporation, Lawrence, KS, 1991.
9. Roskam, Jan, *Airplane Design: Part VIII, Airplane Cost Estimation: Design Development, Manufacturing and Operating,* DARcorporation, Lawrence, KS, 1990.
10. "Legendary Faculty Honored with KU Engineering's Highest Award," *School of Engineering*Available: http://engr.ku.edu/legendary-faculty-honored-ku-engineering%E2%80%99s-highest-award.
11. "Collection Highlights," *Junkers J.I - Canada Aviation and Space Museum*Available: https://ingeniumcanada.org/aviation/collection-research/artifact-junkers-j-i.php.
12. "WWI Planes: Crews, Cockpits, Crashes, Contraptions," *HistoryNet*Available: http://www.historynet.com/gallery-wwi-planes.htm.
13. "Junkers J.I," *Wikipedia*Available: https://en.wikipedia.org/wiki/Junkers_J.I.
14. "Curtiss A-12 (Shrike) Strike Aircraft," *Military Weapons*Available: https://www.militaryfactory.com/aircraft/detail.asp?aircraft_id=716.
15. "Heinkel He 178 Jet-Powered Technology Demonstrator Aircraft," *Military Weapons*Available: https://www.militaryfactory.com/aircraft/detail.asp?aircraft_id=214.
16. "Boeing GA-1," *Wikipedia*Available: https://en.wikipedia.org/wiki/Boeing_GA-1.
17. "The Sirens of Death – 11 Amazing Facts About the Ju 87 Stuka," *MilitaryHistoryNow.com*Available: http://militaryhistorynow.com/2015/06/04/screaming-death-10-amazing-facts-about-the-ju-87-stuka/.
18. "Junkers Ju 87," *Wikipedia*Available: https://en.wikipedia.org/wiki/Junkers_Ju_87.
19. "Supermarine Spitfires and Hawker Hurricanes: World War II Aircraft," *HistoryNet*Available: http://www.historynet.com/supermarine-spitfires-and-hawker-hurricanes-world-war-ii-aircraft.htm.
20. *Polikarpov U 2 Po 2*Available: http://www.century-of-flight.net/Aviation%20history/photo_albums/timeline/ww2/2/Polikarpov%20U%202%20Po%202.htm.
21. "Hawker Typhoon," *Wikipedia*Available: https://en.wikipedia.org/wiki/Hawker_Typhoon.
22. "The Mighty "Jug" – 11 Cool Facts About the Republic P-47 Thunderbolt," *MilitaryHistoryNow.com*Available: http://militaryhistorynow.com/2015/04/20/the-jug-10-cool-facts-about-the-p-47-thunderbolt/.
23. "Republic P-47 Thunderbolt," *Wikipedia*Available: https://en.wikipedia.org/wiki/Republic_P-47_Thunderbolt.

24. "Boeing," *Boeing: Historical Snapshot: AD/A-1 Skyraider Attack Bomber*Available: http://www.boeing.com/history/products/ad-a-1-skyraider-bomber.page.
25. "Douglas A-1 Skyraider," *Wikipedia*Available: https://en.wikipedia.org/wiki/Douglas_A-1_Skyraider.
26. Boyd, R., "AH-64 Apache Longbow," *Military.com*Available: http://www.military.com/equipment/ah-64-apache-longbow.
27. "Boeing AH-64 Apache," *Wikipedia*Available: https://en.wikipedia.org/wiki/Boeing_AH-64_Apache.
28. "A-10 Thunderbolt (Warthog)," *Airforce Technology*Available: http://www.airforce-technology.com/projects/a-10/.
29. "Fairchild Republic A-10 Thunderbolt II," *Wikipedia*Available: https://en.wikipedia.org/wiki/Fairchild_Republic_A-10_Thunderbolt_II.
30. "Dr. Willem A.J. Anemaat," *W Anemaat*Available: http://www.darcorp.com/About_Us/Profile/Willem_Anemaat/.
31. "Adrian Lewis," *Department of History* Available: https://history.ku.edu/adrian-lewis.
32. Disrud, Colonel. "Experience with A-10." 5 Sept. 2017.
33. Lewis, Major. "Experienced Army Major and KU Professor" 12 Sept. 2017.
34. Barrett, R., "Statistical Time and Market Predictive Engineering Design (STAMPED) Techniques for Aerospace System Preliminary Design," Journal of Aeronautics & Aerospace Engineering, Omics Publishing, Vol. 3, No. 1, Feb. 2014.
35. *Civil Turbojet/Turbofan Specifications* Available: http://jet-engine.net /civtfspec.html.
36. "Thomson Linear Motion Optmized." *Motor not included, Direct Drive, Inline, 267 mm Stroke, No Brake, 15000 N. | Thomson*, www.thomsonlinear.com/en/product/T13-B4040MU056-36.
37. "High Force Industrial Actuator IP-66." *High Force Industrial Actuator*, www.progressiveautomations.com/high-force-industrial-actuator.
38. "Start Here and We'll Help You FindAviation Tires." *Home | Goodyear Aviation Tires*, www.goodyearaviation.com/index.html.
39. "EXACTO Guided Bullet Demonstrates Repeatable Performance against Moving Targets." *Defense Advanced Research Projects Agency*, www.darpa.mil/news-events/2015-04-27.
40. Schumacher, L., "The Design Requirements and Application of Guided Hard-Launch Munitions for use on Aerial Platforms," copyright 2016.

## Appendix

All appendices can be found though: https://frankjbonet.wixsite.com/fboneta21